AN ABSTRACT OF THE THESIS OF

Connee S. Mitchell for the degree of Master of Science in Atmospheric Sciences presented on May 6, 1985. Title: The Use of Climate Classification Schemes to Assess the Performance of General Circulation Models

Abstract approved: Redacted for Privacy

Michael E. Schlesinger

Two climate classification schemes, W. Köppen's and C. W. Thornthwaite's, were used to analyze the performance of the OSU AGCM in simulating both the present climate (model verification) and the climatic change induced by an increase in the atmospheric CO_2 (sensitivity study). Climate classification maps were generated for each of the two schemes based on the observed data of Crutcher and Meserve (1970), Taljaard et al. (1969), and Jaeger (1976), as well as for each set of model simulation data.

Both Köppen's and Thornthwaite's schemes showed that the model did well in simulating the observed climate, but no significant

change in climate types was detected by either scheme for a quadrupling of atmospheric CO_2 in the OSU AGCM with seasonally-varying insolation and prescribed sea-surface temperatures. Thornthwaite's scheme also detected no significant change in climate types in the OSU AGCM with annual-averaged insolation and a swamp ocean for a doubling of atmospheric CO_2.

The interannual variability of the simulated climate types was also investigated. It was determined that the climate based on one year of model simulation data should not be taken as representative of the model climate because of the level of noise and the differing extents and intensities of the climate regions between simulation years.

The climate classification schemes provide a different view of the GCM results by combining the raw data from the model to yield a description of the climate in terms of what type of vegetation could be supported. They also have the potential for detecting climate change in GCM experiments, although a method for determining the significance of such changes needs to be developed.

The Use of Climate Classification Schemes to Assess the Performance of General Circulation Models

by

Connee S. Mitchell

A THESIS

submitted to

Oregon State University

in partial fulfillment of
the requirements for the
degree of

Master of Science

Completed May 6, 1985

Commencement June 1985

APPROVED:

Redacted for Privacy

Professor of Atmospheric Sciences in charge of major

Redacted for Privacy

Head of Department of Atmospheric Sciences

Redacted for Privacy

Dean of Graduate School

Date thesis is presented May 6, 1985

Typed by Doris Swan for Connee S. Mitchell

ACKNOWLEDGEMENTS

I would like to thank my major professor, Dr. Michael Schlesinger, for all the help and guidance he gave to me during the preparation of this thesis. I also appreciate the valued suggestions given by Dr. Gerald Potter and Dr. Hugh Ellsaesser and the other members of my committee, Drs. W. Lawrence Gates, Steven Esbensen, David Enfield, and Walter Loveland.

I would also like to thank Dr. Gates, the Director of the Oregon State University Climatic Research Institute, for his support of the research described herein; Robert Mobley, William McKie, and Shiang-Meei Heh for their assistance in performing the simulations and with the graphics; the Technical Information Department of the Lawrence Livermore National Laboratory for drafting and photographing the figures; Doris Swan, Nancy Badal, Floy Worden, and Pam Drumtra for typing the manuscript; and the Atmospheric and Geophysical Sciences Division of Lawrence Livermore National Laboratory for their overall support and encouragement.

This research was supported by the National Science Foundation and the Department of Energy under grants ATM 80-01702 and ATM 82-05992.

TABLE OF CONTENTS

LIST OF FIGURES

LIST OF TABLES

THE USE OF CLIMATE CLASSIFICATION SCHEMES TO ASSESS THE PERFORMANCE OF GENERAL CIRCULATION MODELS

1. INTRODUCTION

Climate is usually defined in terms of the means, extremes, and variations of such elements as temperature, precipitation, evaporation, humidity, cloudiness, and wind. Before the industrial revolution climatic change was primarily due to natural causes, such as continental drift, mountain building, variations in orbital parameters, volcanic emissions, and hypothesized fluctuations in insolation. But today the side effects of technology may also lead to climatic change. For example, the albedo of the earth's surface is being changed through land-use practices such as deforestation, and the atmospheric CO_2 concentration is being increased by the burning of fossil fuels. These changes in the radiative properties of the earth's surface and atmosphere may induce changes in the earth's climate.

To determine whether such anthropogenic activities will change the climate we can simply wait until the climate system itself performs the experiment, that is, does or does not change. Ideally, however, we should have a method for predicting the response of the climatic system. For this reason several types of mathematical models of the earth's climatic system have been developed. The models in this climate model hierarchy may be classified by the number and

treatment of the interacting physical processes, and by the number of spatial dimensions (Schneider and Dickinson, 1974; Saltzman, 1978).

Energy balance models (EBMs) calculate an effective planetary temperature from the balance between the incoming solar (shortwave) and outgoing terrestrial (longwave) radiation. EBMs may be zero dimensional, one dimensional (latitude), or two dimensional (latitude and longitude), and are useful in examining the sensitivity of temperature to changes in the radiative properties of the earth's surface and atmosphere. Radiative-convective models (RCMs) determine the vertical distribution of temperature by computing both the radiative fluxes and the vertical convective heat transport, the latter by adjusting the temperature so that its rate of decrease with height does not exceed a critical value. RCMs are useful in studying the sensitivity of the vertical temperature structure to changes in the radiative properties of the atmosphere and surface.

The most comprehensive mathematical model of the earth's climate system is the general circulation model (GCM). A GCM consists of a set of time-dependent, nonlinear partial differential equations which represent the physical laws governing the behavior of the atmosphere and underlying surface. Vertical velocity, geopotential height, density, clouds, surface albedo, and the rates of change of surface pressure, temperature, horizontal velocity, water vapor concentration, soil temperature, soil moisture, and snow mass are determined by the governing equations of an atmospheric GCM (AGCM).

The above variables are defined for a three dimensional grid of points spanning the earth. The typical AGCM has from two to about

nine layers in the vertical and a horizontal resolution of a few hundred kilometers. The statistical effects of physical processes such as cloud formation, whose characteristic sizes are smaller than the grid size, are parameterized, i.e., related to processes that are resolved by the model. As with other mathematical climate models, an AGCM is only as good as the mathematical representation of the physical processes involved, the numerical techniques used to solve the mathematical representation, and the power of the computer upon which the climate is simulated by the model.

Because of their completeness and because they are three-dimensional, GCMs are the best suited of the climate models discussed for simulating the earth-atmosphere system and for understanding the mechanisms of regional climatic change.

Before using any climate model to predict an unknown climate, such as that which might result from increased levels of CO_2, it is necessary to verify the model's performance in simulating a known climate. The usual method for verifying the performance of a GCM is to compare its simulation of the present climate with the available observations. This is done in terms of the geographical distributions of such fields as sea-level pressure, temperature, wind, and precipitation.

When the performance of a GCM has been so verified, it can be used in a sensitivity study to simulate the effects of perturbations (such as doubling the atmospheric CO_2 concentration) on the climate. This is done by comparing the fields from a (control) simulation of the present climate with those from a (perturbation) simulation of the

equilibrium climate resulting from introducing a perturbation into the model, the differences between the two simulations being attributed to the perturbation.

In addition to describing a climate in terms of individual climatic elements, it may be useful to classify the climate according to something we can easily relate to, such as energy consumption, type of clothing required, type of food crops, or type of vegetation that could be supported. The vegetation-based climate classification schemes of W. Köppen and C. W. Thornthwaite are two examples of schemes that integrate the effects of the climatic elements. Such climate classification schemes should be especially useful in determining the climatic effects of perturbations. For example, while a perturbation may result in a change in the temperature and precipitation patterns of a region, it may not imply a change in the climatic type of that region.

The purpose of this study is to investigate the utility of climate classification schemes in analyzing the performance of AGCMs in simulating both the present climate (model verification) and the climatic change induced by a perturbation such as an increase of atmospheric CO_2 (sensitivity study). This will be discussed more fully in Section 2.4 below.

Two basic types of AGCMs are examined in this study: AGCMs with seasonally-varying insolation and prescribed sea-surface temperatures, and an AGCM with annual-mean insolation and an interactive "swamp" ocean. Since it is important to be aware that different AGCMs may produce different distributions of climate, a description of the AGCMs

is contained in Chapter 2. This chapter also includes a short history of climate classification, describes in detail the two schemes used in this study, presents example climate classification calculations, and briefly discusses the observed global climate distributions in terms of the two schemes. Chapter 3 explains the research strategy and analysis methods used, and Chapter 4 discusses in detail the results of the study and gives a brief summary of these results. Chapter 5 then contains the conclusions drawn from the study and recommendations for future work.

2. BACKGROUND

2.1 General Circulation Models

The treatment of the oceans by GCMs is an important problem. Oceans cover more than 70% of the earth and account for two-thirds of the solar radiation absorbed, and are therefore an integral part of the climatic system. Heat is exchanged at the ocean's surface through shortwave and longwave fluxes, evaporation, and sensible heat transfer. Because of the ocean's large heat capacity, it acts as a huge heat reservoir. Solar energy stored in the surface layer in the tropics is transported poleward by ocean currents; the thermohaline circulation moves cold water from the poles to lower latitudes.

Ideally a complete GCM would consist of an atmospheric GCM (AGCM) coupled to a dynamic oceanic GCM (OGCM). But because of the complexity, a GCM usually goes through various stages of construction and testing, progressively adding more realistic features.

One state of GCM construction consists of an AGCM with a motionless ocean and prescribed sea-surface temperatures, i.e., the sea-surface temperatures are constrained to be the seasonally-varying climatological values. If a perturbation is introduced, such as a doubling of the atmospheric CO_2 concentration, the ocean's temperature is not allowed to respond to the change, with any excess heating by the atmosphere simply passing unnoticed into the ocean. Therefore, the

feedback effects of increased longwave radiation and increased evaporation and condensation over the oceans are absent in a model with prescribed sea-surface temperatures. The Geophysical Fluid Dynamics Laboratory (GFDL) AGCM described by Manabe and Holloway (1975) and the Oregon State University (OSU) AGCM described by Ghan et al. (1982) are examples of models with seasonally-varying insolation and prescribed sea-surface temperatures.

Another stage of GCM construction consists of an AGCM with a "swamp" ocean. A swamp ocean has no ocean currents or heat capacity and, therefore, its surface temperature changes instantaneously in response to the overlying atmosphere. AGCMs with swamp oceans cannot have seasonally-varying insolation, since in winter the zero oceanic heat capacity would result in the freezing of large sections of the oceans.

The feedback effects mentioned above are present for a swamp ocean, and they affect the sensitivity of the model. An example of this sensitivity is the different global-mean surface temperature warmings induced by doubled atmospheric CO_2 obtained by Gates et al. (1981) and by Schlesinger (1984). The global warming due to a doubling of atmospheric CO_2 was only 0.2° C for the OSU AGCM with seasonally-varying insolation and prescribed sea-surface temperatures (Gates et al., 1981), but was 2.0° C for the OSU AGCM with annually-averaged insolation and a swamp ocean (Schlesinger, 1984).

A fully-coupled AGCM and OGCM would be best suited for the present study since both the atmosphere and the ocean play important roles in determining climate. But, since models of this type are still in

the preliminary testing stage and require an enormous amount of computer time to approach an equilibrium state, we will have to work with the results of the other two types of GCMs: AGCMs with seasonally-varying insolation and prescribed sea-surface temperatures (because they have the ability to simulate the seasonal atmospheric cycle), and AGCMs with annual-mean insolation and a swamp ocean (because they allow the ocean to respond to perturbations in the climatic system).

2.2 Climate Classification Schemes

There are two basic approaches to climate classification: genetic and empirical. The former emphasizes origins or causative factors of climate as the organizing principle, while the latter emphasizes climatic elements and their observed effects upon plant and animal life. The ancient Greeks classified climate according to the poleward boundaries of the ecliptic and the limit of the sun's tangential rays in the winter hemisphere at solstice. Surface pressure, air masses, and main wind systems as well as solar radiation are considered to be causative factors of climate by geographers, although the first three are also affected by other features of the general circulation. Therefore, contemporary genetic climate classification schemes are not purely genetic. Examples of contemporary genetic schemes are the ones by Hendl (1963) and Flohn (1950), the latter emphasizing precipitation, sea-level pressure, and wind zones (Trewartha and Horn, 1980).

The trend of climate classification schemes has been toward empirical schemes, partly because most causative factors are much more

difficult to identify than climatic elements, but probably more importantly because our interpretation of the origins of climate is more likely to change than our observations concerning the effects of climate on plants and animals.

The climate of an area is not determined by any single factor, but rather by the distinctive regional integration of several factors. Since vegetation is such a good integrator of the effects of climate, it is the basis of most empirical climate classification schemes. The idea of using vegetation as a basis for classifying climate became accepted in the late 19th century, but Wladimir Köppen was the first to produce a simple, yet practical, scheme using readily-available data.

2.2.1 Köppen's Scheme

Köppen's scheme is the most widely-used climate classification scheme by geographers today. It was first introduced in 1901 with the last version by Köppen appearing in 1931 (Köppen, 1931).

a. Description

Köppen's scheme uses the monthly-mean temperature and precipitation to define five principal types of climate based upon the various kinds of vegetation each type could support, and designates each type by a letter of the alphabet as shown in Table 1.

Table 1. Köppen's climate classification scheme (after Trewartha, 1968).[1]

Principal climate type	Precipitation characteristics
A - tropical rainy (Tmin > 64.4)	f - even rainfall (Rmin ≥ 2.4) w - dry winter (Rmin < 2.4 and Rmin < 3.9-AR/25) m - monsoon (Rmin < 2.4 and Rmin ≥ 3.94-AR/25)
B - dry S - steppe AR ≤ 0.44*AT-8.5 for even rainfall AR < 0.44*AT-14 for dry summer AR < 0.44*AT-3 for dry winter W - desert AR < 0.22*AT-4.25 for even rainfall AR < 0.22*AT-7 for dry summer AR < 0.22*AT-1.5 for dry winter	f - even rainfall (WS < 10*DW and WW < 3*DS) s - dry summer (WW ≥ 3*DS) w - dry winter (WS ≥ 10*DW)
C - warm temperate rainy (26.6 ≤ Tmin ≤ 64.4 and Tmax > 50)	f - even rainfall (not s or w) s - dry summer (WW ≥ 3*DS and Rmin < 1.2) w - dry winter (WS ≥ 10*DW)
D - cold snowy forest (Tmin < 26.6 and Tmax > 50)	f,s,w - same as for C climates
E - polar (Tmax ≤ 50) T - tundra (32 ≤ Tmax ≤ 50) F - perpetual frost (Tmax<32)	

Here, "summer" and "winter" refer to the summer and winter half-years, April through September and October through March in the Northern Hemisphere, and vice versa in the Southern Hemisphere, and:

Tmin = minimum monthly mean temperature (°F)
Tmax = maximum monthly mean temperature (°F)
AT = annual mean temperature (°F)
Rmin = minimum monthly total precipitation (in/mo)
Rmax = maximum monthly total precipitation (in/mo)
AR = total annual precipitation (in/yr)
WW = precipitation of wettest winter month (in/mo)
WS = precipitation of wettest summer month (in/mo)
DW = precipitation of driest winter month (in/mo)
DS = precipitation of driest summer month (in/mo)

[1]The colors shown are used in all Köppen figures within this paper.

Recognizing the fact that plant growth depends not only upon the amount of precipitation, but also upon the intensity of evaporation, Köppen devised formulas combining temperature and precipitation that represent an index of evapotranspiration (the combined process of evaporation of water and transpiration from plants). These formulas (shown in Table 1) are the basis for separating the dry B climate from the other four thermally-defined moist climates in the first-level divisions, as shown in Fig. 1.

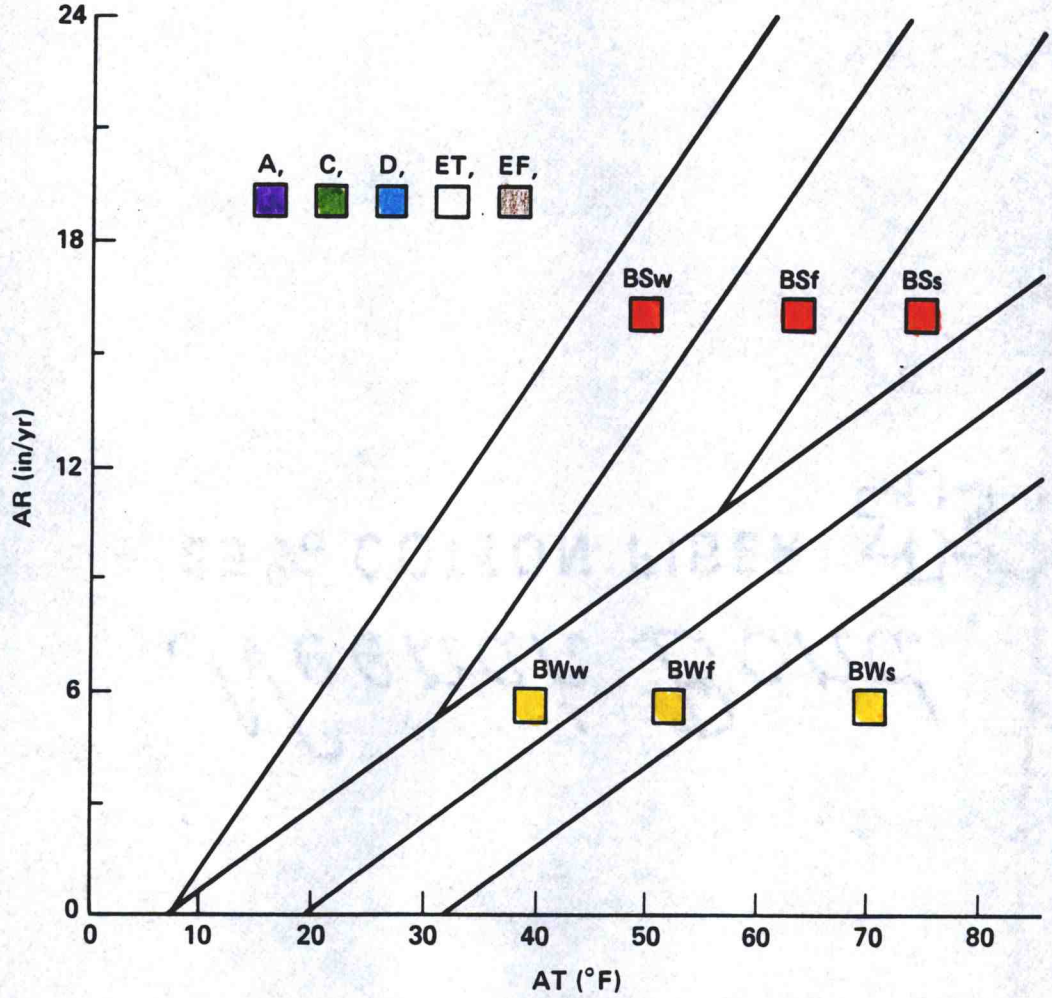

Fig. 1. Köppen's first-level subdivisions between dry and moist climates. (Colors used in all figures relating to Köppen correspond to those used in Table 1.) Adapted from Haurwitz and Austin (1944).

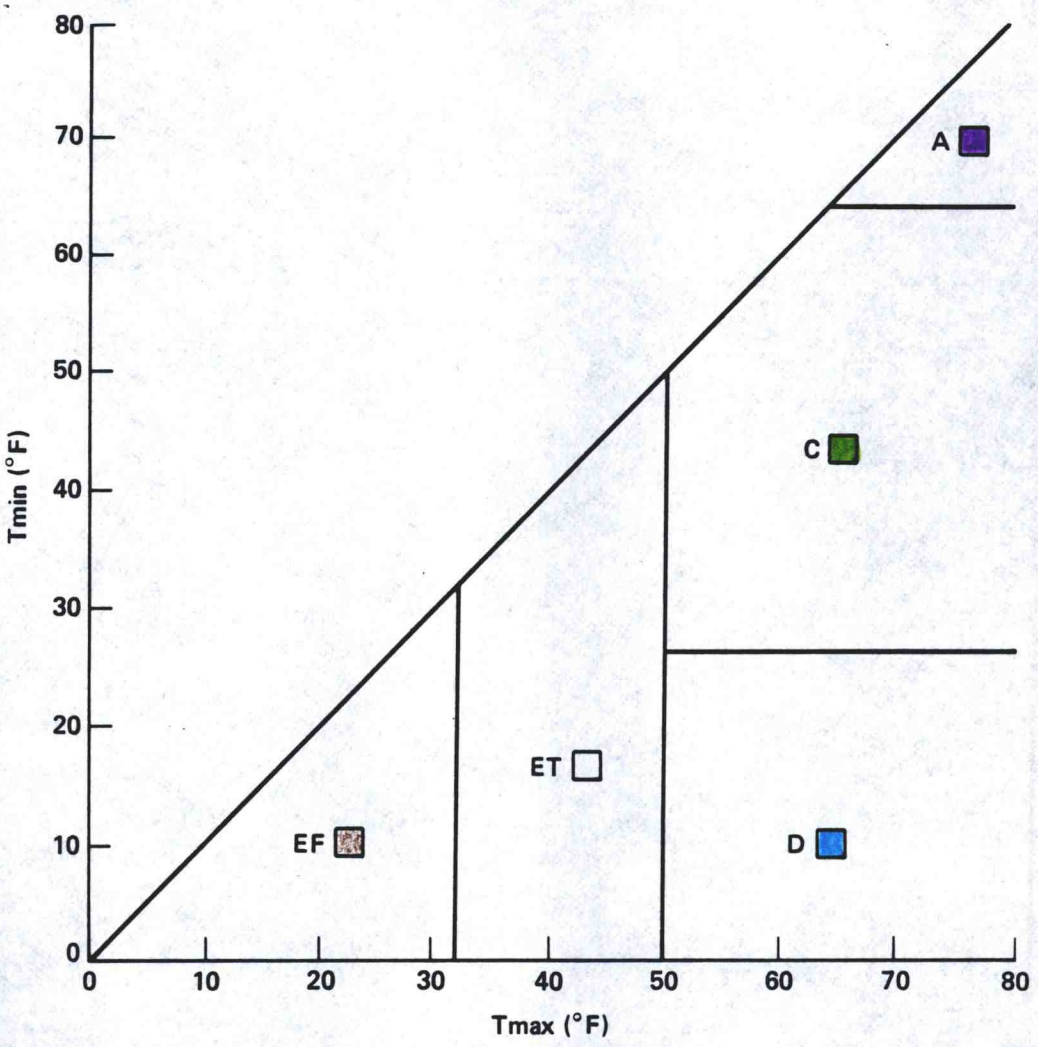

Fig. 2. Köppen's first-level subdivisions among the moist climates. Adapted from Haurwitz and Austin (1944).

The boundaries among the moist climates are based solely on temperature, as shown in Fig. 2. The tropical rainy A climate has continuously high temperature. The minimum temperature of 64.4°F for the coolest month for the A climate was chosen because some tropical crops cannot thrive at lower temperatures. The minimum temperature of 26.6°F of the coldest month separates the temperate C climate from the cold snow-forest D climate, since it is believed that frozen

ground and a snow cover would last less than a month at warmer temperatures. A maximum temperature of 50°F of the warmest month represents the poleward limit of forest, thus separating the cold snow-forest D climate from the polar E climate. A maximum temperature of 32°F separates the perpetually frozen EF climate from the tundra ET climate (Trewartha, 1968).

After the major climate type is determined, the precipitation characteristics for that specific major climate type are determined according to the second column of Table 1. These second-level subdivisions, or moisture indices, are based upon the seasonal distribution of precipitation: f, no distinct dry season; s, dry summers; w, dry winters; m, monsoon. The precipitation characteristic of a tropical A climate can be represented by a point with coordinates (AR,Rmin) in Fig. 3. However, B, C, and D climates require two points with coordinates (DW,WS) and (WW,DS), which can be connected by a line segment as shown in Fig. 4, to determine the precipitation characteristic. If any part of the line segment is in the "w" section and not in the "s" section, then the climate type is "w" - dry winter (line segments 1 and 5); if any part of the line segment is in the "s" section and not in the "w" section, then the climate type is "s" - dry summer (line segments 3 and 7); if the line segment is entirely within the "f" section, then the climate type is "f" - even rainfall (line segments 2 and 6); if the line segment extends into both the "w" and "s" sections, then the climate type is also "f" - even rainfall (line segments 4 and 8).

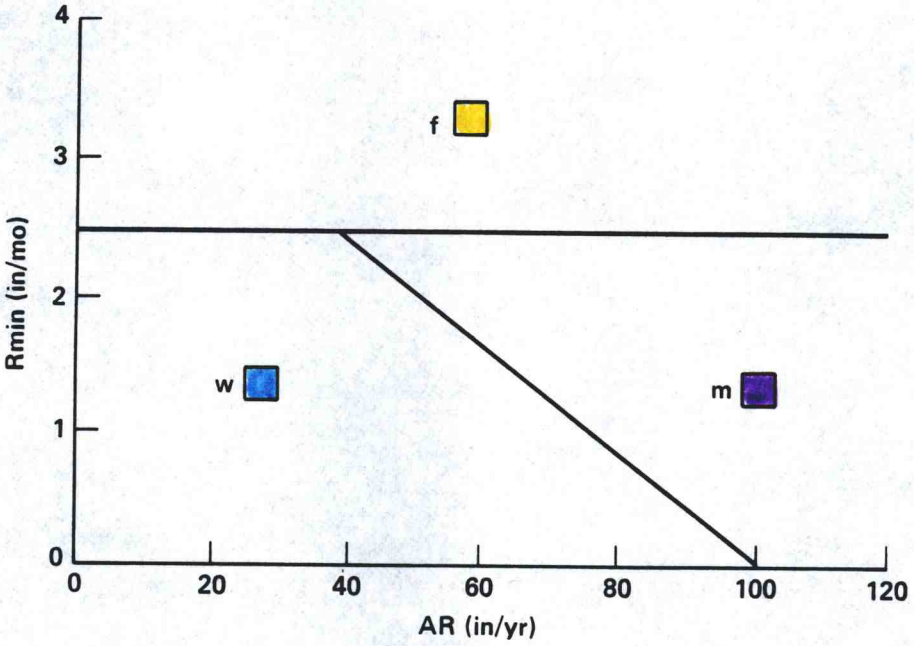

Fig. 3. Köppen's second-level subdivisions for A climate. Adapted from Haurwitz and Austin (1944).

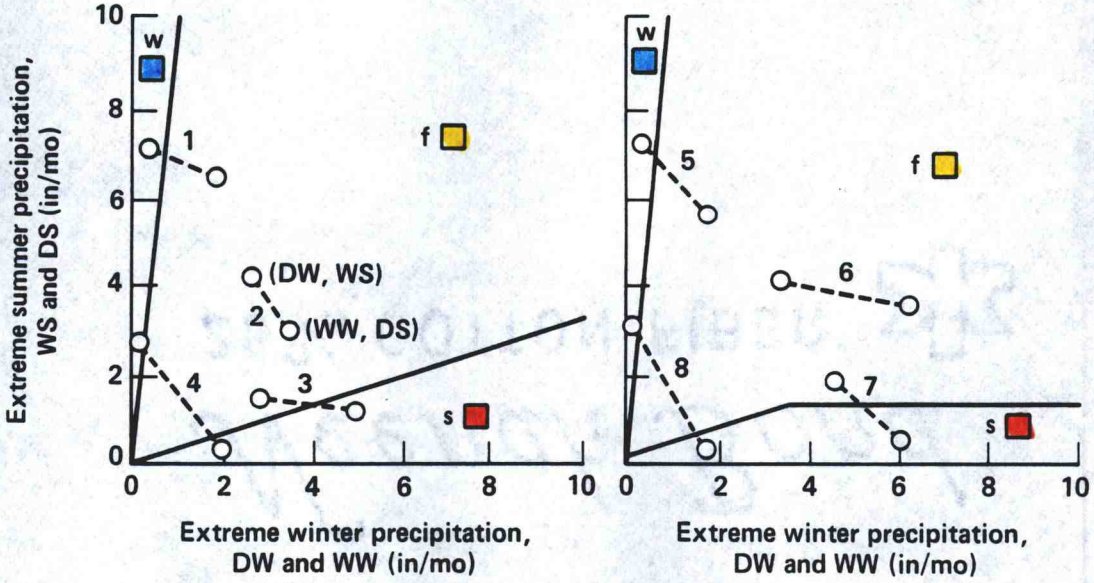

Fig. 4. Köppen's second-level subdivisions for B (left), C (right), and D (right) climates. See text for description of dotted line segments.

There are other lower-level subdivisions based on the occurrence of fog and the duration and intensity of extreme temperatures, but the scope of this study will be limited to the two major levels.

b. Example

As an example of the calculation of the first two levels of Köppen's scheme, assume a region has the monthly-mean temperature and precipitation shown in Table 2.

Table 2. Sample data for Köppen scheme.

Month	Jan	Feb	Mar	Apr	May	Jun	Jul	Aug	Sep	Oct	Nov	Dec
T(°F)	30.0	32.0	45.9	50.2	59.2	70.2	76.6	73.9	65.1	56.5	48.9	29.7
P(inches)	5.7	3.4	3.1	3.5	3.6	6.5	4.1	4.4	7.7	3.3	6.3	2.6

The values of the variables at the bottom of Table 1 are then defined for a northern hemisphere location as:

Tmin = 29.7°F
Tmax = 76.6°F
AT = 53.2°F
Rmin = 2.6 in
Rmax = 7.7 in
AR = 54.2 in
WW = 6.3 in
WS = 7.7 in
DW = 2.6 in
DS = 3.5 in

Since the sequence of steps by which a climate type is arrived at is not specified in Trewartha (1968), we will first determine whether or not the climate is B. Since WS < 10 * DW and WW < 3 * DS, the precipitation characteristic is f if the climate is B (Table 1 and Fig. 4), hence we check to see whether the criterion for a BSf or

a BWf climate is met (Fig. 1). For this example AR > 0.44 * AT - 8.5 and AR > 0.22 * AT - 4.25, therefore, this is not a B climate.

Since Tmax > 50°F and 26.6°F ≤ Tmin ≤ 64.4°F, this is a temperate C climate (Fig. 2). Also, since WW < 3 * DS and WS < 10 * DW, the precipitation characteristic for an even rainfall f climate is satisfied (Fig. 4). Therefore, this region has a Cf climate according to Köppen's scheme.

c. Observed Climatology

A Köppen climate map, or global representation of the distribution of climate types over land, for the present-day climatology from Trewartha (1968, hereafter referred to as T68) is shown in Fig. 5. If not otherwise indicated in the figure captions, a blank region on a climate map denotes that there is no climate type defined for that level, e.g., there are no second-level subdivisions for polar ET and EF climates.

Generally, the equatorial regions have a tropical A climate, and the mid-latitudes have a temperate C climate, which gives way poleward to a cold D climate in the Northern Hemisphere. The polar regions have tundra ET and perpetual frost EF climates. The dry climates BS and BW are located in the subtropical and mid-latitude regions and define the steppe and desert regions, respectively. The present-day climatology will be discussed in more detail in Chapter 4.

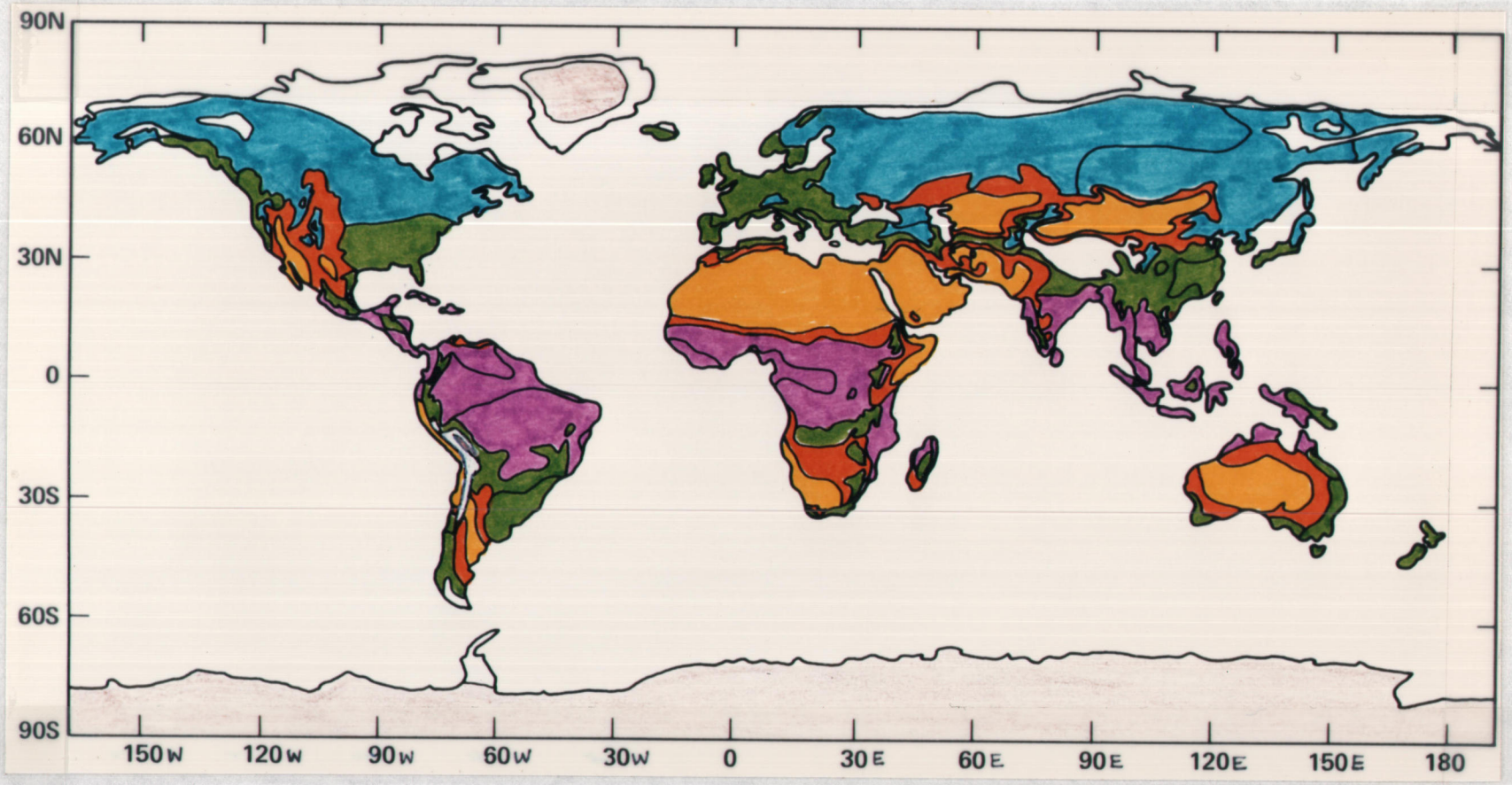

Fig. 5. Köppen climate map for T68 showing first-level (A, BW, BS, C, D, ET, EF) subdivisions (after Trewartha, 1968) over land only.

2.2.2 Thornthwaite's Scheme

Another well-known empirical classification scheme is that devised by C. W. Thornthwaite. Thornthwaite's 1955 scheme is like Köppen's scheme in that it: (1) quantitatively defines climate types; (2) is based ultimately on vegetation; and (3) employs a combination of symbols to designate the climatic types.

a. Description

The concept of potential evapotranspiration is the cornerstone climatic index of Thornthwaite's scheme. Potential evapotranspiration (PE) is the maximum evapotranspiration possible if a plentiful supply of moisture is available. Since the PE is a theoretical moisture loss depending only on the available energy for a region, it is independent of vegetation, soil, and precipitation, and is therefore a means for objective separation of climatic regions on climatic criteria alone (Carter, 1966).

The derivation of a general equation for PE is described in Thornthwaite (1954). The unadjusted PE, or "UPE", is based on a 30-day month with 12 hours of insolation per day and is defined as:

$$UPE(m) = \begin{cases} 16 \left(10 * \frac{T(m)}{I}\right)^{a} & \text{for } T(m) \geq 0°C \\ 0 & \text{for } T(m) < 0°C \end{cases} \qquad (1)$$

where m is the month index, "T(m)" is the monthly mean surface air temperature (°C), "I" is an annual heat index defined as:

$$I = \sum_{m=1}^{12} \left(\frac{T(m)}{5} * H[T(m)] \right)^{1.514} \qquad (2)$$

where

$$H[x] = \begin{cases} 0 \text{ for } x \leq 0 \\ \\ 1 \text{ for } x > 0 \end{cases}$$

is the Heavyside function, and "a" is a coefficient defined as:

$$a = (6.75*10^{-7})\ I^3 - (7.71*10^{-5})\ I^2 + 0.01792\ I + 0.49239 \quad . \qquad (3)$$

Thornthwaite applies a factor to the UPE to adjust for varying lengths of months and daily insolation:

$$PE(m) = UPE(m) * \frac{HSUN(m,\phi)}{(30 \text{ days/mo})*(12 \text{ hr/day})} \quad , \quad \text{mm/month} \qquad (4)$$

where

$$HSUN(m,\phi) = \sum_{i=1}^{m} 2\left[\cos^{-1}\left(\frac{\cos 90.83^\circ}{\cos \phi \cos \delta_i} - \tan \phi \tan \delta_i\right)\right]\frac{12 \text{ hr}}{\pi \text{rad}}$$

$$\text{for } |\phi| < 50^\circ \qquad (5a)$$

$$HSUN(m,\phi) = HSUN(m,50^\circ) \qquad \text{for } \phi > 50^\circ \qquad (5b)$$

$$HSUN(m,\phi) = HSUN(m,-50^\circ) \qquad \text{for } \phi < -50^\circ \qquad (5c)$$

is the number of hours of insolation per month, ϕ is latitude, and

$$\delta = 23.46 * \sin\left(\frac{\text{number of days since vernal equinox}}{365} * 2\pi\right) \quad (6)$$

is the declination angle. Thornthwaite didn't define HSUN for latitudes poleward of 50°; the above formulation for HSUN is taken from Willmott (1977).

A description of the main subdivisions in Thornthwaite's scheme is given in Table 3, and is the same as that of Mather (1966, 1974), except that different letters have been used to designate the dry subhumid, semi-arid, and arid categories.

The annual moisture index

$$Im = 100 * (P/PE-1) \quad , \quad (7)$$

where P is the total annual precipitation (mm/yr) and PE the annual potential evapotranspiration (mm/yr), is used to define the first-level divisions. Since the PE represents the amount of energy available in terms of the amount of water that could be evaporated, it also serves as an index of thermal efficiency, that is, the effect of temperature in determining the rate of plant growth, upon which the second-level divisions are based. Fig. 6 gives a graphical representation of the first-level moisture regions and the second-level thermal efficiency divisions.

Table 3. Thornthwaite's 1955 climate classification scheme (after Mather 1966, 1974)[1].

1st Level - Moisture Regions

A - perhumid	Im $\geq$ 100	
B - humid	20 $\leq$ Im < 100	
C - moist subhumid	0 $\leq$ Im < 20	
D - dry subhumid	-33.3 $\leq$ Im < 0	
E - semi-arid	-66.7 $\leq$ Im < -33.3	
F - arid	-100.0 $\leq$ Im < -66.7	

2nd Level - Thermal Efficiency

A - megathermal	PE $\geq$ 1140	mm/yr
B - mesothermal	570 $\leq$ PE < 1140	
C - microthermal	285 $\leq$ PE < 570	
D - tundra	142 $\leq$ PE < 285	
E - frost	PE < 142	

3rd Level - Relative Dry Season

Moist (Im $\geq$ 0) climates:
- r - little or no water deficiency (Ia < 10 or Ps = Pw)
- s - exceptional (Ia $\geq$ 10) summer water deficiency (Ps < Pw)
- w - exceptional (Ia $\geq$ 10) winter water deficiency (Pw < Ps)

Dry (Im < 0) climates:
- d - little or no water surplus (Ih < 16.7 or Ps = Pw)
- s - exceptional (Ih $\geq$ 16.7) winter water surplus (Pw > Ps)
- w - exceptional (Ih $\geq$ 16.7) summer water surplus (Ps > Pw)

4th Level - Summer Concentration of Thermal Efficiency

a - smallest concentration	PESC $\leq$ 48%
b - smaller concentration	48.0% < PESC $\leq$ 68.0%
c - larger concentration	68.0% < PESC $\leq$ 76.3%
d - largest concentration	PESC > 76.3%

---

[1]The colors shown apply to all Thornthwaite figures within this paper. See Eqs. 4, 7, 8, 10, and 14 for definitions of PE, Im, Ih, Ia, and PESC, respectively.

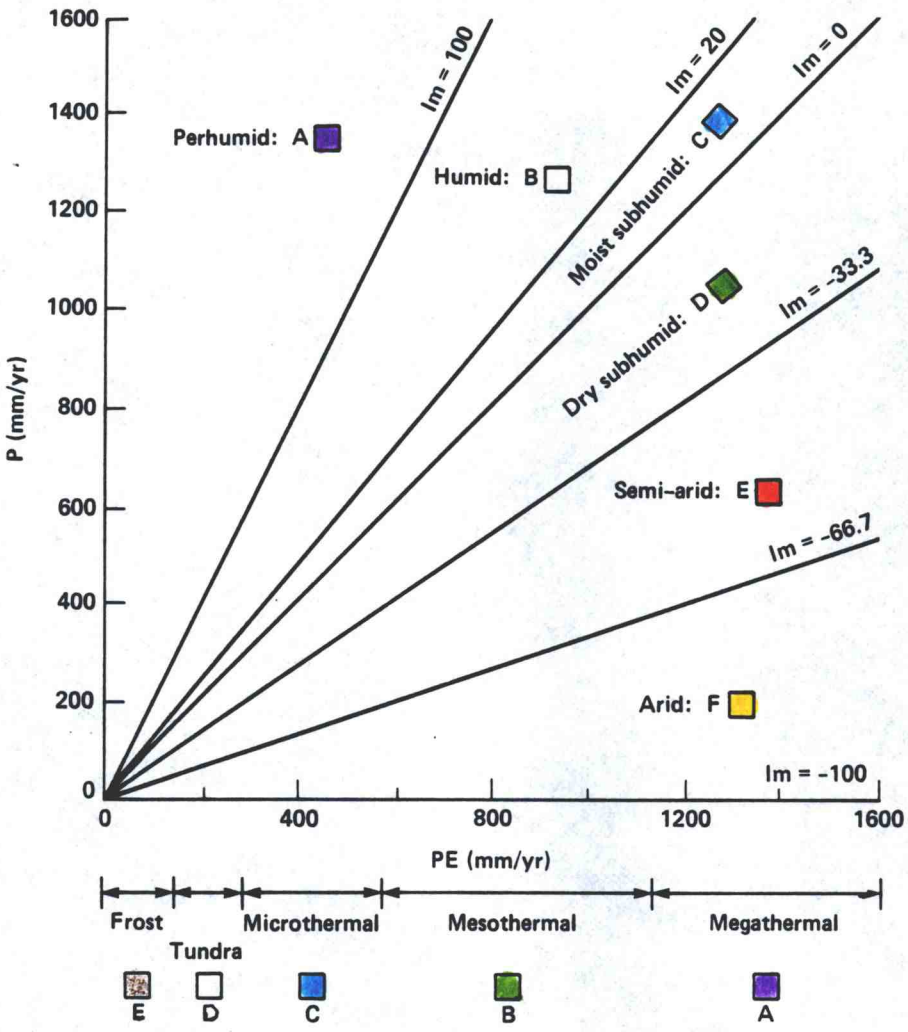

Fig. 6. Thornthwaite's first-level subdivisions of moisture regions (shown in terms of P and PE) and second-level subdivisions of thermal efficiency (shown in terms of PE). (Colors used in all figures relating to Thornthwaite correspond to those used in Table 3.)

The third-level divisions indicate the seasonality of precipitation. The seasonality of precipitation is determined by a combination of the moisture index, a humidity index, an aridity index, and the number of moist (Im > 0) months for the summer (Ps) and for the winter (Pw) half-years, where summer and winter are defined as April through September and October through March for the Northern

Hemisphere, and vice versa for the Southern Hemisphere.

The annual humidity index

$$Ih = 100*(S/PE) \quad , \tag{8}$$

where

$$S = P - AE \qquad (mm/yr) \tag{9}$$

is the annual moisture surplus and AE the actual evaporation, is used to determine if there is a season of exceptional precipitation for a dry climate (more precipitation than evaporation is exceptional in a dry climate). Also, the annual aridity index

$$Ia = 100 * (D/PE) \quad , \tag{10}$$

where

$$D = PE - AE \qquad (mm/yr) \tag{11}$$

is the annual moisture deficit, which is used to determine if there is a season of exceptional precipitation for a moist climate (less precipitation than evaporation is exceptional in a moist climate). The precipitation and PE are used to determine AE from a moisture budget for the year.

If a region has an exceptional season (determined by Im, Ih, and Ia, as defined in Table 3), the seasonality of precipitation is also dependent upon Ps and Pw, otherwise it is independent of Ps and Pw. Inserting (7) and (9) into (8), and (11) into (10), we can get expressions for the humidity and aridity indices in terms of Im and AE/PE,

$$Ih = Im + 100 * (1 - AE/PE) \tag{12}$$

$$Ia = 100 * (1 - AE/PE) , \tag{13}$$

and then represent the seasonality of precipitation as shown in Fig. 7.

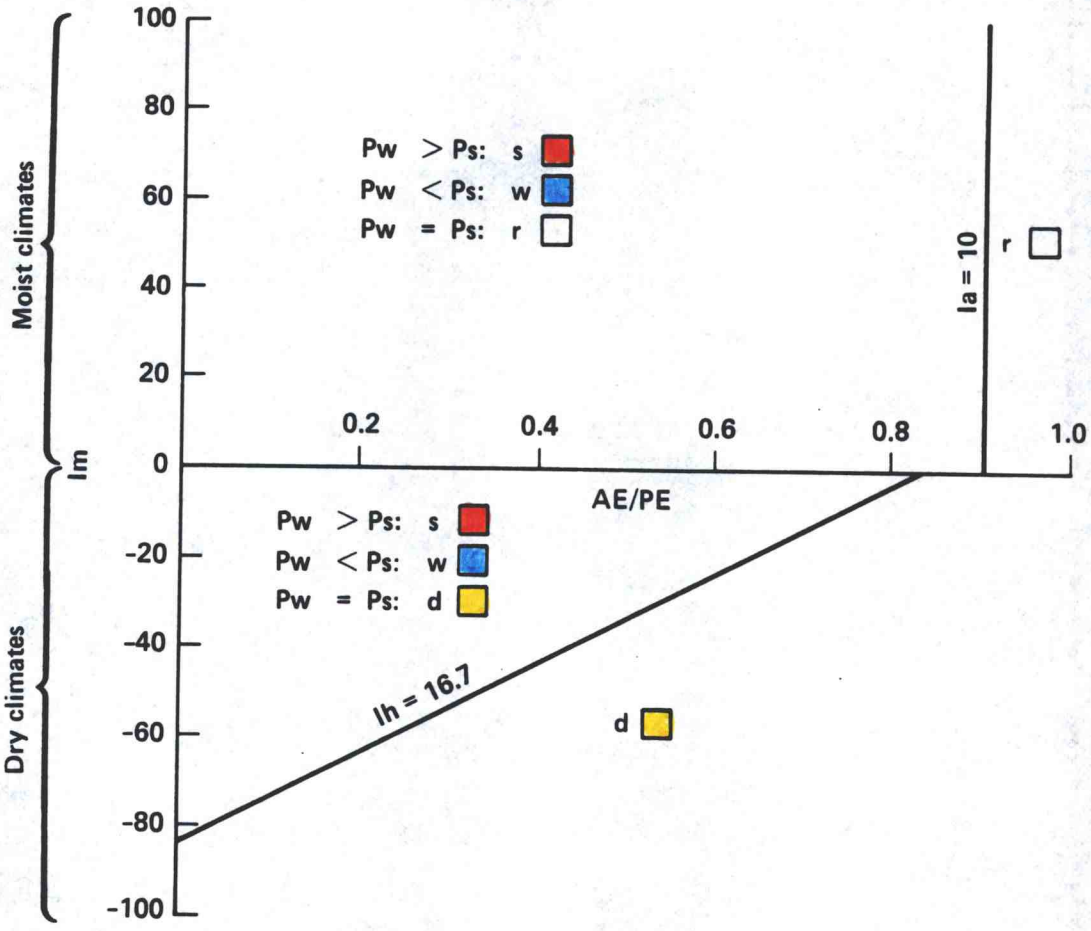

Fig. 7. Thornthwaite's third-level subdivisions of precipitation seasonality.

The fourth-level divisions represent the summer concentration of thermal efficiency PESC, defined as

$$\text{PESC} = 100 * (\text{PE for 3 summer months})/(\text{annual PE}) , \qquad (14)$$

where the three summer months are June, July, and August for the Northern Hemisphere, and December, January, and February for the Southern Hemisphere. These subdivisions are illustrated in Fig. 8.

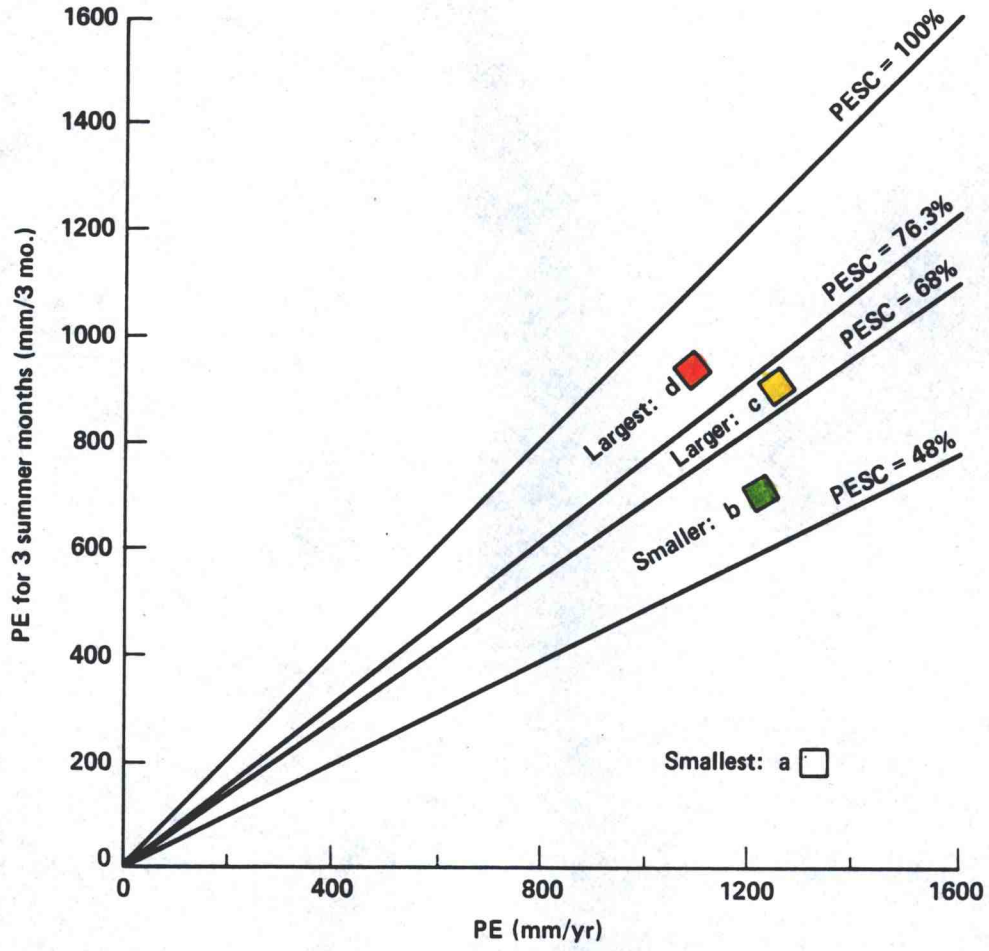

Fig. 8. Thornthwaite's fourth-level subdivisions of summer concentration of PE.

The maximum PESC is located near the poles and the minimum near the equator, since almost all of the solar radiation at the poles is concentrated in the three summer months, while only a quarter of the solar radiation is received at the equator during the three summer months. Continental regions will tend to have a higher PESC than oceanic regions because the surface air temperature over the ocean lags that over land due to the land's smaller heat capacity, hence the numerator of (14) is greater for land than for oceans (Mather, 1974; Thornthwaite and Mather, 1955; Mather, 1966).

b. Example

As an example of the use of Thornthwaite's scheme, suppose we are given the same monthly observations of temperature and precipitation at 40°N latitude as were used in the Koppen example. Table 4 contains these data in metric units, as well as the other variables used in applying Thornthwaite's scheme. The following discussion explains the steps involved in obtaining a Thornthwaite climate classification for a region.

The annual heat index given by (2) is

$$I = 0 + 0 + 1.92 + 2.90 + 5.33 + 8.91 + 11.30 + 10.28 + 7.19 + 4.55 + 2.60 + 0$$
$$= 54.97$$

and the exponent "a" from (3) is

$$a = (6.75 \times 10^{-7}) * (54.97)^3 - (7.71 \times 10^{-5}) * (54.97)^2 + 0.01792 * 54.97 + 0.49239$$
$$= 1.3567 .$$

The unadjusted PE from (1) is then

$$UPE(m) = 16 \left(10 * H[T(m)] * \frac{T(m)}{54.97} \right)^{1.3567} .$$

Table 4. Sample data for Thornthwaite's scheme. Asterisks denote that the quantity is undefined for that month.

Month	Jan	Feb	Mar	Apr	May	Jun	Jul	Aug	Sep	Oct	Nov	Dec
T,(°C)	-1.1	0	7.7	10.1	15.1	21.2	24.8	23.3	18.4	13.6	9.4	-1.3
P,(mm)	144	87	78	90	91	165	103	112	196	85	159	65
rainfall	0	87	78	90	91	165	103	112	196	85	159	0
snowfall	144	0	0	0	0	0	0	0	0	0	0	65
UPE, (mm)	0	0	25	37	63	100	124	114	82	55	33	0
HSUN,(hr)	300	297	368	397	446	449	455	424	371	342	297	290
PE,(mm)	0	0	26	40	78	124	155	133	85	52	27	0
AE,(mm)	0	0	26	40	78	124	155	130	85	52	27	0
S,(mm)	0	161	188	50	13	41	0	0	41	33	132	0
D,(mm)	0	0	0	0	0	0	0	3	0	0	0	0
soil moisture,(mm)	150	150	150	150	150	150	98	80	150	150	150	150
snowfall storage, (mm)	209	135	0	0	0	0	0	0	0	0	0	65
snowmelt, (mm)	0	74	135	0	0	0	0	0	0	0	0	0
Im	*	*	200	125	17	32	-34	-16	131	63	489	*
seasons for Ps and Pw	—NH winter—><				——NH summer———					><	——NH winter	
	—SH summer—><				——SH winter———					><	——SH summer	
seasons for PESC	SH summer—>				<——NH summer——>							<——

The hours of insolation per month are given by (5) as

$$\text{HSUN}(m,40^\circ) = \sum_{i=1}^{m} 2\left[\cos^{-1}\left(\frac{\cos 90.83^\circ}{\cos 40^\circ \cos \delta_i} - \tan 40^\circ \tan \delta_i\right)\right]\frac{12 \text{ hr}}{\pi \text{rad}}$$

The values of UPE(m) and HSUN(m,40°) are given in Table 4 along with the PE(m) calculated from (4). Since the moisture budget calculation is iterative (see section 3.2), only the equilibrium values of the surplus (S), deficit (D), soil moisture, snowfall storage, and snowmelt for our example are shown in Table 4. Basically, we start with a field capacity of 150 mm. During the winter the snowfall accumulates on top of the ground (denoted as "snowfall storage" in Table 4). As the temperature rises above freezing, the snow melts (denoted as "snowmelt" in Table 4), but since the ground moisture is already at field capacity, the snowmelt and any additional rainfall run off as surplus (denoted as "S" in Table 4). As the temperature continues to rise into summer, the PE also increases. When the PE exceeds the rainfall, the ground starts to dry out, decreasing the soil moisture. As the ground drys out, it becomes more resistive to moisture removal, so that if the PE exceeds the maximum moisture that can actually be evaporated (the AE), a deficit (denoted as "D" in Table 4) will occur.

The annual moisture index from (7) is then

$$Im = 100 * (1375/720 - 1) = 91$$

which indicates a first-level humid (B) climate, since $20 \leq Im < 100$

(Table 3 and Fig. 6). The annual PE is 720 mm, which satisfies the criterion for a second-level mesothermal (B) climate, since 570 ≤ PE < 1140.

To determine the third-level classification, we first note that this region has a moist (Im > 0) climate, so we need to determine if this region has an exceptionally dry season by calculating the aridity index from (10):

$$Ia = 100 * 3/720 = 0.4 .$$

Since Ia < 10, this region has little or no water deficiency, i.e., an r climate. From (14), the PESC is

$$PESC = 100 * (124 + 155 + 133)/720 = 57\% ,$$

which satisfies the criterion for a fourth-level b climate, since 48% < PESC ≤ 68%. Therefore the complete Thornthwaite classification is BBrb for this example.

c. Observed Climatology

A set of climate maps for the present-day climatology for the United States from Thornthwaite (1948, hereafter referred to as T48) is shown in Fig. 9. The second and fourth levels of Thornthwaite's scheme show the general zonal characteristics of climate based on temperature. More regional detail is provided by the first and third levels, which combine temperature and precipitation in a consistent manner.

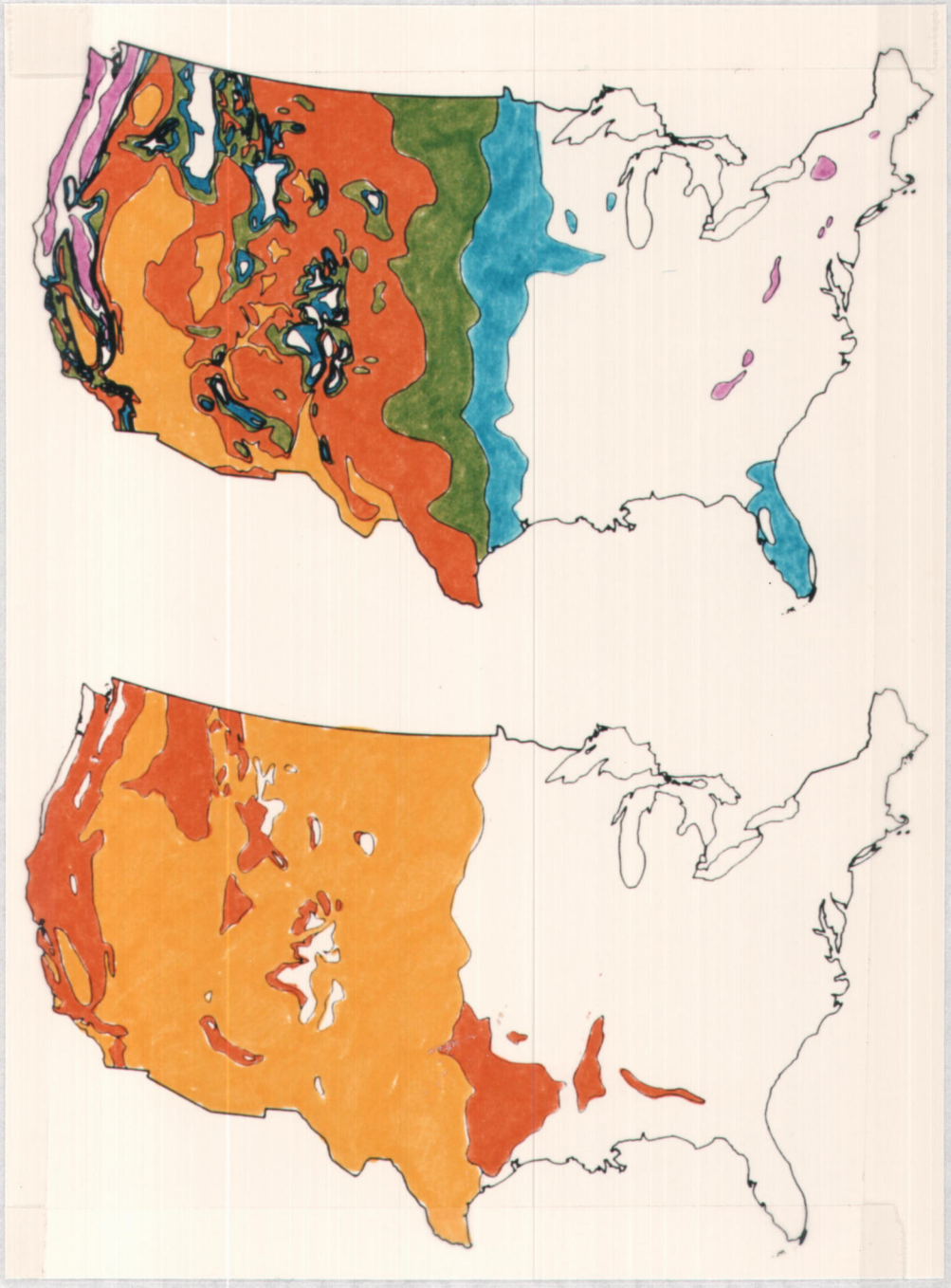

Fig. 9a. Thornthwaite climate maps for T48: first-level sub-divisions (top) of moisture regions ([]A, []B, []C, []D, []E, []F) and third-level subdivisions (bottom) of relative dry season ([]r, []d, []s, []w).

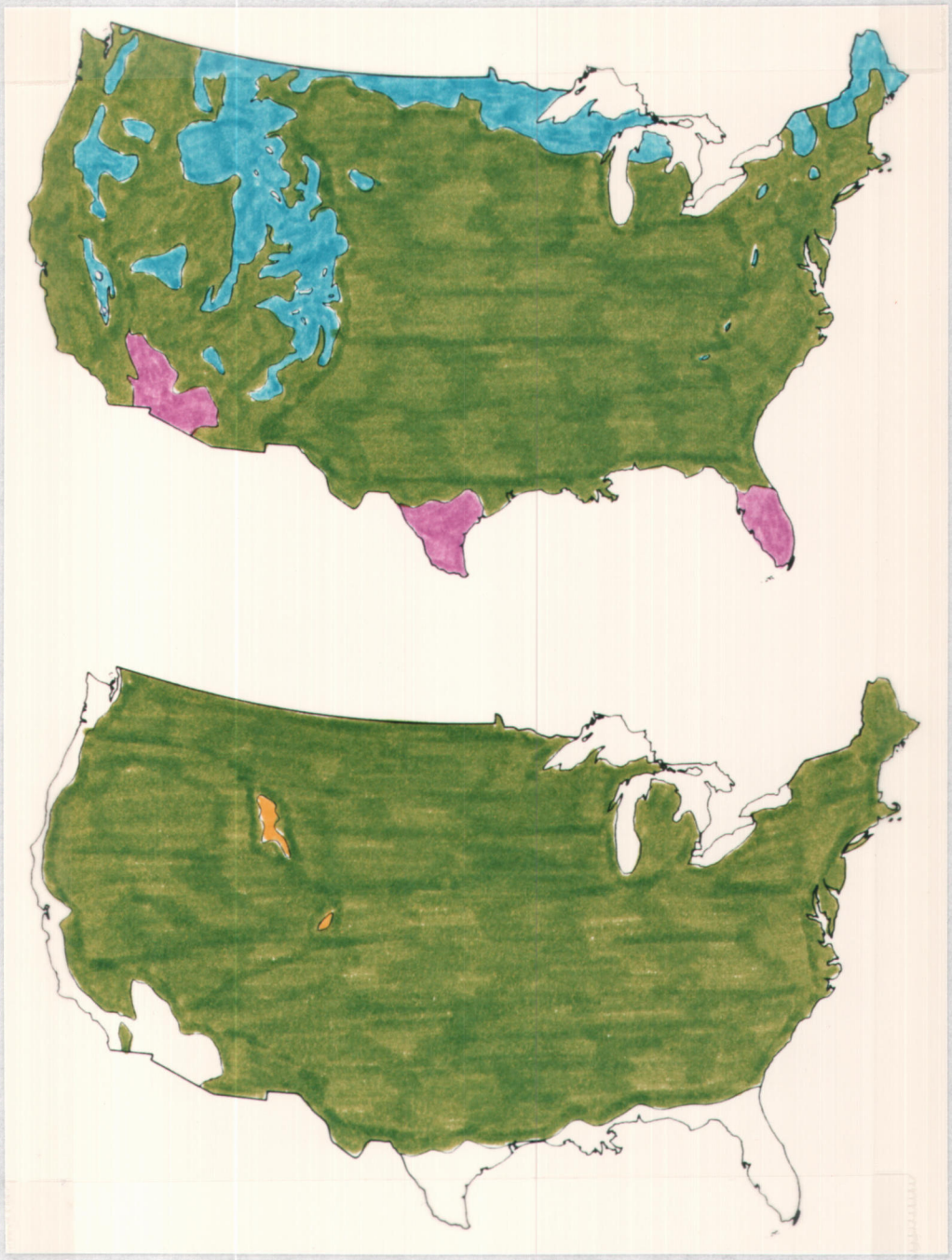

Fig. 9b. Thornthwaite climate maps for T48: second-level sub-divisions (top) of thermal efficiency (A, B, C, D, E) and fourth-level subdivisions (bottom) of summer concentration of thermal efficiency (a, b, c, d).

The eastern half of the United States has primarily a humid, evenly-moist (Br) climate, while the western half has primarily a semi-arid, evenly-dry (Dd) climate. Most of the United States has a mesothermal (B) climate except for some microthermal (C) in the mountains and along the northern border, and some megathermal (A) in southern Florida, Texas, California, and Arizona. The summer concentration of PE or thermal efficiency is in the range 48% to 68% (b) for most of the United States except for some areas along the Pacific coast and the Gulf coast that have less than 48% (a). The present-day climatology based on Thornthwaite's scheme will be discussed in more detail in section 4.2.1.

2.3 Climate Classifications of Previous GCM Simulations

While climate classification schemes were developed to describe the observed distribution of climate using the available observations of such meteorological variables as temperature and precipitation, they can also be used to classify the distribution of climate simulated by GCMs. Such an application could potentially be useful in the verification of the ability of a GCM to simulate the observed climate, and to describe the effects of perturbations such as a doubling of the atmospheric CO_2 concentration on the climate. However, very few GCM simulations have been analyzed in terms of a climate classification scheme, perhaps because the utility of such classification schemes over and above the "raw" data has not been clearly demonstrated.

2.3.1 Rand Two-Level Model

Bregman (1978) used a truncated version of Köppen's scheme based only on January and July data for the Rand AGCM (Gates et al., 1971; Gates and Schlesinger, 1977; Schlesinger and Gates, 1980). The first level of Köppen's scheme was used with the following assumptions: (1) January is the coldest month of the year and July the warmest month for the Northern Hemisphere, and vice versa for the Southern Hemisphere, (2) the drier month of the two months is the driest month of the year, and (3) the wetter month of the two months is the wettest month of the year.

The model did fairly well overall in simulating the general features of the climate. However, the adaptation of any climate classification scheme based on monthly-mean data, such as Köppen's scheme, to annual-mean or only two months of data can lead to faulty conclusions as to the ability of the model to simulate the climate, since the extremes of temperature and precipitation can occur in other months besides January and July.

2.3.2 GFDL 9- and 11- Level Models

Manabe and Holloway (1975, hereafter referred to as MH75) have produced a climate map based on Köppen's classification scheme for a

control simulation of a GFDL AGCM with 11 vertical levels, an approximately uniform horizontal grid cell size of 265 km, seasonally-varying insolation, and prescribed sea-surface temperatures. To verify the ability of the GFDL AGCM to simulate the present-day climate, MH75 compared the climate map based on the first year of the control model simulation (Fig. 10) to the T68 climate map (Fig. 5).

The polar temperatures of MH75's model are cooler than T68, extending the ET climate southward into Scandinavia, and establishing a perpetual frost EF climate along the northern coast of the USSR; EF climates should only exist over the permanent ice caps of Antarctica and Greenland. The cold DF climate of the rest of Canada is simulated well by the model. The three spots of Dw climate in Canada and the section in the north-central United States in the simulation may be due to interannual variability. The model does not simulate the BS climate of the Rocky Mountains and the southwestern United States, and incorrectly simulates BS and BW climates in the central United States.

The desert (BW) region simulated in southern Argentina isn't as large, dry, or far north as is observed, and the southern border of Brazil is simulated to be a BW climate rather than the observed tropical climate. MH75 suggest that the excessively dry region in southern Brazil simulated by their model may be due to the penetration of the subtropical dry air in the Pacific Ocean through an unrealistically large gap in the Andes Mountains due to smoothing in the model's topography.

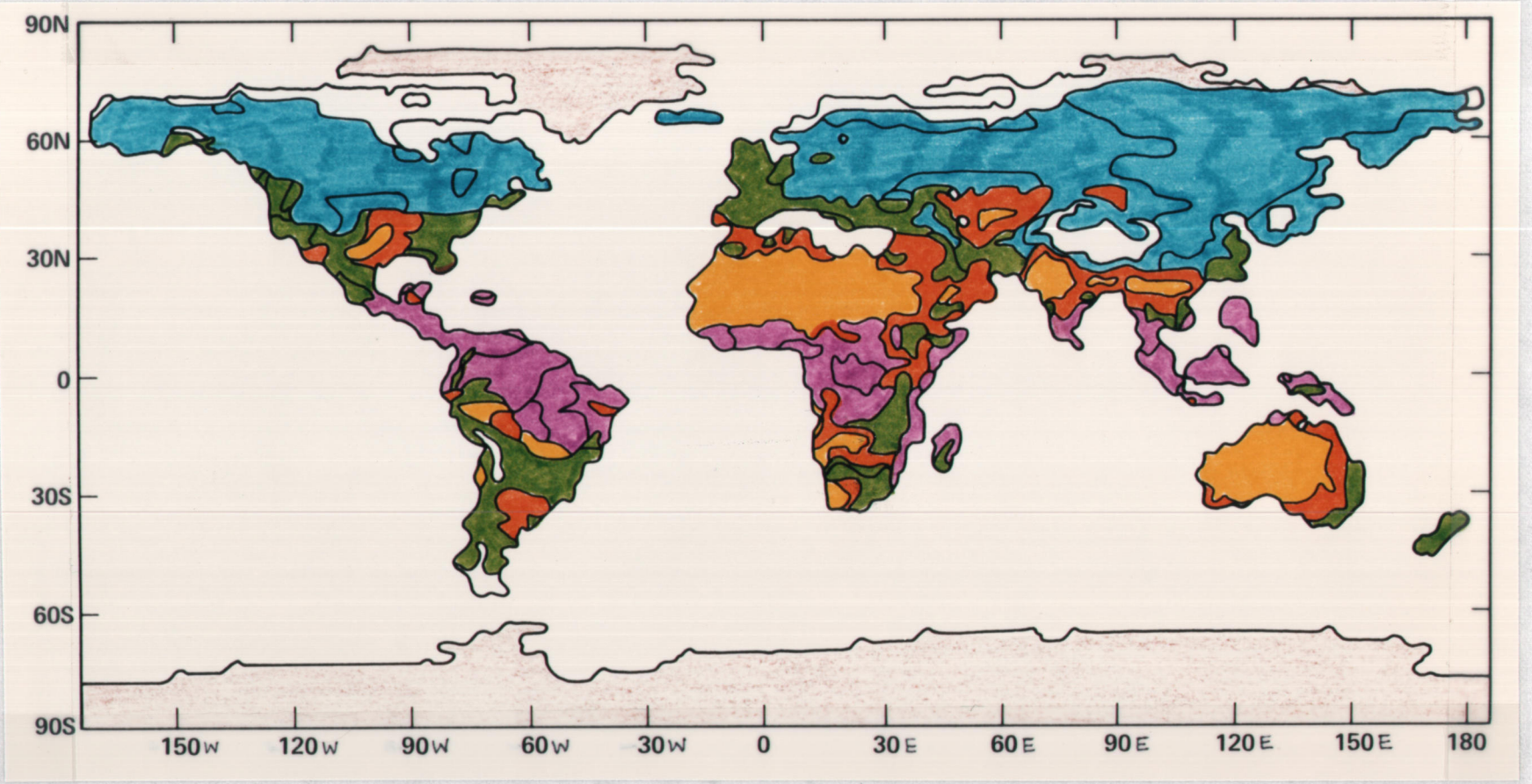

Fig. 10. Köppen climate map for MH75 (Manabe and Holloway, 1975) showing first-level (A, BW, BS, C, D, ET, EF) subdivisions over land only.

The temperate band in the Congo Basin is simulated by the model, but doesn't extend as far eastward as observed. The desert region simulated in southern Africa is cut in half by a band of Cf and Cw climate, unlike the observed, and the simulated Kalahari Desert extends all the way to the southern tip of Africa, replacing the observed C climate there. The MH75 model simulates the seasonal distribution of rainfall in tropical Africa well, reproducing the even-rainfall Af climate of T68 along the equator, with dry winters to the north and south. However, the model doesn't simulate the observed Cs climate along the Mediterranean coast of northeast Africa.

The cold Df climate simulated for northeastern Europe extends farther westward and southward than is observed, and as mentioned earlier, the northern Scandinavian coast is incorrectly simulated to be a tundra ET climate. The polar ET climate of Tibet and the dry BS-BW region east of the Caspian Sea are reproduced well by the model, but the simulated Gobi Desert is smaller than observed. The simulated cold dry-winter Dw climate of the USSR extends farther northward than the observed. MH75 explain that the extensive Dw area results from very cold dry winters produced there by the dry northerly winds around the strong Asian anticyclone during winter.

The simulated desert Bw climate of the Sahara doesn't extend to Saudi Arabia and western India as is observed. The model's simulation shows a mostly BS climate in Saudi Arabia, with some temperate Cs and Cf in the north, and Cf in Iran, Afghanistan, and West Pakistan. The simulated climate of India is drier than observed,

although some tropical Aw climate is reproduced in southern India. Due to underestimated summer rainfall in the simulation, the observed temperate climate in northern India is represented as a dry BS-BW climate by the model. The simulated desert region in central India extends eastward to the coast, and replaces the observed temperate and tropical climates in northern Southeast Asia and southeast China with a dry BW-BS climate. MH75 say that this is due to the lack of maritime air in southeastern China caused by the excessive development of tropical cyclones in the western Pacific.

The MH75 model simulates a temperate Cf climate along the coast of eastern China as observed, but the temperate climate observed in the rest of eastern China is simulated as cold Df and Dw climates. While the model incorrectly simulates all of Japan as a Df climate, it accurately reproduces the Af and Aw of Indonesia, the Am of the Philippines, and the Af and C climates of New Guinea.

The MH75 model simulates much of Australia to be drier than observed as shown by the large desert region. The observed temperate climate on the southwest coast is incorrectly simulated as a steppe BS climate, while the observed Cf climate along the southeastern coast is reproduced by the model. Except for a very small section, the observed tropical Aw climate along the northern coast is simulated as a dry BS-BW climate.

Manabe et al. (1979, hereafter referred to as MHH79) also produced a climate map using the last year of data from a three-year run of their spectral AGCM (note that all other models discussed in this paper are gridpoint models) with 9 vertical levels and an east-west

grid spacing of 5.625° (referred to as model M21 in MHH79). It has problems similar to those of MH75 discussed above in simulating the climate of T68. In addition, the dry regions of Argentina, the Sahara Desert, the Kalahari Desert, the Gobi Desert, and Australia are too small or nonexistent in the model simulation. However, overall, both MH75 and MHH79 do fairly well in simulating the gross features of the global climate over land.

2.3.3 GISS 9-Level Model

Hansen et al. (1984) produced maps of vegetation types using the Köppen (1936) scheme for five-year-mean data from a simulation of the present-day climate and a simulation of an ice age climate 18,000 years ago. Their model has nine vertical layers, a horizontal resolution of 8° latitude by 10° longitude, a prescribed variable ocean mixed layer depth, and prescribed ocean heat transport.

A map of vegetation types based on the observed data for the model grid resolution was not included in Hansen et al. (1984). However, it was stated that the model did a fair job of reproducing the present-day vegetation patterns. Differences included simulating too much forest on the east coast of Africa and not simulating enough boreal forest in central Asia.

The vegetation map for the ice age simulation has more ice and tundra in Canada, Europe, and Asia than the one for the control simulation. There was also less treed grassland in the United States, and more desert in Africa and Australia in the ice age simulation.

The magnitude of the simulated climatic changes shown by the vegetation maps is smaller than that suggested by the paleoclimatic evidence (Hansen et al., 1984). This may be due to deficiencies of the model and/or its prescribed boundary conditions or the inability of Köppen's scheme to detect climate changes.

2.4 Motivation for Present Study

In the past GCM validation and sensitivity studies have primarily focused on comparing contour plots of such fields as temperature and precipitation from the model simulation and the observed data. This study suggests the use of climate classification schemes as an additional tool in analyzing the performance of GCMs. Climate classification schemes such as Köppen's and Thornthwaite's use a combination of meteorological data to obtain a description of the climate in terms of which types of vegetation could be supported. This is not an attempt to imply that climate maps are superior to individual comparisons of temperature and precipitation, only that they provide an alternative perception of the data at a quick glance.

This paper will evaluate the performance of the OSU model by comparing climate maps from the mean of a ten-year simulation of the present-day climate with the climate maps from the observed data. Climate maps for the first three years of this ten-year simulation will also be compared with each other and with the ten-year mean to determine the magnitude of the interannual variability of the simulated climate types. A brief comparison of the performances of both

the OSU model and the GFDL model will also be given with the caveat that differing averaging times, observed data sets, and resolutions are used by the MH75 model.

The CO_2-induced climate changes simulated by the two OSU models (quadrupled CO_2 by the seasonal model and doubled CO_2 by the swamp model) will be evaluated in terms of vegetation changes by comparing the climate maps of the perturbed simulations with those of the control simulations.

The results from each of the two climate classification schemes, Köppen's and Thornthwaite's, used in this study will also be compared with each other to evaluate the relative sensitivity of the schemes.

3. STRATEGY AND METHODS OF ANALYSIS

3.1 Research Strategy

The purpose of this study is to investigate the utility of climate classification schemes in analyzing the performance of AGCMs in simulating both the present climate (model verification) and the climatic change induced by a perturbation such as an increase of atmospheric CO_2 (sensitivity study).

To accomplish the model verification part of this study, climate classification maps based on data from a 10-year control simulation of the OSU AGCM with seasonally-varying insolation and prescribed sea-surface temperatures will be compared to maps based on observed data. However, the climate classification maps of T68 (Fig. 5) and T48 (Fig. 9) cannot be used for this purpose because their resolution is different from that of the model (4° latitude by 5° longitude), and because T48 does not include the entire world. Therefore, present-day climate maps have been generated with the model's resolution using the observed data of Crutcher and Meserve (1970), Taljaard et al. (1969) and Jaeger (1976).

The climate maps based on each of the first three years of the control simulation will also be compared with each other and with the 10-year simulation to estimate the uncertainty of climate classifications resulting from the limited sample size and the interannual variability of the simulation.

For the sensitivity study the climate resulting from a quadrupling of atmospheric CO_2 in the OSU AGCM with seasonally-varying insolation and prescribed sea-surface temperatures will be compared to the 10-year simulation using both climate classification schemes. The conclusions drawn concerning the interannual variability of the model will be especially valuable for this sensitivity study, since only one year of data from the quadrupling experiment was available.

The climate resulting from a doubling of atmospheric CO_2 in the OSU AGCM with annual-averaged insolation and a swamp ocean will also be compared to a control simulation of the swamp model using only the first and second level subdivisions of Thornthwaite's scheme, since only annual-mean data are available from the swamp model. (The first and second level subdivisions of Thornthwaite's scheme do not require monthly means as do Köppen's and the other two levels of Thornthwaite's scheme.)

A list of data sets and sources used in this study is given in Table 5, and the climate map comparisons made for each scheme are given in Table 6. The climate maps in this paper show the distribution of climate types over both the land and ocean, although the classification schemes were designed for use over land only. The climate types over oceans are shown in this paper for completeness and to provide clues as to the movement of climatic regions, but will not be discussed in this paper.

Table 5. List of data sets and published climate maps used.

Abbreviation	Source
OBS	Observed monthly-mean temperature data (Crutcher and Meserve, 1970; Taljaard et al., 1969) and precipitation data (Jaeger, 1976).
YR1	Monthly-mean temperature and precipitation data from the first year of the 10-year control simulation of the OSU AGCM with seasonally-varying insolation and prescribed sea-surface temperatures.
YR2	Same as YR1 except for second year of the simulation.
YR3	Same as YR1 except for third year of the simulation.
A10	Same as YR1 except for the mean of the 10-year simulation.
QAD	Monthly-mean temperature and precipitation data from the first year of the quadrupled CO_2 simulation of the OSU AGCM with seasonally-varying insolation and prescribed sea-surface temperatures (Gates et al., 1981).
SWP	Annual-mean precipitation and PE data from the last 180 days of the control simulation of the OSU AGCM with annual-averaged insolation and a swamp ocean (Schlesinger, 1984).
SCO2	Same as SWP except for the perturbed (doubled-CO_2) simulation of the model (Schlesinger, 1984).

Table 6. Comparisons made for each classification scheme.

Reason for comparison	Köppen climate map comparisons	Thornthwaite climate map comparisons
Description of general climate; effect of resolution and data source	OBS T68	OBS T48
Performance of control simulation of OSU AGCM	A10 OBS	A10 OBS
Interannual variability of OSU AGCM	YR1 YR2 YR3 A10	YR1 YR2 YR3 A10
Climate type change due to quadrupled CO_2 in seasonal OSU AGCM	QAD A10	QAD A10
Climate type change due to doubled CO_2 in annual OSU AGCM	--- ---	SCO2 SWP

3.2 Analysis Methods

The only input data needed for both Köppen's and Thornthwaite's schemes are the monthly mean temperatures and precipitation for a year. For Köppen's scheme these data are used directly in the equations of Table 1. For Thornthwaite's scheme the temperatures are used to compute the PE from Eqs. (1)-(6), and then the precipitation and PE are used to determine AE from a moisture budget for the year. The moisture budget method used in this study is that described by Willmott (1977). Willmott's method is a more complete and documented version of Thornthwaite's (1948) moisture budget method. A flowchart outlining the basic steps used to construct the moisture budget is given in Appendix A. The values of Im, Ih, Ia, and PESC are then calculated from Eqs. (7)-(11), and (14), and are used in Table 3.

Thornthwaite's method of calculating PE is based on mid-latitude climatic regions. Therefore the validity of extending his PE calculations to the very warm tropics and the very cold polar regions is questionable. Bailey and Johnson (1972) suggest that the annual heat index (I) may be used as an indicator of the regions where Thornthwaite's PE calculations are reasonable. While Thornthwaite's (1948) nomogram shows heat indices only between 20 and 120, Bailey and Johnson (1972) expand this range slightly to between 16 and 146. This generally excludes regions poleward of 60°N and 50°S, and the very warm regions of northeast Brazil, northwest Africa, India, southeastern Asia, Indonesia, and the northern coast of Australia.

Lacking a better method, this paper treats these extreme regions no differently from the mid-latitude regions. However, one should be aware that a method for calculating PE based solely on mid-latitude regions does not necessarily hold for polar and equatorial regions.

The same method of analysis was used for all data sets, except those from the swamp model. Although the OSU AGCM constructs its own moisture budget, Willmott's method was used for all GCM (except the swamp model) and observed data sets, so that differences between the climate types of the data sets would not be due to the use of different moisture budget routines. For this same reason, the model-simulated PE was not used, since observed PE was not available. For cases where the annual PE is zero, both the moisture index (Im) and the PESC are set equal to zero, since they would otherwise be undefined according to (7) and (14), respectively. These cases will be noted in the discussion of the results.

The climates of the swamp model data sets were not defined in terms of Köppen's scheme because of the lack of monthly-mean values of temperature and precipitation. However, no adaptations need to be made for Thornthwaite's scheme if the model-simulated PE is available. Input data consist of the model-generated PE and annual precipitation, from which the moisture index, Im, is calculated. Therefore, no moisture budget calculations are required. Only the first two levels (see Table 3) of the Thornthwaite climate type were determined for the swamp model data sets.

Listings of the codes used to classify climates according to Köppen's and Thornthwaite's schemes for the OSU AGCM with seasonally-varying insolation are presented in Appendices B and C, respectively. The code used for classifying the climate according to Thornthwaite's scheme for the swamp model is a truncated version of the code in Appendix C, since monthly-mean values are not computed.

4. RESULTS

4.1 Köppen Climate

4.1.1 Description of Observed Climatology (OBS)

In this section we present the present-day climatology described in terms of Köppen's scheme. Specific features of the new observed climatology (OBS) using the model grid resolution (4° latitude by 5° longitude) will be discussed, noting any differences from the classical climatology of T68 (Fig. 5). Differences not accounted for by model grid resolution are assumed to be due to differing sources of input data, however this cannot be verified since the data used to construct the climate map of T68 are not available.

The climate maps for OBS are shown in Fig. 11. If not otherwise stated in the figure captions, a blank region on a climate map indicates that there is no climate type defined for that level, e.g., there are no second-level subdivisions for polar ET and EF climates.

Canada has a mostly cold Df climate with a tundra ET climate in the north. There is a temperate Cs climate along the coast of British Columbia and the United States Pacific Northwest. However OBS shows a dry BS climate only in the southwestern United States, while BS extends along the Rockies into Canada in T68. This difference is probably due to cooler temperatures and/or more precipitation in OBS,

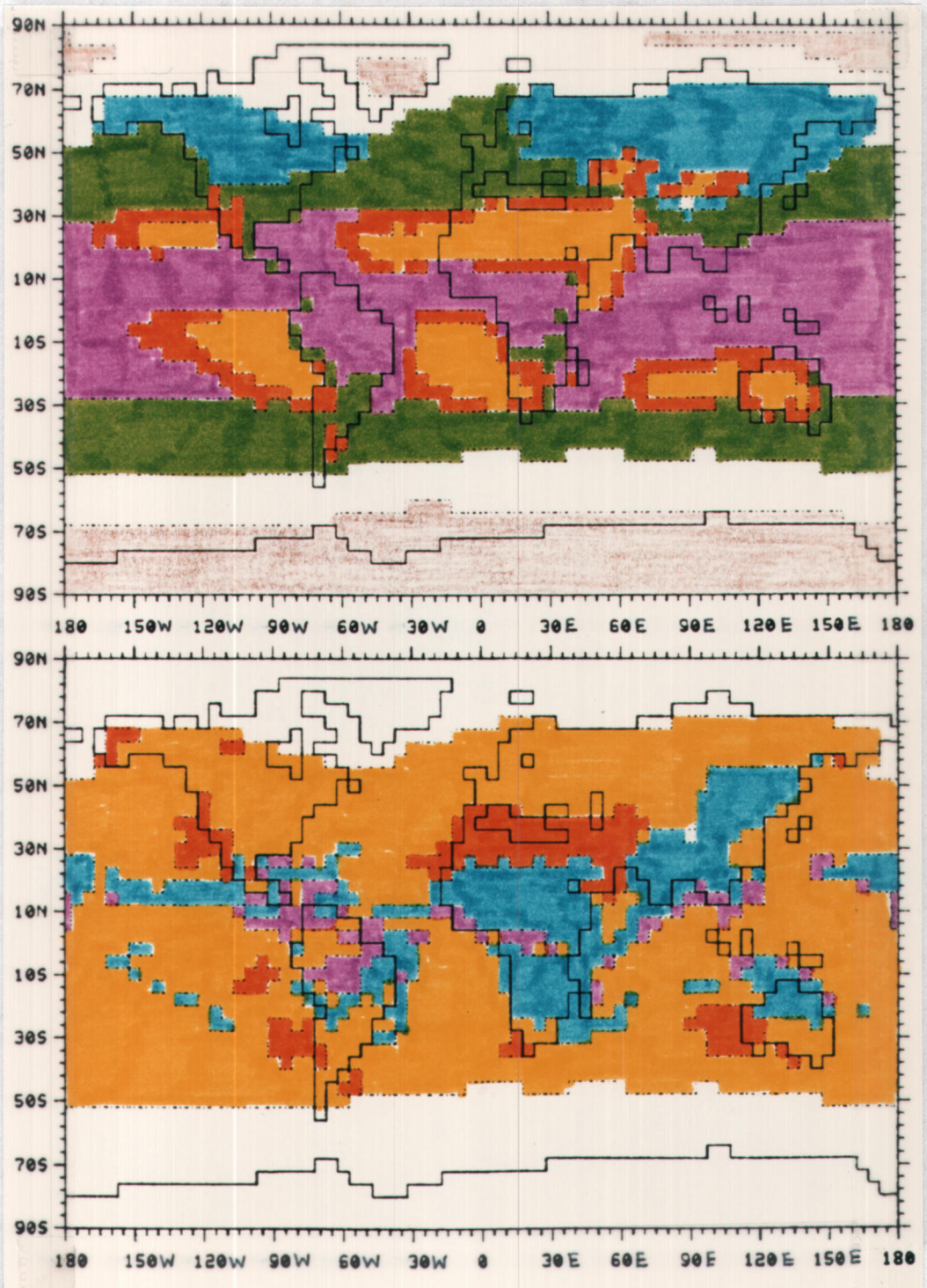

Fig. 11. Köppen climate maps for OBS: First-level subdivisions (top) of major groups (A, BW, BS, C, D, ET, EF) and second-level subdivisions (bottom) of relative dry season (f, s, w, m). Blank regions on the bottom map indicate no second-level subdivision for that region.

since the T68 feature is large enough not to be averaged out by the 4°x5° resolution. The eastern half of the United States has a cold Df climate in the north and a temperate Cf climate in the south.

The seasonal movement of precipitation in tropical Brazil is apparent, with monsoon Am and even-rainfall Af climates along the equator, and a dry-winter Aw climate to the north and south. However the monsoon climate of OBS is much larger and extends farther southward than that of T68. Ecuador has a tropical Aw climate, with temperate climates to the south and a section of dry BS climate near Peru and Bolivia. The region around Paraguay, Uruguay, and northern Argentina has a temperate Cf climate. Southern Argentina has a dry BS climate and the southern tip of South America has a cold ET climate. The Chilean coast has mostly a Cf climate with some Cs climate. The grid resolution of OBS is too coarse to show any detail along the western coast, e.g., the tundra ET climate of the Andes shown by T68 has been averaged out in OBS.

The Mediterranean coast of Africa has a temperate Cs climate along Morocco and Algeria, with dry BS and BW climates to the east. To the south is the desert BW climate of the Sahara, bordered on the north and south by a steppe BS climate. Farther south, the seasonal distribution of rainfall in the tropics is shown. In the region between Gambia and Nigeria there is a dry-winter climate with a monsoon climate along the coast. The Congo Basin region has mostly a dry-winter climate, with a section of monsoon and even-rainfall climates along the equator. There is a band of temperate Cw climate

in Angola and Zambia, with tropical Aw climate to the east in Mozambique and Madagascar. Farther south are the dry BS and BW climates of the Kalahari Desert, with a temperate Cf climate along the east coast and a Cs climate at the southern tip of Africa.

Along the Mediterranean coast in Spain, Italy, the Balkans, and Turkey, there is a temperate Cs climate, with a Cf climate along the rest of the coast. The rest of Europe has a Cf climate with a cold Df climate to the north in Sweden and Finland and along the U.S.S.R. border. Most of the U.S.S.R. has a cold Df climate with a patch of Dw climate in the southeast and tundra ET climate along the northern coast. The section of Dw climate in OBS doesn't extend quite as far north or as far west as that in T68.

The Gobi is shown as a desert BW climate bordered by BS to the east and west. The extent of the tundra ET climate in Tibet in OBS is smaller than that in T68, consisting of only one grid point bordered by a cold Dw climate. Iran, western Pakistan, Afghanistan, and the region east of the Caspian Sea are also shown as desert BW climates bordered by BS. India has a tropical Aw climate with a temperate Cw climate to the northeast and a dry BS climate to the northwest. Some of the detail in western India is lost due to the coarse grid resolution of OBS.

Eastern China has a temperate Cf climate with Cw to the west. The coast of Burma and Thailand has a tropical Am climate with Aw to the north, and Indonesia and New Guinea have tropical Af climates. T68 shows Japan with a cold Df climate in the north and a temperate Cf climate in the south, while OBS shows a Cf climate for all of Japan.

Central Australia has a desert BW climate surrounded by a steppe BS climate. The northern coast has a tropical Aw climate. In OBS the east coast has a temperate Cw climate to the north where T68 shows a Cs climate, and a Cf climate to the south. The southwest corner of the coast also has a temperate Cf climate, although if one doesn't take the continental outlines of the grid map too literally, it could also have a Cs climate such as T68 shows.

4.1.2 Comparison of Model Climatology (A10) to Observed Climatology (OBS)

Section 4.1.1 described the present-day climatology in terms of Köppen's scheme. The purpose of this section is to discuss how well the OSU AGCM simulates the observed climate. The Köppen climate maps for the mean of the first ten years of the control simulation of the OSU AGCM are shown in Fig. 12. The model does fairly well in simulating the major climate regions of the world with the following exceptions.

Temperatures in the polar regions are much higher in the model, especially in the winter hemisphere, causing the observed polar ET climate along the northern coast of the U.S.S.R. and most of the northern Canadian coast to be represented by the warmer Df climate in the model. The cold Df climate of the rest of Canada and the perpetual frost EF climate of Antarctica and central Greenland are represented well.

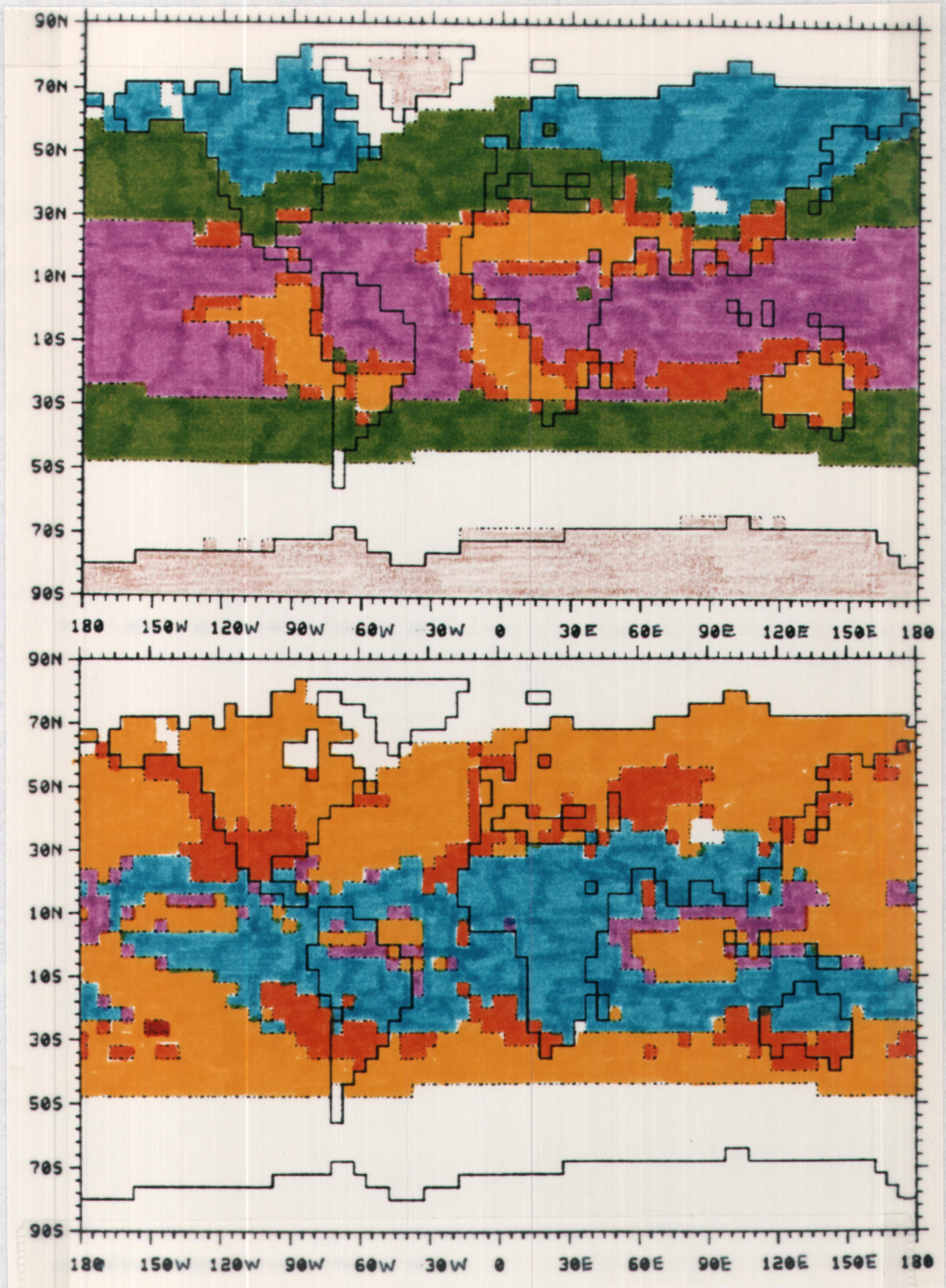

Fig. 12. Köppen climate maps for A10: first-level subdivisions (top) of major groups (A, BW, BS, C, D, ET, EF) and second-level subdivisions (bottom) of relative dry season (f, s, w, m). Blank regions on the bottom map indicate no second-level subdivision for that region.

The model fails to simulate the dry BS climate of the Rocky Mountains, and the observed dry BS climate in the southwestern United States is represented incorrectly as a temperate Cs climate due to cooler temperatures and more precipitation. The observed temperate Gulf Coast climate is simulated as a BS climate because of a large deficit of summer precipitation and generally warmer temperatures, especially in the summer. The observed dry summers characteristic of the western coast of the United States are extended across the country to the east coast by the model. Generally there is more rainfall west of the Rockies all year long, and less rainfall in the eastern half of the United States simulated by the model, especially in the summer in the south.

The combination of warmer temperatures and smaller rainfall simulated by the model for Peru yields a dry BS climate instead of the observed temperate climate. The equatorial monsoon (Am) and even-rainfall (Af) regions are simulated less extensively than observed, with drier winters (Aw) to the north and south. The southern border of Brazil is simulated as a dry BS climate rather than the observed tropical climate. Farther south, the simulated warmer than observed temperatures and smaller than observed rainfall, especially in the summer, represent the observed temperate region in northeast Argentina as a desert; the reverse occurs in southeastern Argentina because of the simulated larger than observed rainfall, especially during the summer. The simulated polar ET climate at the southern tip of South America extends farther northward in the model because the simulated temperatures are colder than observed,

especially in the summer.

The observed temperate band in the Congo Basin is not simulated by the model, and is instead represented as tropical Aw and dry BS climates. The simulated climate is cooler and drier there in summer than observed and much warmer in winter. In contrast to the observations, the BS and BW climates of southern Africa extend eastward in the simulation to cover tropical Madagascar, as a result of the smaller than observed rainfall simulated there, especially in summer. Along the equator in Africa the simulated climate is slightly wetter in summer and slightly drier in winter than observed, causing the observed monsoon and even-rainfall climates there to be represented as dry-winter climates.

Along the Mediterranean coast the simulated summer and winter precipitations are larger and smaller than observed, respectively, hence the observed dry-summer climate is simulated as a dry-winter climate. The northwestern coast of Europe is simulated to be slightly warmer in the summer and much colder in the winter than is observed, which causes the simulated cold Df climate to extend too far westward and replace the observed temperate Cf climate. The region east of the Caspian Sea is simulated with mostly a temperate Cs climate in contrast to the observed BS-BW climate as a result of the larger than observed rainfall simulated by the model especially during the winter. The model simulation agrees with the observation in the region of the Sahara east to India, but the dry BS-BW climate has also penetrated into India, replacing the observed tropical Aw climate there. India's summer monsoon region appears to be simulated

farther southwestward over the Arabian Sea than is observed.

Along the southern border in Manchuria, the simulated winter is wetter and the summer is drier than the observed. Thus the observed Dw climate of the eastern section is simulated as a Df climate, and the observed Df climate of the western section is simulated as a Ds climate. Except for a section of temperate C climate in the north, eastern China is simulated to have a steppe BS climate which is drier than the observed. The Gobi Desert is not simulated by the model because the rainfall is greater than that observed, especially during the summer. The simulated polar ET region of Tibet is a little farther north than observed.

In southeastern Asia the simulated summer is much drier than observed, so that instead of a monsoon Am climate simulated in the south, there is only a dry-winter Aw climate simulated by the model. The climate of the rest of southeastern Asia is simulated well by the model, including the temperate Cw climate to the north. Northern Japan is simulated as a Df climate, which is cooler than observed. All of Japan is simulated to have less rainfall than observed, but the southern half is simulated to have an especially dry summer, resulting in a Cs climate there instead of the observed Cf climate. The simulated winter in all of Indonesia and New Guinea is drier than observed; most of the observed even-rainfall climate there is simulated as a dry-winter Aw climate.

Australia is simulated to be almost all desert, with warmer temperatures than observed and decreased rainfall over most of the continent. The observed even-rainfall climate is simulated as a

dry-winter climate in central Australia and as a dry-summer climate in the south. The observed temperate climate on the southwest coast is simulated as a steppe BS climate, and the observed Cf climate along the southeastern coast is simulated as a Cs climate. The observed tropical Aw climate along the northern coast is simulated as a dry BS-BW climate.

4.1.3 Interannual Variability of the OSU AGCM (YR1, YR2, YR3, and A10)

The purpose of this section is to investigate the interannual variability of the model. Because of sampling errors it is preferable to use the average of several years of a model simulation. The average of the ten-year control simulation (A10) should provide a more accurate representation of the steady-state climate of the model than any single year of the simulation. This section will compare the climate maps for each of the first three years of the control simulation of the OSU AGCM (Fig. 13-15) with each other and with the climate maps for A10 (Fig. 12).

The first three years show basically the same climate (mostly Df and Ds) for Canada. A10 is different (and more like the observed) in the seasonality of precipitation, since it is entirely Df with no Ds. The steppe BS climate of A10 in the southwestern United States isn't present in YR1, YR2, or YR3 except for a grid point in northwest Mexico in YR3.

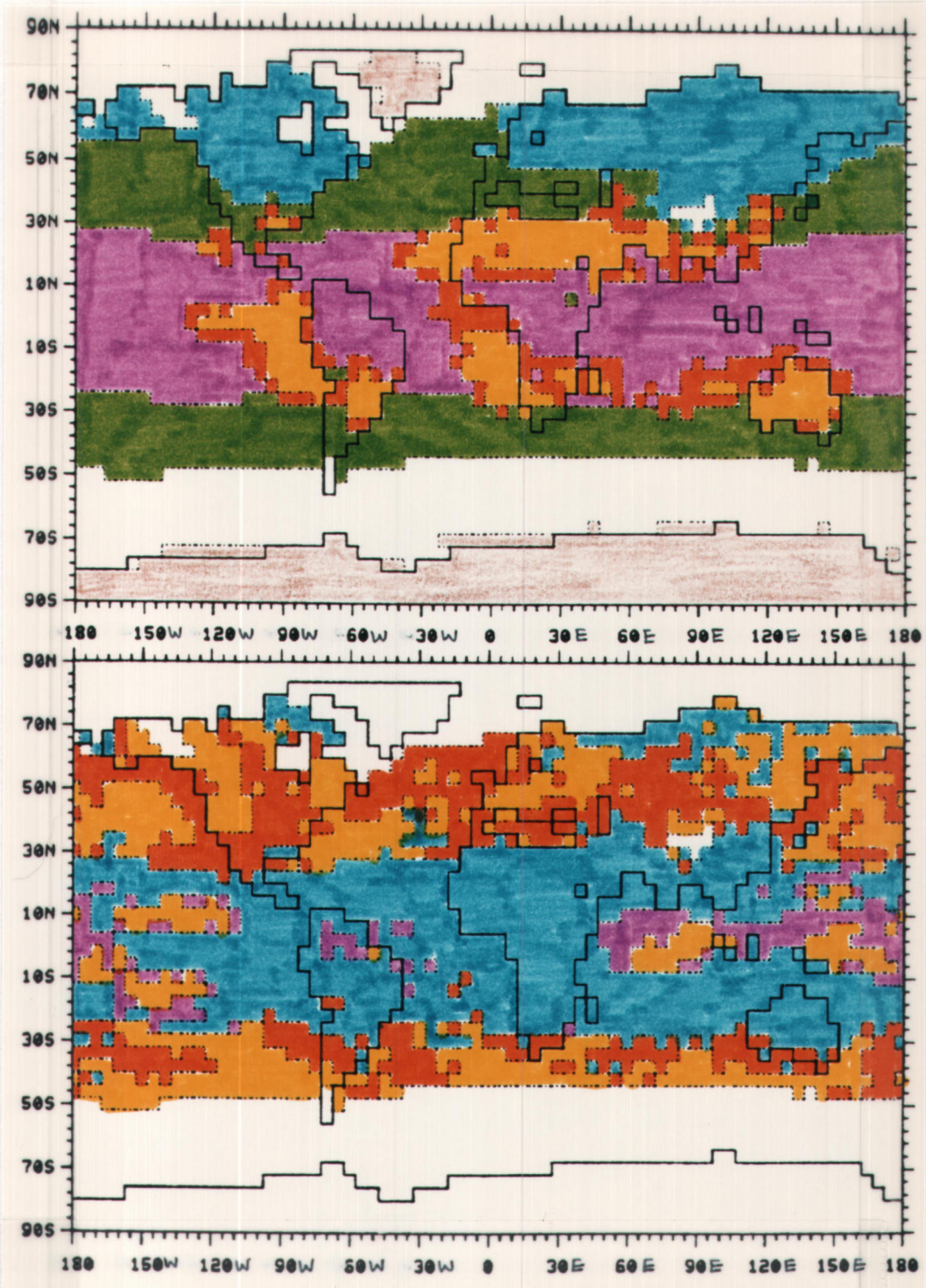

Fig. 13. Köppen climate maps for YR1: first-level subdivisions (top) of major groups (A, BW, BS, C, D, ET, EF) and second-level subdivisions (bottom) of relative dry season (f, s, w, m). Blank regions on the bottom map indicate no second-level subdivision for that region.

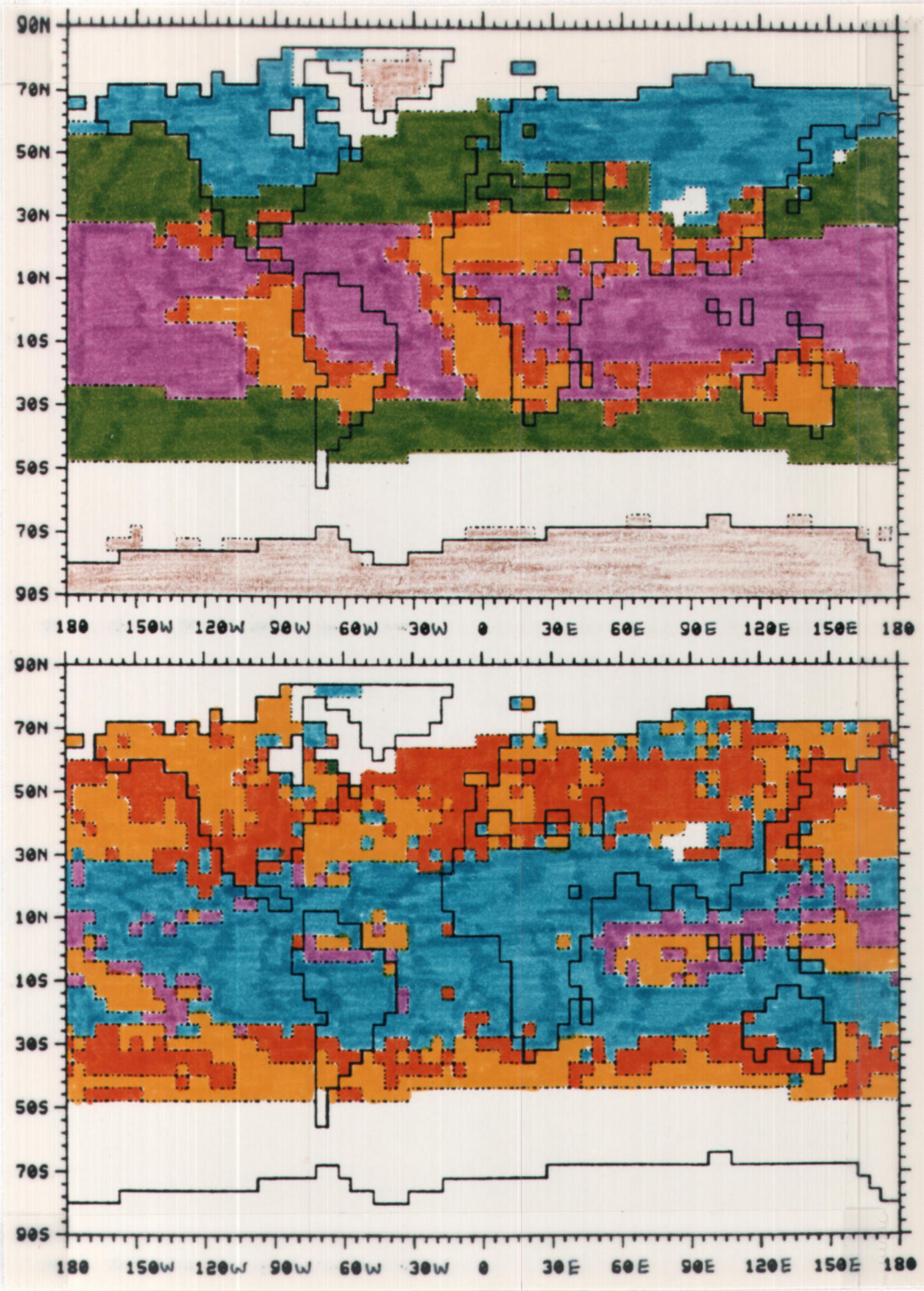

Fig. 14. Köppen climate maps for YR2: first-level subdivisions (top) of major groups ([]A, []BW, []BS, []C, []D, []ET, []EF) and second-level subdivisions (bottom) of relative dry season ([]f, []s, []w, []m). Blank regions on the bottom map indicate no second-level subdivision for that region.

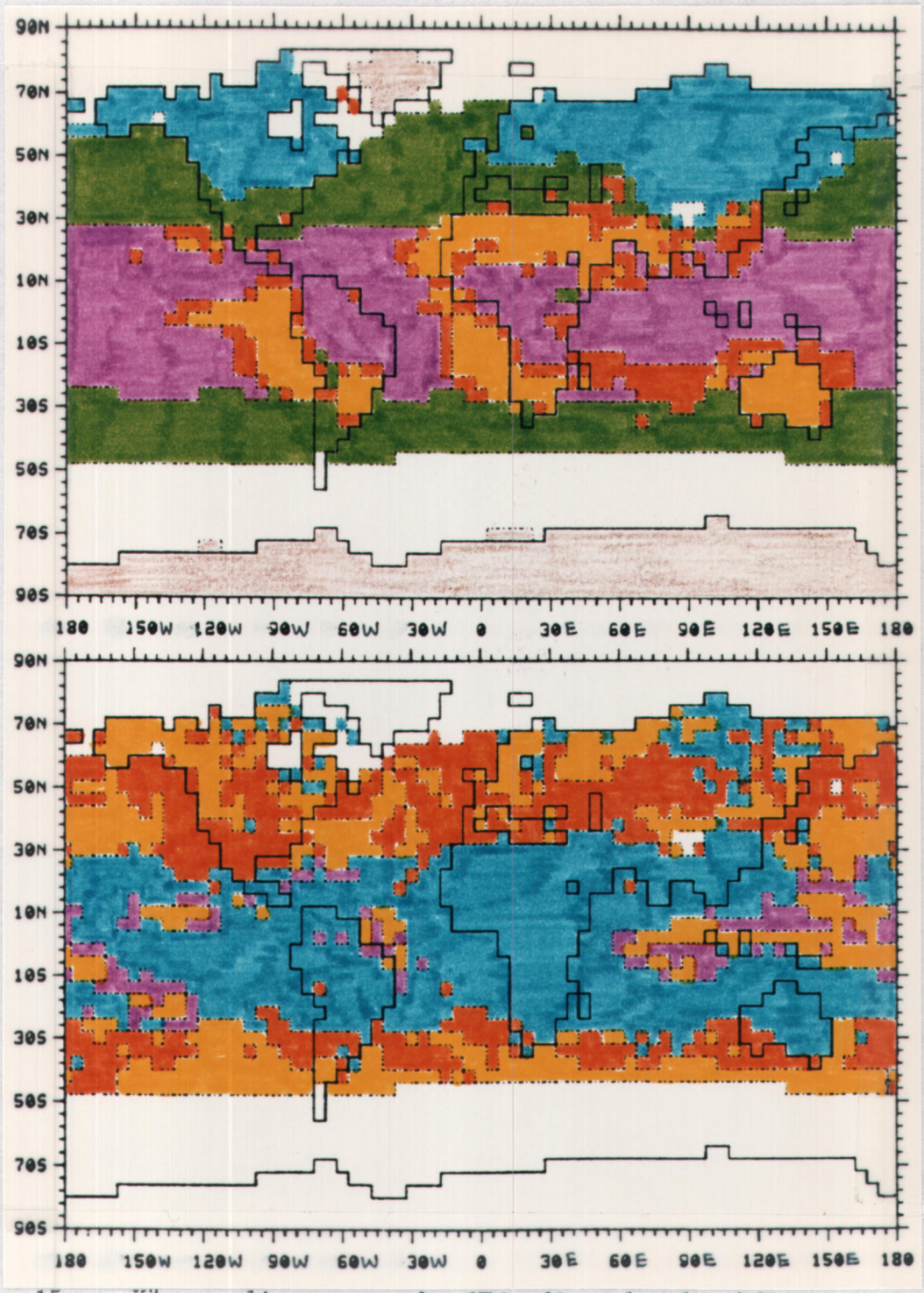

Fig. 15. Köppen climate maps for YR3: first-level subdivisions (top) of major groups (A, BW, BS, C, D, ET, EF) and second-level subdivisions (bottom) of relative dry season (f, s, w, m). Blank regions on the bottom map indicate no second-level subdivision for that region.

In the United States the boundary between the cold D climate and the temperate C climate simulated by the model in the Pacific Northwest is moved slightly southward in YR2, but is in the same location in YR3 and A10 as in YR1. In the east this boundary is far southward in YR1 and is progressively farther northward in YR2 and YR3 so that the location of the boundary in YR3 is the same as for A10. A dry BS patch along the Gulf Coast in YR1 and YR2 is almost absent in YR3, but is present again in A10. Overall, the most striking difference in the simulated North American climate is in the seasonality of precipitation, since it is a chaotic jumble in each of the first three years, but is much more organized into definable regions in A10.

The only real differences in the simulated climate of South America are in the seasonality of precipitation: the extent of the monsoon and even-rainfall regions along the equator and the dry-summer region of northern Argentina grow and shrink in size from year to year of the simulation. The distribution of simulated climate types in Africa is also basically the same in all four cases.

The boundary between the cold D climate of the north and the temperate C climate of the south of the model simulation is at about the same location in Europe in the first three years, but is farther north in A10. The simulated seasonal distribution of rainfall is a mixture of dry winters, dry summers, and even-rainfall in the first three years, while A10 has an even-rainfall climate with some dry-summer climate along the Mediterranean coast. The simulated seasonal distribution of rainfall in the U.S.S.R. and Manchuria in the first

three years is a checkerboard mixture of dry winters, dry summers, and even-rainfall, while A10 has an even-rainfall climate except for a region of dry-summer climate east of the Caspian Sea.

The region east of the Caspian Sea is simulated to have about the same proportion of temperate Cs and dry BS climates in all four cases, although the BS region moves around slightly. The extent of the tundra ET region in Tibet varies from four to seven grid points in the four cases.

Japan's simulated climate fluctuates between a cold D climate and a temperate C climate, and the seasonal distribution of rainfall also changes from year to year of the simulation. Eastern China is simulated to be a mixture of dry BS and BW climates and temperate C climates in the first three years, settling down to a mostly BS climate with a bit of temperate C climate in the north in A10. Southeastern Asia is simulated to be mostly a tropical Aw climate with some dry BS regions scattered about in various locations in the four cases.

The simulated climate of the islands of Indonesia is the same for all four cases except for the seasonal distribution of rainfall of one gridpoint. New Guinea's simulated climate remains constant in all four cases. The dry BS regions simulated along the coast of Australia tend to move around from year to year of the simulation. The extent of the simulated dry-summer climate in the south also varies from year to year of the simulation and is quite large in A10.

4.1.4 Model Sensitivity to Quadrupled CO_2 (QAD and A10)

The purpose of this section is to describe the changes in climate types due to a quadrupling of CO_2 in the OSU AGCM. This perturbation experiment was chosen because it was the only one for which at least one year of a seasonal simulation was complete. It should again be stressed that since this experiment was not run for several years, the interannual variability has not been averaged out, adding another cause (other than a definite climate change) for differences between QAD and A10.

The climate maps for the quadrupled-CO_2 simulation are shown in Fig. 16. A quadrupling of CO_2 results in essentially no change of climate type in the OSU AGCM with seasonally-varying insolation and prescribed sea-surface temperatures. If the climate maps for QAD were put alongside the maps for YR1, YR2, YR3, and A10, no distinction could be made between them. The climate is essentially the same because the precipitation and, to some extent, the temperature differences (QAD minus A10) were not statistically significant (Gates et al., 1981). An AGCM with prescribed sea-surface temperatures is relatively insensitive to increased CO_2 concentration, as was discussed in the Introduction.

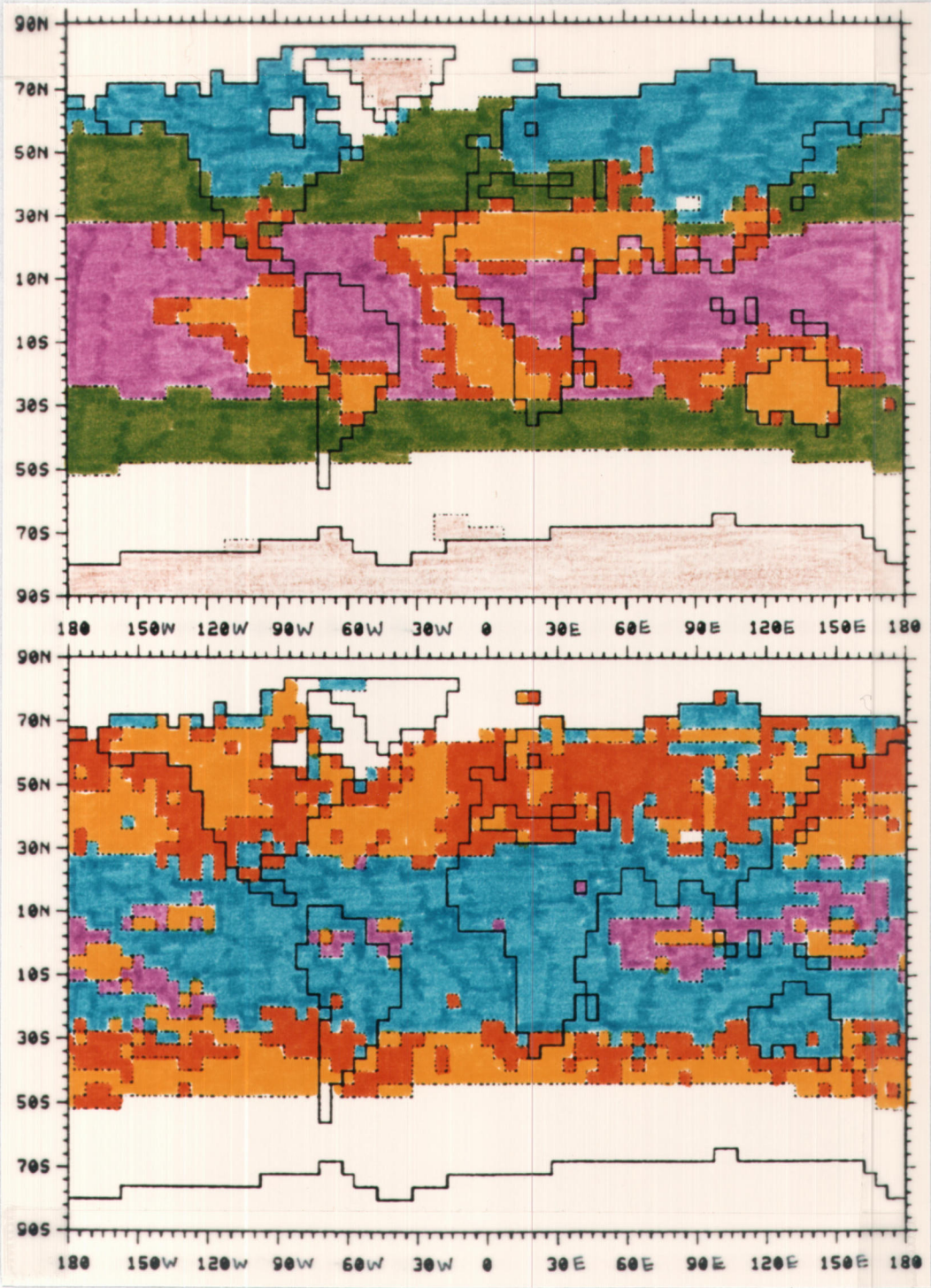

Fig. 16. Köppen climate maps for QAD: first-level subdivisions (top) of major groups (A, BW, BS, C, D, ET, EF) and second-level subdivisions (bottom) of relative dry season (f, s, w, m). Blank regions on the bottom map indicate no second-level subdivision for that region.

4.2 Thornthwaite Climate

4.2.1 Description of Observed Climatology (OBS)

Climate maps based on Thornthwaite's 1948 scheme are shown in Fig. 9, and those for OBS based on Thornthwaite's 1955 scheme are shown in Fig. 17[1]. The Thornthwaite climatology of OBS will be discussed, noting any differences from the climate maps of Thornthwaite's 1948 paper (previously referred to as T48). T48 contains a set of climate maps only for the United States; there is no published set of climate maps for the world to which we can compare the set for OBS. It should also be noted that the climate type boundary definitions of Thornthwaite's 1948 scheme differ slightly from the updated 1955 scheme (Mather, 1966).

Figure 17 shows that in general, perhumid A climates are usually located where the temperatures are cool and/or the precipitation is high, such as in Tibet, Japan, along the Canadian Pacific coast, and the latitude band 45°S to 60°S. Deserts and other very hot and dry regions have arid Fd climates. In polar regions such as Greenland and Antarctica, where the maximum monthly-mean temperature is below freezing, Im is set equal to zero (i.e., moist-subhumid Cr climate), since the PE is zero. In the Arctic region usually at least one

---

[1]Since the first, second, and fourth levels of Thornthwaite's scheme are each subdivided using a single index, regular contours can be used in the climate maps instead of the "box" contours used for the Köppen maps.

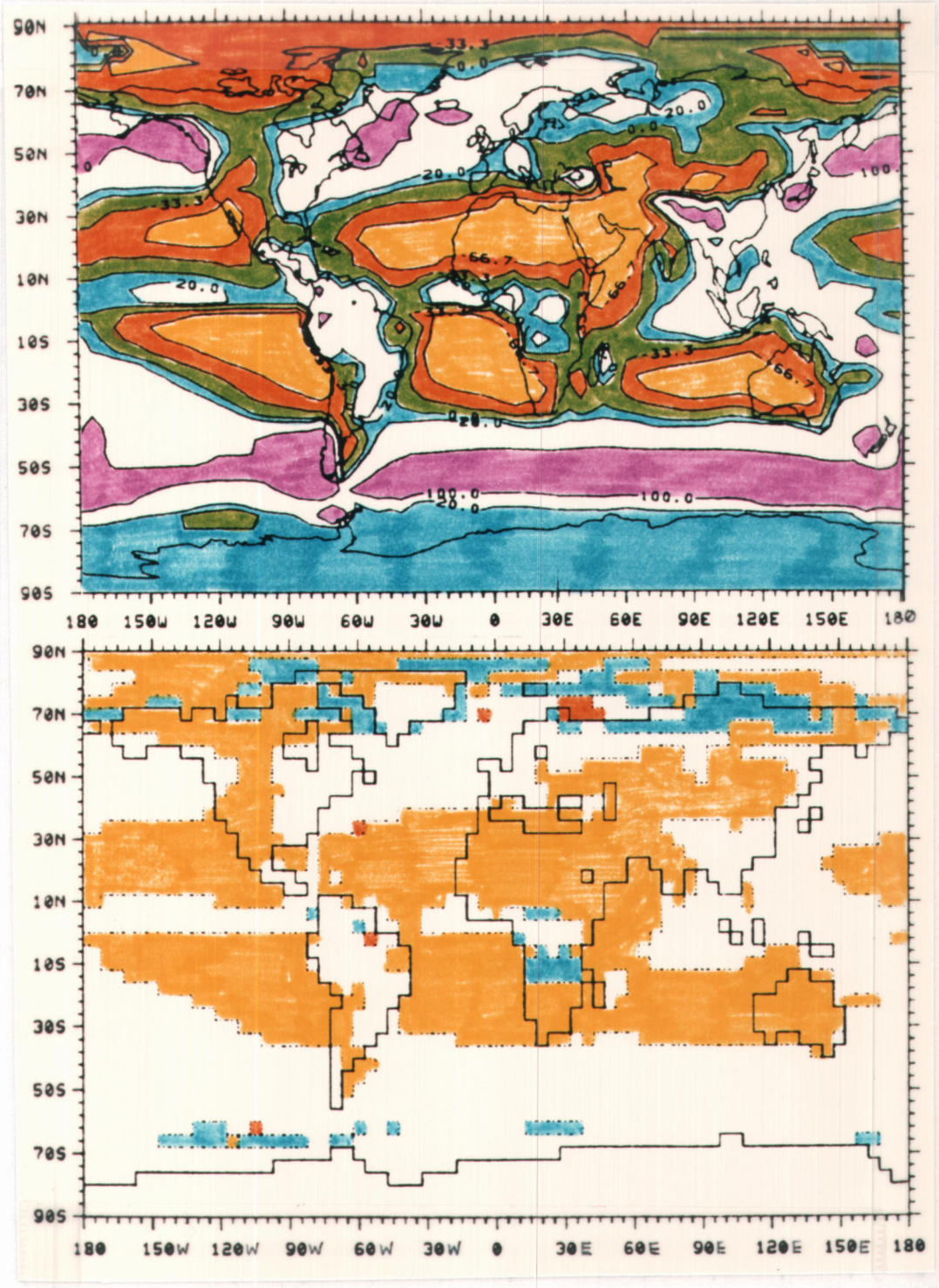

Fig. 17a. Thornthwaite climate maps for OBS: first-level subdivisions (top) of moisture regions ([]A, []B, []C, []D, []E, []F) and third-level subdivisions (bottom) of relative dry season ([]r, []d, []s, []w).

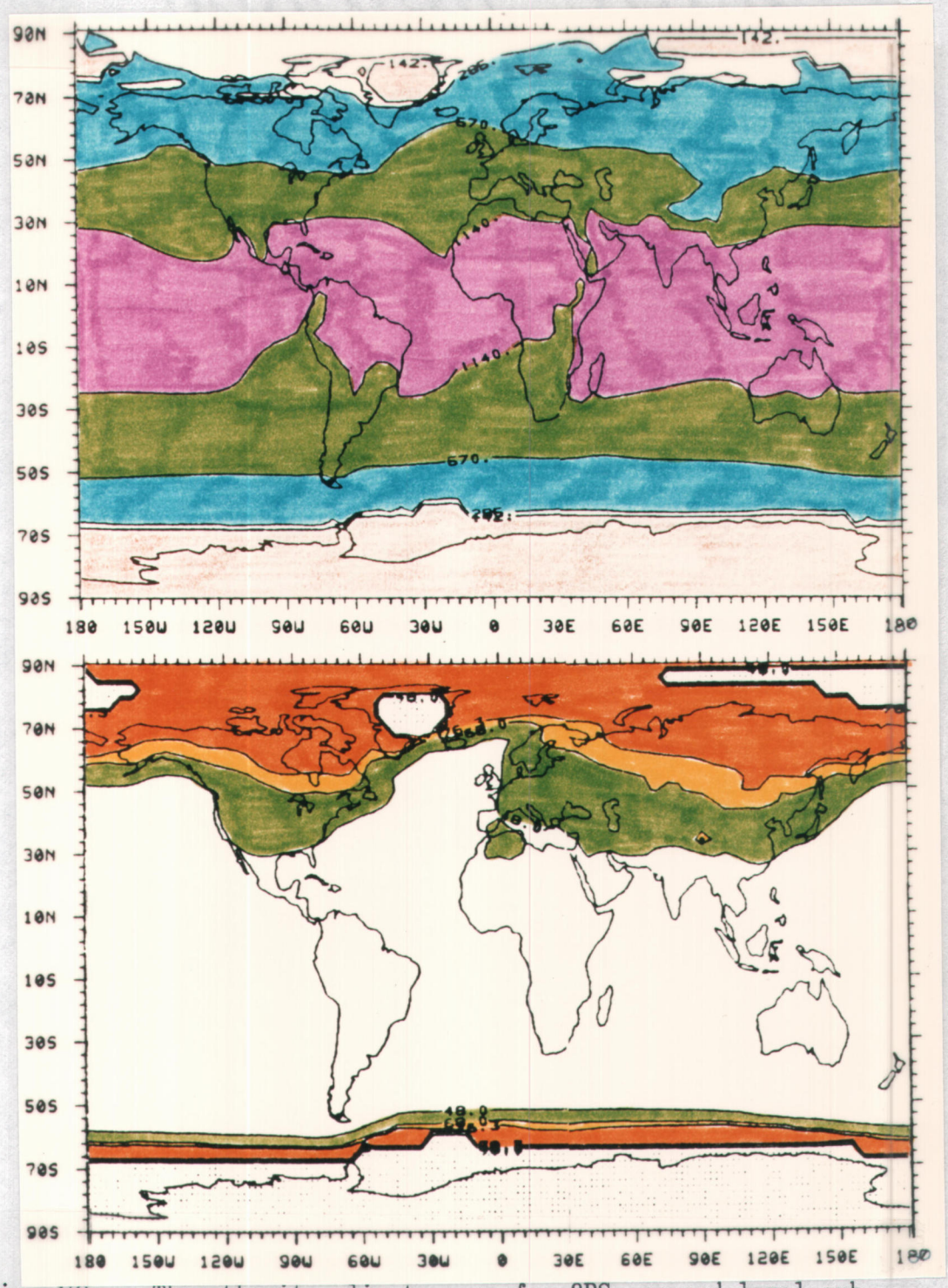

Fig. 17b. Thornthwaite climate maps for OBS: second-level subdivisions (top) of thermal efficiency (A, B, C, D, E) and fourth-level subdivisions (bottom) of summer concentration of thermal efficiency (a, b, c, d). Dotted areas indicate regions where the maximum monthly PE is zero.

month has an above-freezing temperature in OBS, so that the PE is slightly greater than zero, resulting in a mostly semi-arid Ed climate classification.

Central Canada has a dry-subhumid Dd climate, with a semi-arid Ed climate to the north, perhumid Ar along the west coast, and a humid Br climate in Quebec and Ontario. The climate along the west coast of the United States starts out with a humid Br climate in the northwest, and progressively dries out as one moves southward, ending with an arid Fd climate in southern California. Most of Mexico, the southwestern United States, and the Rockies have a semi-arid Ed climate. A narrow band of moist-subhumid Cr climate separates the dry western half of the United States from the humid Br climate of the eastern half. The climate of T48 (Fig. 9a) is essentially the same as that of OBS for the United States, except that the arid Fd region in the southwest extends farther northward in T48 than in OBS, due probably to the differing boundary definitions in the 1948 and 1955 schemes (Mather, 1966).

Peru and most of Brazil have a humid Br climate. The east central coast is drier than the interior and the PE of the former is larger because the monthly-mean temperatures are slightly higher and almost constant throughout the year. Therefore the ratio of precipitation to PE is much smaller, so that the climate is a mixture of dry-subhumid Dd and semi-arid Ed climates.

There are two grid points along the equator in Brazil whose aridity indices are large enough to indicate that an exceptionally dry season might exist. The rainfall is greater than the PE for more

of the half-year April-September than for the period October-March for both stations. The half-year October-March is winter for the Northern Hemisphere station, but it is summer for the Southern Hemisphere station. Hence the two climates are classified Cw and Cs, respectively.

Northern Argentina has a humid Br climate with a transition zone of subhumid Cr and Dd climate to the west and south. Southern Argentina and northern Chile have a semi-arid Ed climate, which changes rather abruptly to a perhumid Ar climate in southern Chile.

Except for a semi-arid Ed section of climate in the west, the Mediterranean coast of Africa has an arid Fd climate. This Fd climate covers all of the Sahara Desert except for the Ed climate along the southern border.

Just north of the equator in Africa along 6°N are three grid points whose climate types are Cw, Dw, and Cw. The seasonal variations of temperature and precipitation are the same for all three locations. The temperature (and therefore the PE) and the precipitation are both greater for the second location than for the other two locations, but the important thing is that the ratio of precipitation to PE is smaller for the second location, such that the moisture index (Im) is slightly negative, giving the second location a dry-subhumid D climate. The other two locations have slightly positive moisture indices, and therefore moist-subhumid C climates. The rainfall of all three locations is concentrated in the summer. The aridity indices of the two moist locations are large enough to indicate an exceptionally dry season, which happens to be the winter

season, so that they both have a Cw climate. The humidity index of the dry location is also large enough to indicate an exceptionally moist season, which is the summer season, so that it has a Dw climate.

The Congo Basin is a mixture of humid and moist-subhumid climates, and most of the northern half is evenly moist (Cr and Br climates) while the southern half has exceptionally dry winters (Cw and Bw climates). Southern Africa has a dry-subhumid Dd climate in the north and along the east coast, and an arid Fd climate on the west coast. Madagascar also has a dry-subhumid Dd climate.

Spain has a dry-subhumid Dd climate in the south and a moist-subhumid Cr climate in the north. This Cr climate extends northward through France, along the southern edge of the Baltic Sea, up into Finland, and then eastward into the U.S.S.R. The British Isles, Norway, Sweden, and most of the region from Germany and Poland southward to Italy has a humid Br climate.

The northwestern U.S.S.R. has mostly a humid Br climate surrounded by a moist-subhumid C climate, with some dry-subhumid Dd climate to the south. This band of dry-subhumid Dd climate extends eastward through Mongolia and western Manchuria and covers most of eastern U.S.S.R. The winters are drier in the north where Dw, Cw, and Bw climates exist. The Gobi Desert has an arid Fd climate bordered by a semi-arid Ed climate. Tibet has a perhumid Ar climate surrounded by a humid Br climate that extends into southeast Asia, Indonesia, New Guinea, eastern China, and along the coast of Manchuria. Japan has a perhumid Ar climate.

Central Australia has an arid Fd climate bordered by a semi-arid Ed climate and a dry-subhumid Dd climate along the coast to the north, east, and south. The eastern coast also has a bit of moist-subhumid Cr climate.

The top panel of Fig. 17b shows that megathermal A climates exist in Florida, Central America, Brazil, much of Africa, Saudi Arabia, India, southeast Asia, Indonesia, New Guinea, and the northern half of Australia. These are tropical regions of greatest thermal efficiency or largest annual PE, which result from high, consistent temperatures. Mesothermal climates occupy the mid-latitudes from about 30° to 50° latitude. Microthermal climates are generally found from about 50° to 70° latitude, and also extend into Tibet. From 70°N to 90°N the climate is a mixture of microthermal, tundra, and frost, the latter dominant in Greenland and parts of the Arctic Ocean. In the southern polar region the climates have hardly any longitudinal variation. There is a very narrow transition band of tundra at about 65°S separating the frost climate of the Antarctic from the warmer microthermal climate to the north.

The thermal efficiency of T48 (Fig. 9b) differs slightly from that of OBS (Fig. 17b) in that the microthermal C climate of Canada has extended southward into the United States along the Rockies in T48. The lower panels of Figs. 9b and 17b show that the concentration of thermal efficiency is the same for both T48 and OBS. Less than half of the thermal efficiency (annual PE) is concentrated in the three summer months between 50°S and 30°N (up to 60°N over ocean areas). The PESC is between 48% and 68% over the United States,

southern Canada, Algeria, much of Europe and in Asia south of Mongolia and north of India and southeast Asia.

The next level of PESC (68% to 76.3%) occupies a small area in Tibet and serves as a narrow transition zone to the largest concentration (76.3% to 100%), the latter covering Siberia, northern Canada, and most of the Arctic. The PESC is zero in Greenland, part of the Arctic, and over Antarctica, since the mean monthly temperature is always below freezing. These regions of zero PESC are filled in with dots on the climate maps.

The locations of the boundaries for PESC and the thermal efficiency are similar, except that the former tends to highlight the seasonal cycle of PE. This difference is especially evident along the coastlines. The PESC is much greater in the Northern Hemisphere because of the large land mass, while the range of PESC from 48% to 100% covers only about ten degrees of latitude in the Southern Hemisphere.

4.2.2 Comparison of Model Climatology (A10) to Observed Climatology (OBS)

Section 4.2.1 described the present-day climatology in terms of Thornthwaite's scheme. This section compares the Thornthwaite maps for A10 (Fig. 18) to those for OBS (Fig. 17). There is general agreement between A10 and OBS with the exceptions discussed below.

Comparison of Figs. 18a and 17a shows that the areas where the moisture index of A10 is much greater than that of OBS, (i.e., where there is more precipitation and/or it is cooler in A10 than OBS) are: eastern Alaska, northwestern Canada, the United States west of the Rockies, off the eastern United States coast, the southern tip of Africa, off the coast of Somalia, the western Mediterranean, Tibet, and off the southeastern and southwestern coasts of Australia. The moisture index of A10 is much smaller than that of OBS (i.e., where there is less precipitation and/or it is warmer in A10 then in OBS), in the following regions: off the western Canadian coast, Central America, Peru, southern Brazil, northern Argentina, off the southern Chilean coast, Liberia and the Ivory Coast, off the coast of Burma, eastern China, Japan, and New Guinea.

The moist region over the North Pacific is larger in A10 than in OBS, extending farther inland into eastern Asia and western North America, replacing the observed dry-subhumid and semi-arid climates of central and northern Canada, and the central and southwestern United States with simulated perhumid, humid, and moist-subhumid climates.

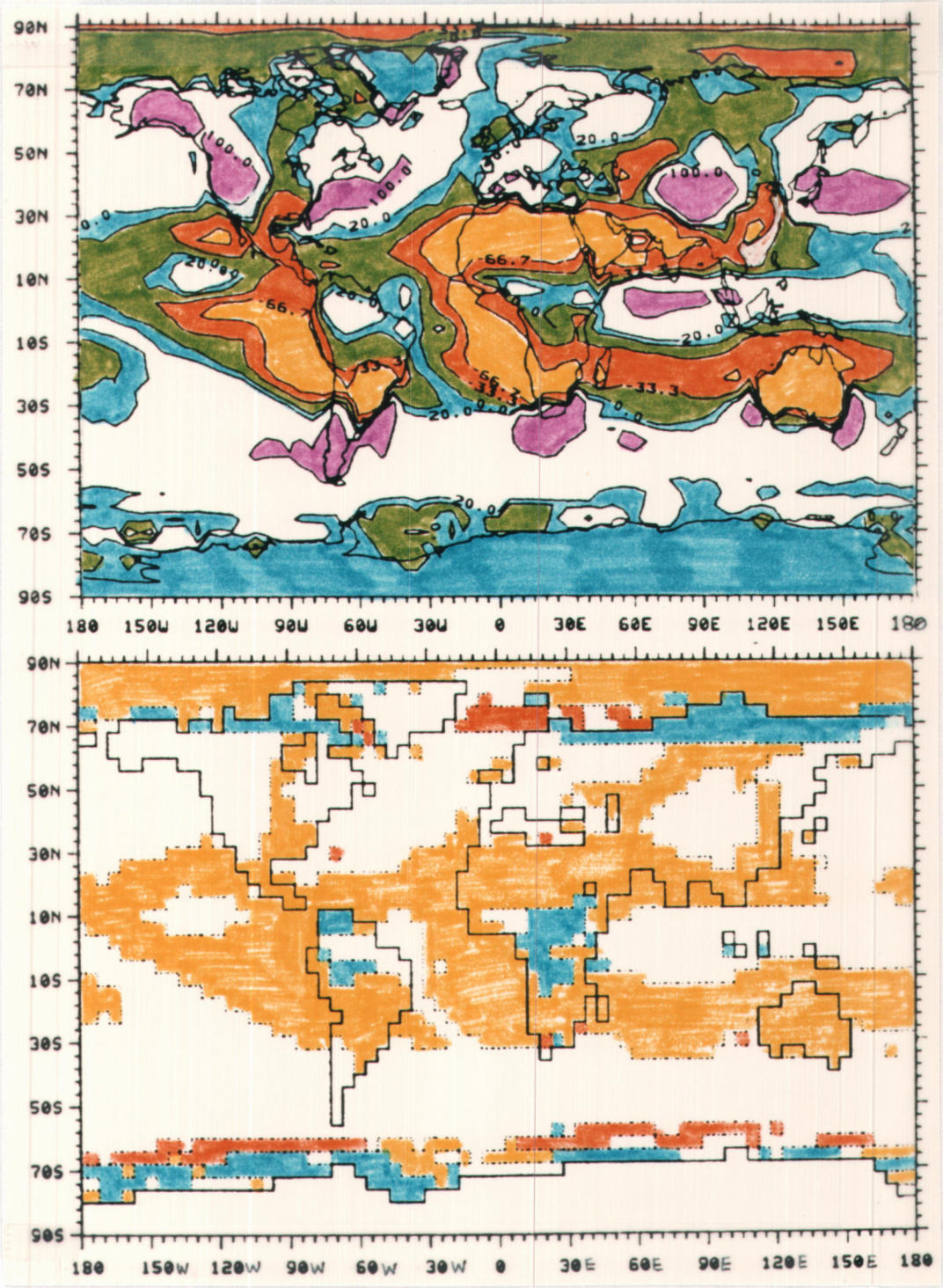

Fig. 18a. Thornthwaite climate maps for A10: first-level subdivisions (top) of moisture regions ([]A, []B, []C, []D, []E, []F) and third-level subdivisions (bottom) of relative dry season ([]r, []d, []s, []w).

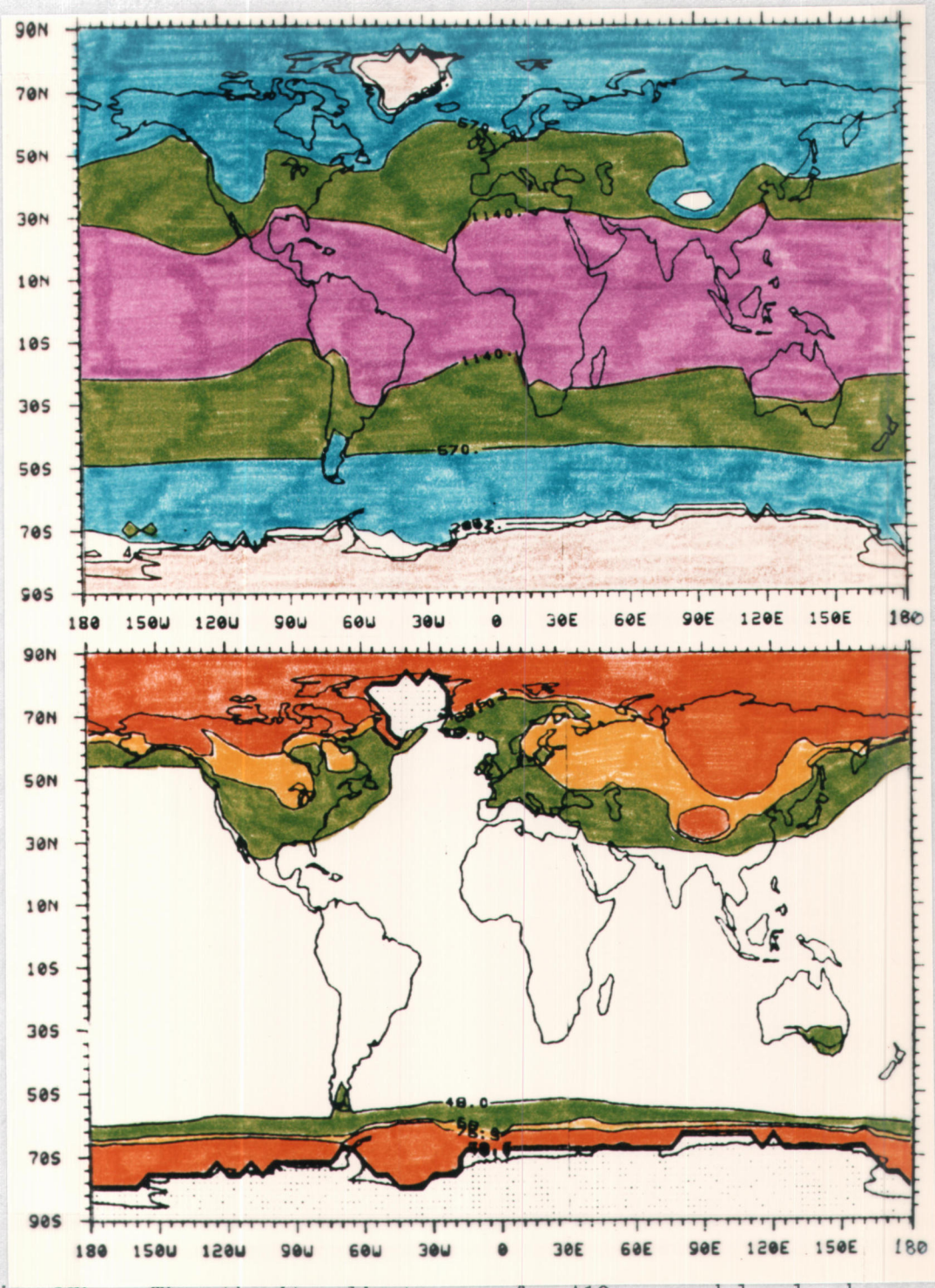

Fig. 18b. Thornthwaite climate maps for A10: second-level subdivisions (top) of thermal efficiency ([]A, []B, []C, []D, []E) and fourth-level subdivisions (bottom) of summer concentration of thermal efficiency ([]a, []b, []c, []d). Dotted areas indicate regions where the maximum monthly PE is zero.

Along most of the northern Canadian coast the amount of rainfall is greater than the PE only for a month or two at the beginning and end of summer in OBS, which does not constitute an exceptionally-moist season in a dry climate; therefore the second-level classification is "evenly-dry" or "d" for OBS. In A10 the precipitation is about three times greater than that of OBS, so that the annual precipitation is larger than the annual PE, and therefore the climate is a moist climate. The rainfall is greater than PE for only a few months in summer in A10 as in OBS, but while a dry season is not exceptional in a dry climate, it is exceptional in a moist climate, and this results in the dry-winter Bw and Cw classifications for A10 along the northern Canadian coast.

The humid region in the North Pacific extends farther southward in A10 than in OBS, so that the observed semi-arid region of southwestern United States and Mexico is not present in A10. The two large semi-arid observed regions in the eastern Pacific are simulated as one semi-arid region extending across Central America and the southern United States in A10.

The semi-arid Ed region of the eastern South Pacific extends farther inland in A10 than in OBS, so that Venezuela, Columbia, Ecuador, and Peru are simulated as semi-arid Ed and dry-subhumid Dd climates instead of the humid Br climate of OBS. At about 25°S, the arid Ed region of the eastern South Pacific has penetrated farther eastward in A10 than in OBS, and the observed humid Br climates of southern Brazil, Paraguay, and northern Argentina are absent in A10. However this simulated dry region did not penetrate as far southward

as in OBS, leaving southern Argentina and Chile with a large region of perhumid Ar climate in A10. These differences in first-level climate types are primarily due to the fact that the simulated precipitation is less than the observed precipitation in most of South America each month, except in northern Brazil and southeastern Argentina.

There are dry-winter climates in South America in bands just north and south of the equator in A10 instead of the evenly-moist climates of OBS. In these regions, the simulated half-year temperatures for winter are warmer than those for summer. Therefore, the ratio of rainfall to PE is smaller in winter (drier winters) and larger in summer (moister summers) in A10 than in OBS, resulting in the dry-winter Dw and Bw classifications there.

The semi-arid Ed region of the eastern South Atlantic is merged with that of the eastern North Atlantic and with that of Australia in A10. The humid and moist-subhumid climates of central Africa only cover a narrow band along 6°N in A10, with dry-subhumid and semi-arid climates along the western coast and in the Congo Basin. This band of moist climate extends farther eastward in A10 than in OBS, with the observed arid Fd climate of Somalia simulated as moist-subhumid Cr and dry-subhumid Dd climates, and merges with the moist region of the eastern Indian Ocean to create a pool of perhumid Ar climate in the Indian Ocean. The larger amount of precipitation at the southern tip of Africa in A10 results in the observed semi-arid Ed climate there to be simulated as a perhumid Ar climate instead.

The simulated humid Br and moist-subhumid Cr climates along the western coast of Europe extend farther inland than in OBS and replace the observed dry-subhumid Dd climate of western Europe. The observed moist region in southern Asia is not simulated in A10 and the arid climate of the Gobi Desert is also not simulated in A10. The simulated arid region of the Sahara extends farther eastward through India, Burma, northern Thailand and Indochina, and eastern China than is observed, while the observed arid region east of the Caspian Sea is simulated as a semi-arid region. The observed perhumid Ar climate of southern Japan is located in northern Japan in A10 and extends farther eastward than is observed.

Australia is much drier in A10 than in OBS, being simulated as a completely arid Fd climate, except for a small sliver of semi-arid Ed climate along the eastern coast. However there are two small sections of perhumid Ar climate just off the southwestern and southeastern coasts in A10 due to the large amount of precipitation there.

Antarctica and Greenland have moist-subhumid Cr climates since the temperature remains below freezing in both A10 and OBS. The warmer-than-observed Arctic temperatures result in one or two more above-freezing months in A10. Although the number of months with nonzero PE is larger in A10 than in OBS, the annual PE of A10 is less than that of OBS. Therefore, the moisture index of A10 in the Arctic is larger than in OBS, so that the predominantly semi-arid Ed climate of OBS is simulated as a predominantly dry-subhumid Dd climate in A10.

The top panels of Figs. 18b and 17b show that the megathermal climate extends farther southward in A10 than in OBS to cover the Congo Basin, Peru, and northern Argentina, and farther northward to cover Egypt, eastern China, and the Gulf Coast. Even though the temperatures over Antarctica are much warmer in A10 than in OBS, they still aren't above freezing, so that the climate south of about 45°S is the same in both A10 and OBS, except that the microthermal climate of A10 at the southern tip of South America is located farther inland than in OBS. Except for Greenland, the tundra and frost climates of the Northern Hemisphere polar latitudes are simulated as microthermal climates, because of the much warmer-than-observed temperatures in A10 in this region. The microthermal climate also extends farther down into the western United States in A10 than in OBS and the observed microthermal climate in Tibet is simulated as a tundra climate in A10.

The lower panels of Figs. 18b and 17b show that the PESC of the Southern Hemisphere is basically the same in A10 as in OBS, except that southeastern Australia and the southern tip of South America have a larger PESC in A10 than in OBS. The PESC of the Northern Hemisphere is generally slightly larger in A10 than in OBS. Algeria, southwestern Europe, the region around and to the north of Tibet, and the region in the Arctic between 75°E and 155°W all have noticeably larger PESC in A10 than in OBS. The difference in the last region is due to a maximum monthly-mean temperature that is above freezing.

4.2.3 Interannual Variability of the OSU AGCM (YR1, YR2, YR3, and A10)

The Thornthwaite climate maps for A10, YR1, YR2, and YR3 are shown in Figs. 18-21. The positioning of the major moisture regions of the four sets of data is essentially the same, although the extent varies from year to year. As with the Koppen climate maps, the Thornthwaite climate maps of the A10 data are somewhat more organized and less jumbled than maps from YR1, YR2, or YR3.

Figs. 18a-21a show that the climate type of the western half of North America is basically the same in all four data sets, although the two large perhumid Ar regions of western Alaska and in the northwestern United States tend to join and separate from year to year. Similarly, a perhumid Ar region appears in Quebec in YR1 and YR3, but is not in YR2 and A10. The intensity of the dry region in the central third of the continent varies slightly from year to year.

The climate types of South America remain essentially unchanged in the four cases, except that the boundary between the moist climate of northern Brazil and the dry climate of southern Brazil changes positions slightly.

The extent and strength of the arid region of the Sahara doesn't vary from year to year. The extent of the moist band along 6° N latitude remains essentially constant, although the strength (moist B to moist-subhumid C) varies in the four cases. The annual precipitation in the Congo Basin progressively decreases slightly in the first three years, expanding the arid F region there.

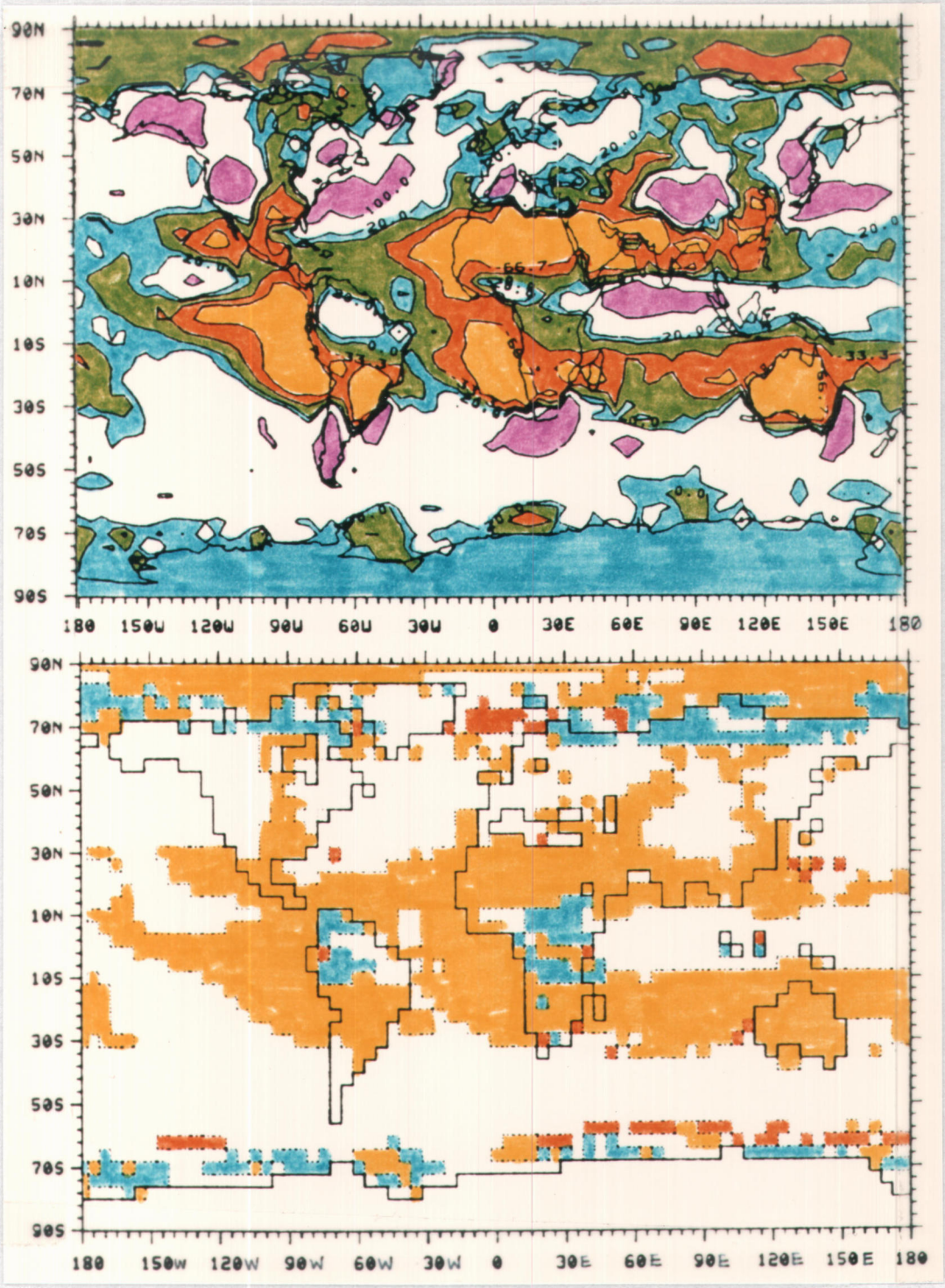

Fig. 19a. Thornthwaite climate maps for YR1: first-level subdivisions (top) of moisture regions ([]A, []B, []C, []D, []E, []F) and third-level subdivisions (bottom) of relative dry season ([]r, []d, []s, []w).

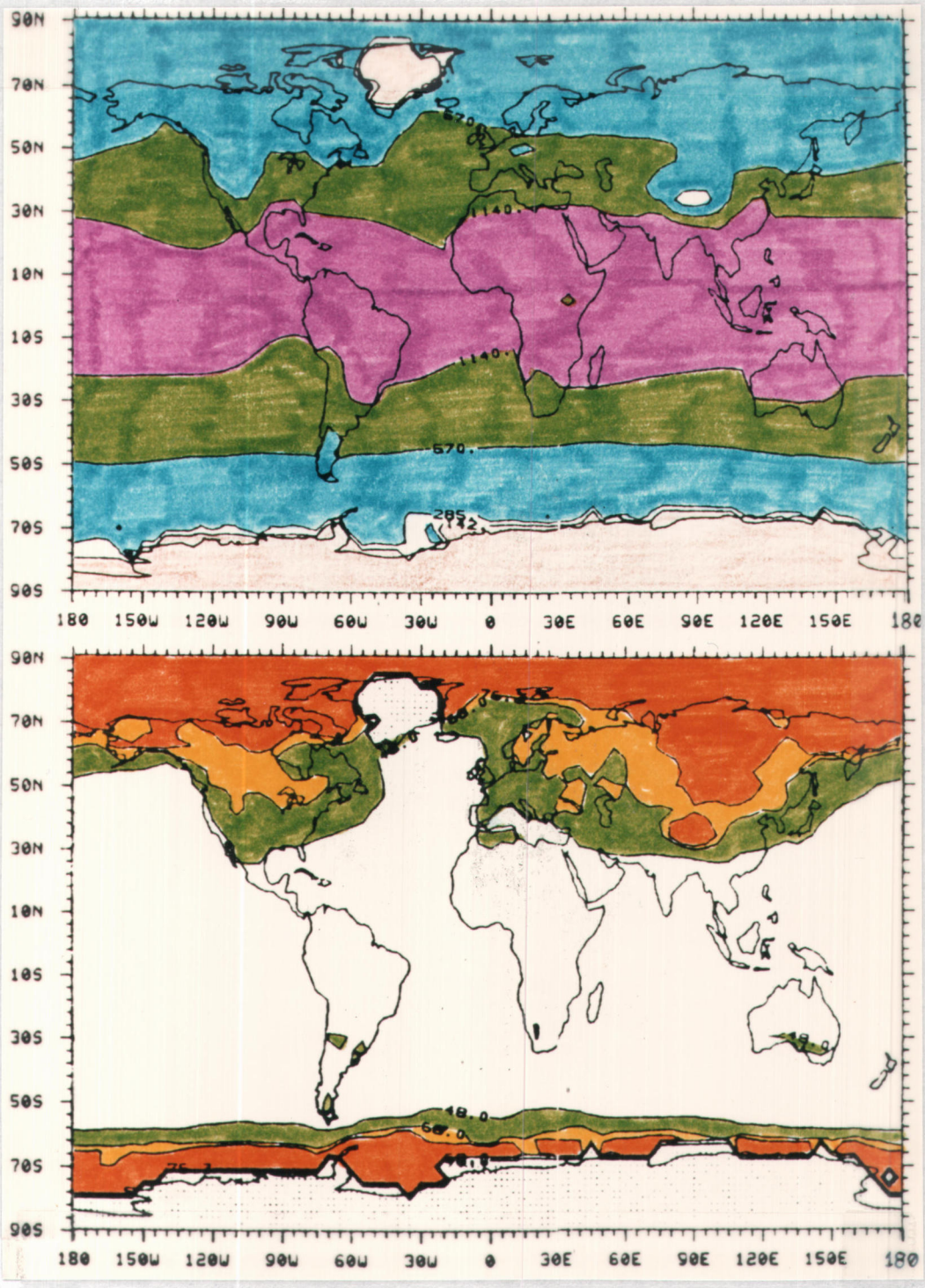

Fig. 19b. Thornthwaite climate maps for YR1: second-level subdivisions (top) of thermal efficiency ([]A, []B, []C, []D, []E) and fourth-level subdivisions (bottom) of summer concentration of thermal efficiency ([]a, []b, []c, []d). Dotted areas indicate regions where the maximum monthly PE is zero.

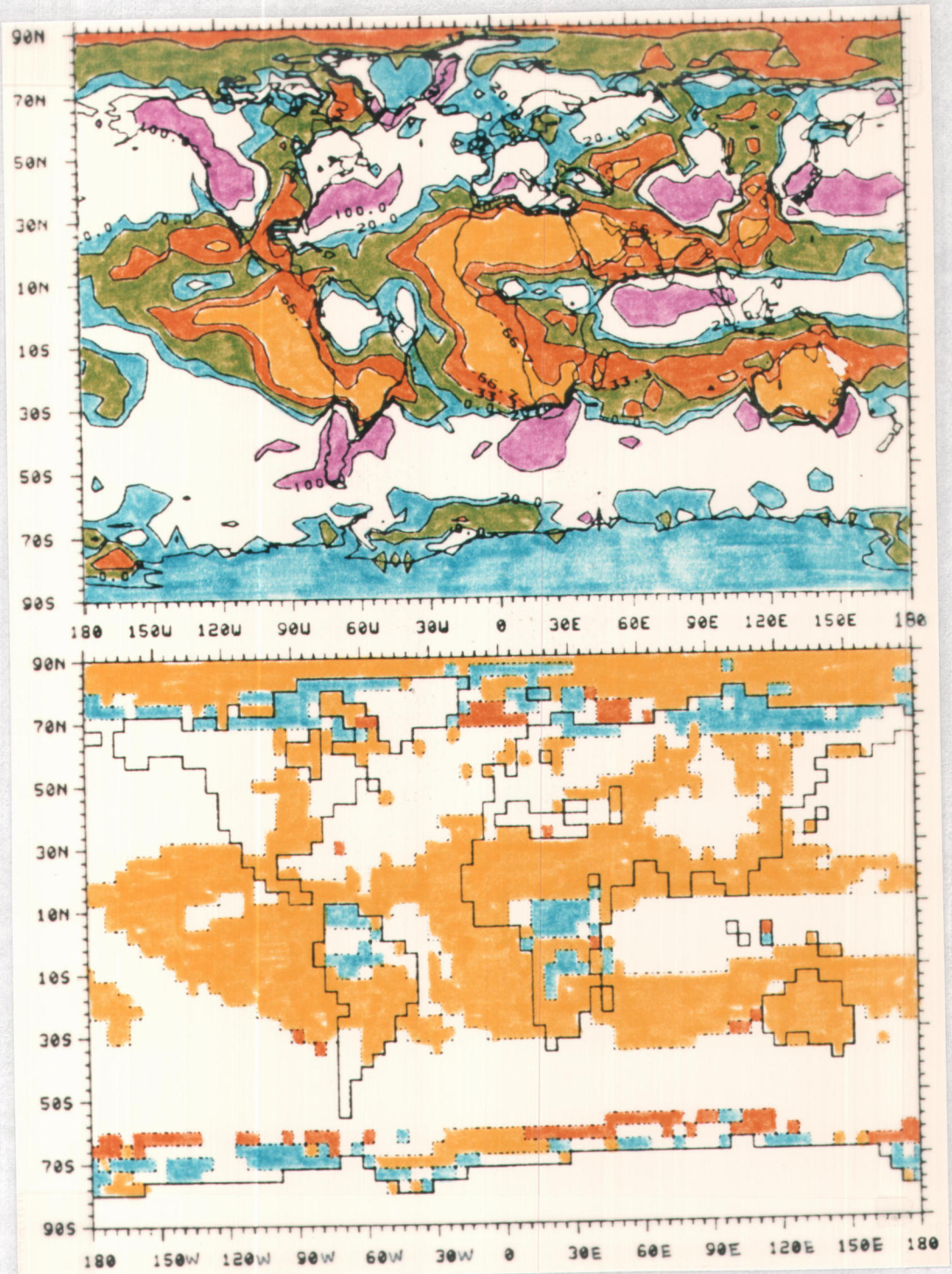

Fig.20a. Thornthwaite climate maps for YR2: first-level subdivisions (top) of moisture regions ([]A, []B, []C, []D, []E, []F) and third-level subdivisions (bottom) of relative dry season ([]r, []d, []s, []w).

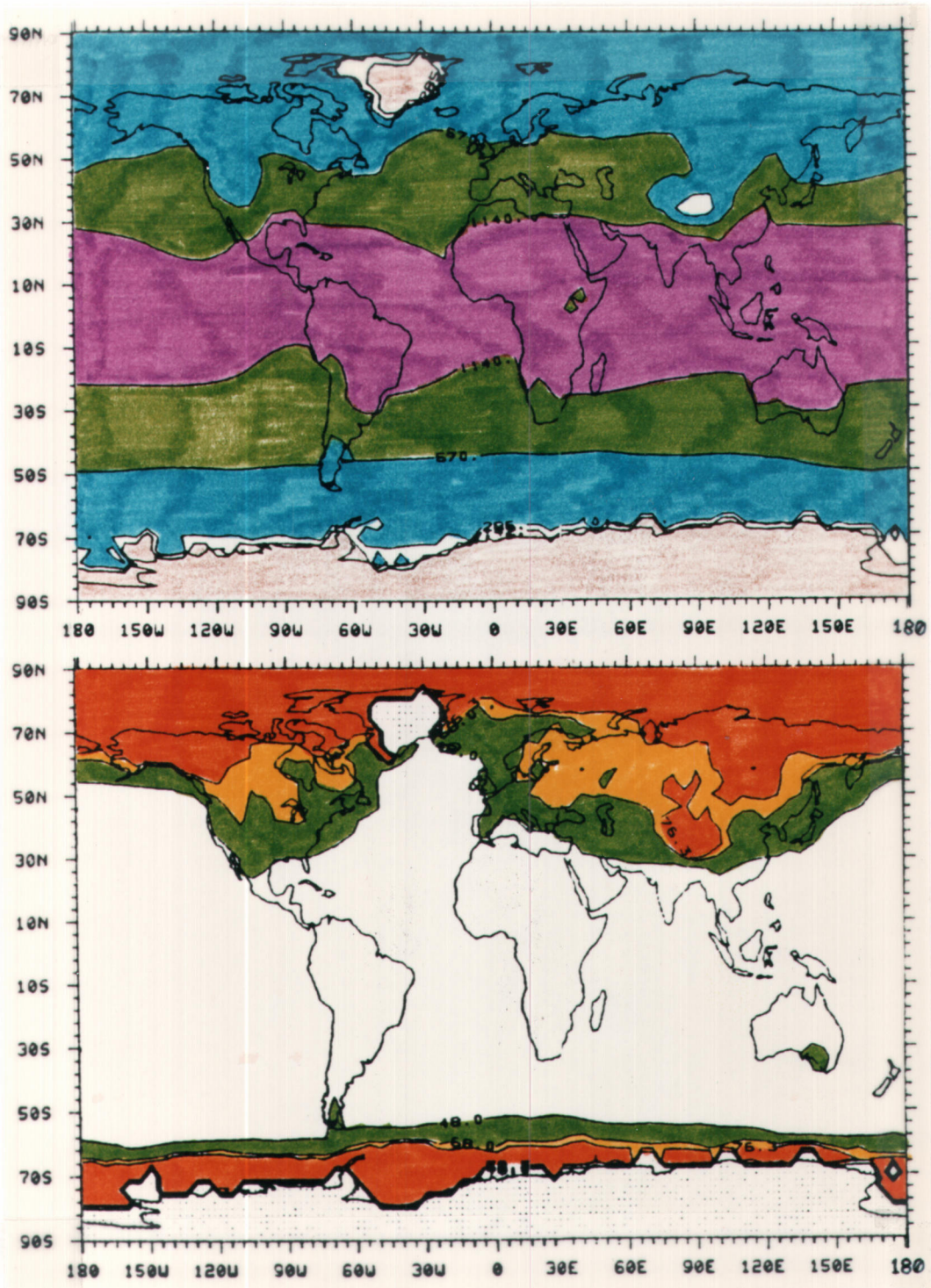

Fig. 20b. Thornthwaite climate maps for YR2: second-level subdivisions (top) of thermal efficiency ([]A, []B, []C, []D, []E) and fourth-level subdivisions (bottom) of summer concentration of thermal efficiency ([]a, []b, []c, []d). Dotted areas indicate regions where the maximum monthly PE is zero.

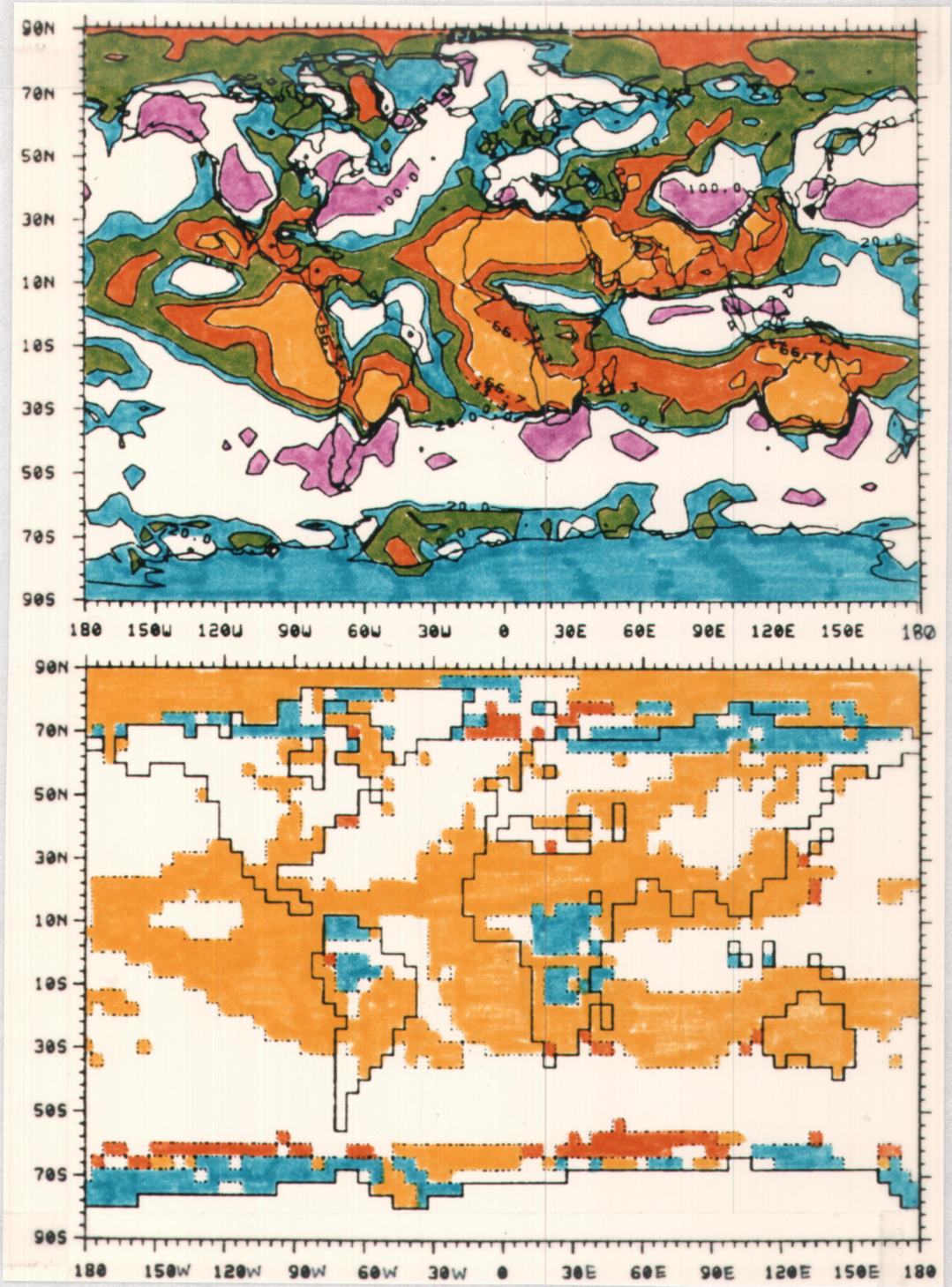

Fig. 21a. Thornthwaite climate maps for YR3: first-level subdivisions (top) of moisture regions ([]A, []B, []C, []D, []E, []F) and third-level subdivisions (bottom) of relative dry season ([]r, []d, []s, []w).

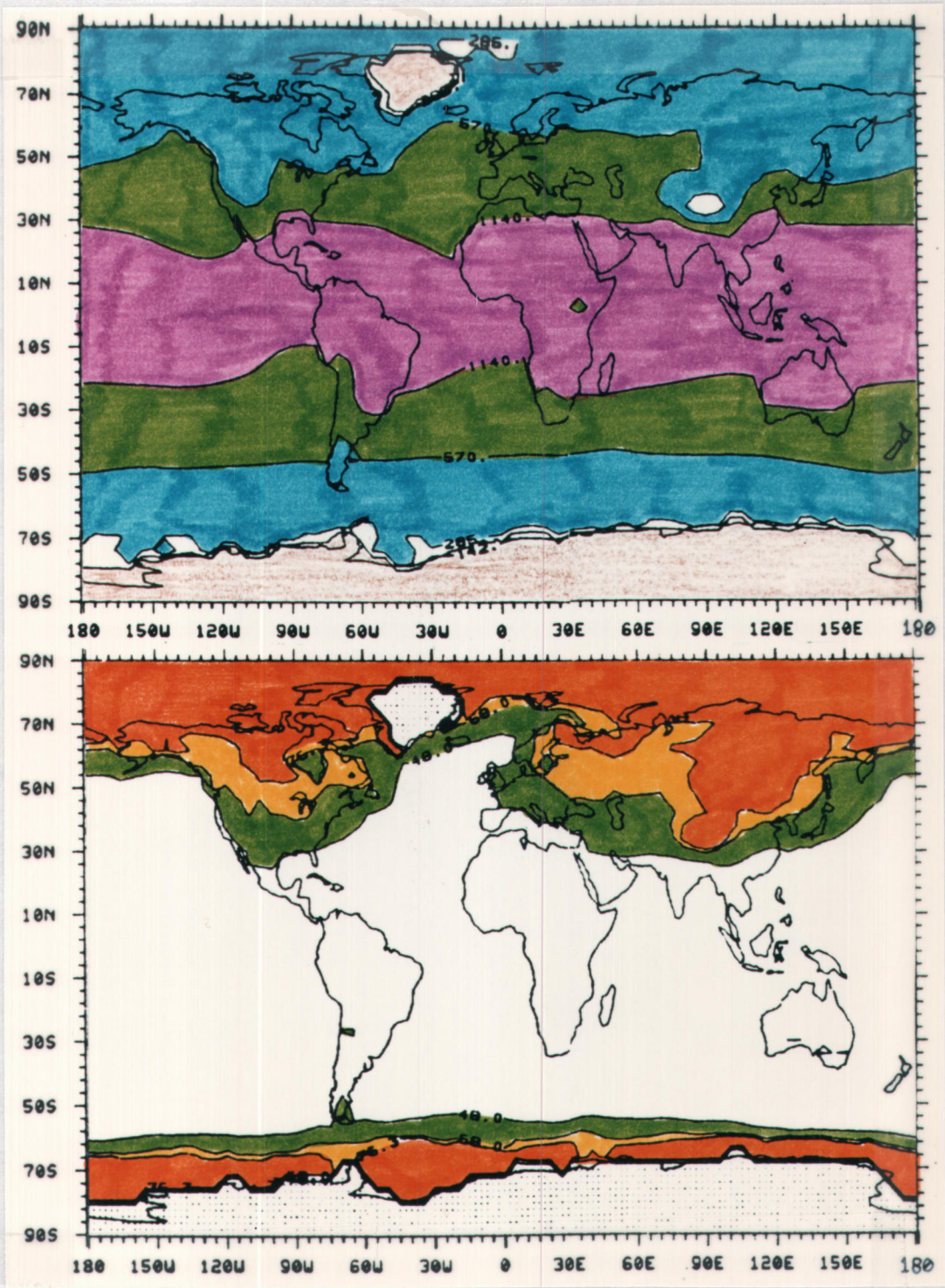

Fig. 21b. Thornthwaite climate maps for YR3: second-level subdivisions (top) of thermal efficiency ([]A, []B, []C, []D, []E) and fourth-level subdivisions (bottom) of summer concentration of thermal efficiency ([]a, []b, []c, []d). Dotted areas indicate regions where the maximum monthly PE is zero.

The climate type of Europe is fairly constant from year to year. The perhumid Ar region in the Sea of Japan and east of Japan is about the same in YR2, YR3, and A10, but it extends westward into Manchuria in YR1. The width of the strip of dry-subhumid Dd climate along 120° E longitude in China varies slightly, being largest in YR2 with some regions of semi-arid Ed climate scattered throughout. The extent of the dry-subhumid Dd region in the central U.S.S.R. increases in the first three years, with YR3 basically the same as A10. The climates of Indonesia, New Guinea, and Australia are the same for each of the four cases.

Figs. 18b-21b show that there is virtually no interannual variation in the distribution of thermal efficiency. However the distribution of PESC is organized into smoother homogeneous bands in A10 than in any of the individual years. The boundaries between the PESC subdivisions b,c, and d in the Northern Hemisphere shift from year to year, more so in Eurasia than in North America. In Europe and western Asia the b-c border is farther north in YR1 than in the other three cases. The distributions of d climate in Asia in YR1 and A10 are the same. In YR2 the penetration of d climate into Asia isn't as great as in YR1 and the section over Tibet extends farther northward. In YR3 these two sections are joined. These variations in PESC are due to the variations in the temperature extremes, e.g., the summer (winter) of YR3 was warmer (cooler) than that of YR1, so that the summer concentration of thermal efficiency is larger.

Africa, Australia, and South America have a PESC of a, with spots of b appearing in southeastern Australia and the southern tip

of South America in each of the four cases, and also around Algeria, Morocco, and northern Argentina in YR1.

4.2.4 Model Sensitivity to Quadrupled CO_2 (QAD and A10)

As can be seen by comparing the climate maps of QAD (Fig. 22) to those of A10 (Fig. 18), there are no major differences in the distribution of the climate types. The locations of boundaries between climate types has changed only slightly (e.g., the perhumid region in western North America is not as extensive in QAD as it is in A10), but these differences are no greater than the interannual variations among YR1, YR2, and YR3. The Thornthwaite scheme could detect no significant climate change resulting from a quadrupling of CO_2 in the OSU AGCM with prescribed sea-surface temperatures.

4.2.5 Description of Swamp Model Climatology (SWP)

This section will describe the climatology resulting from a simulation of the OSU AGCM with annual-averaged insolation and a swamp ocean. The first and second levels of the Thornthwaite classification (moisture regions and thermal efficiency, respectively) for SWP are shown in Fig. 23.

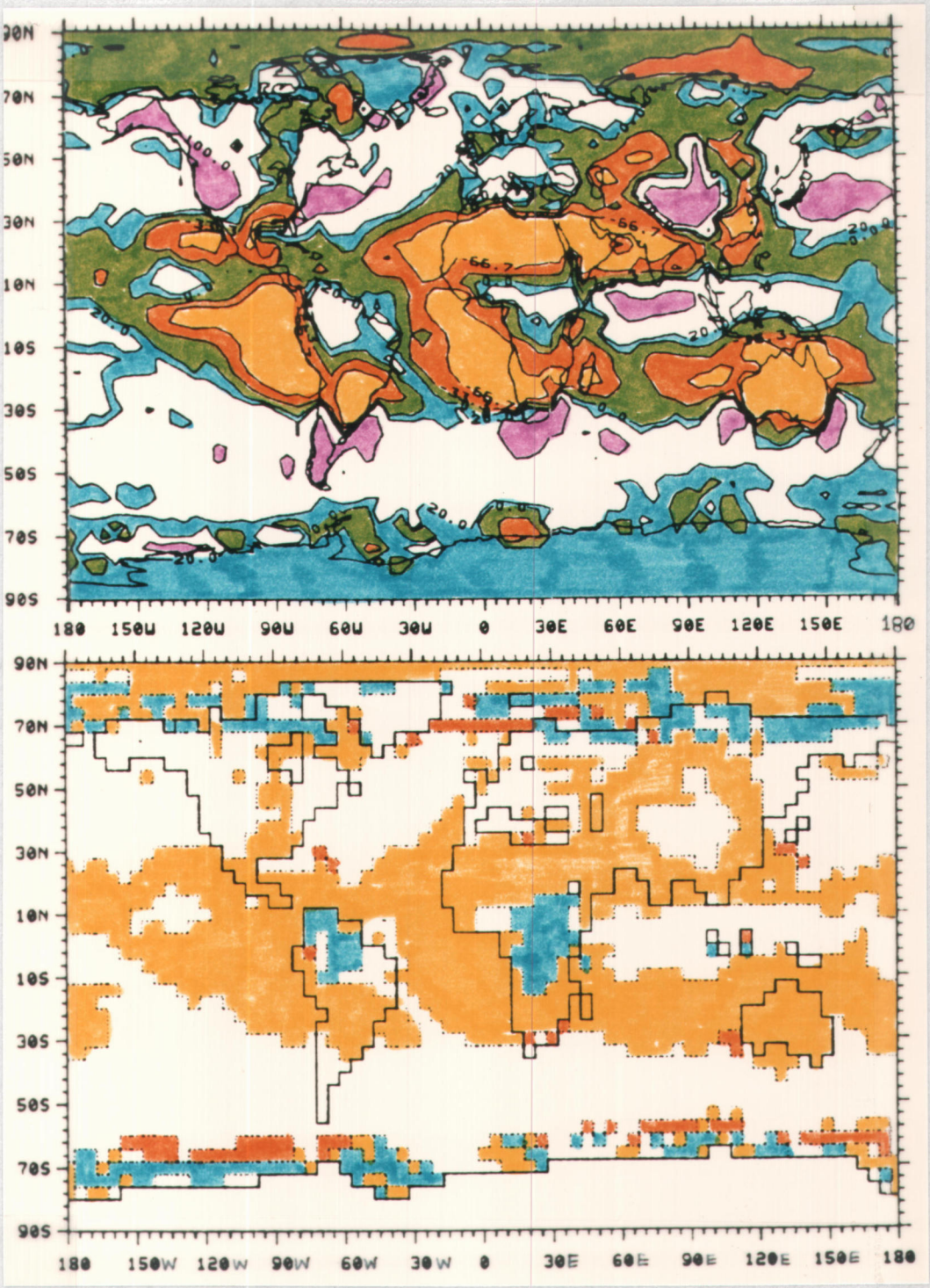

Fig. 22a. Thornthwaite climate maps for QAD: first-level subdivisions (top) of moisture regions ([]A, []B, []C, []D, []E, []F) and third-level subdivisions (bottom) of relative dry season ([]r, []d, []s, []w).

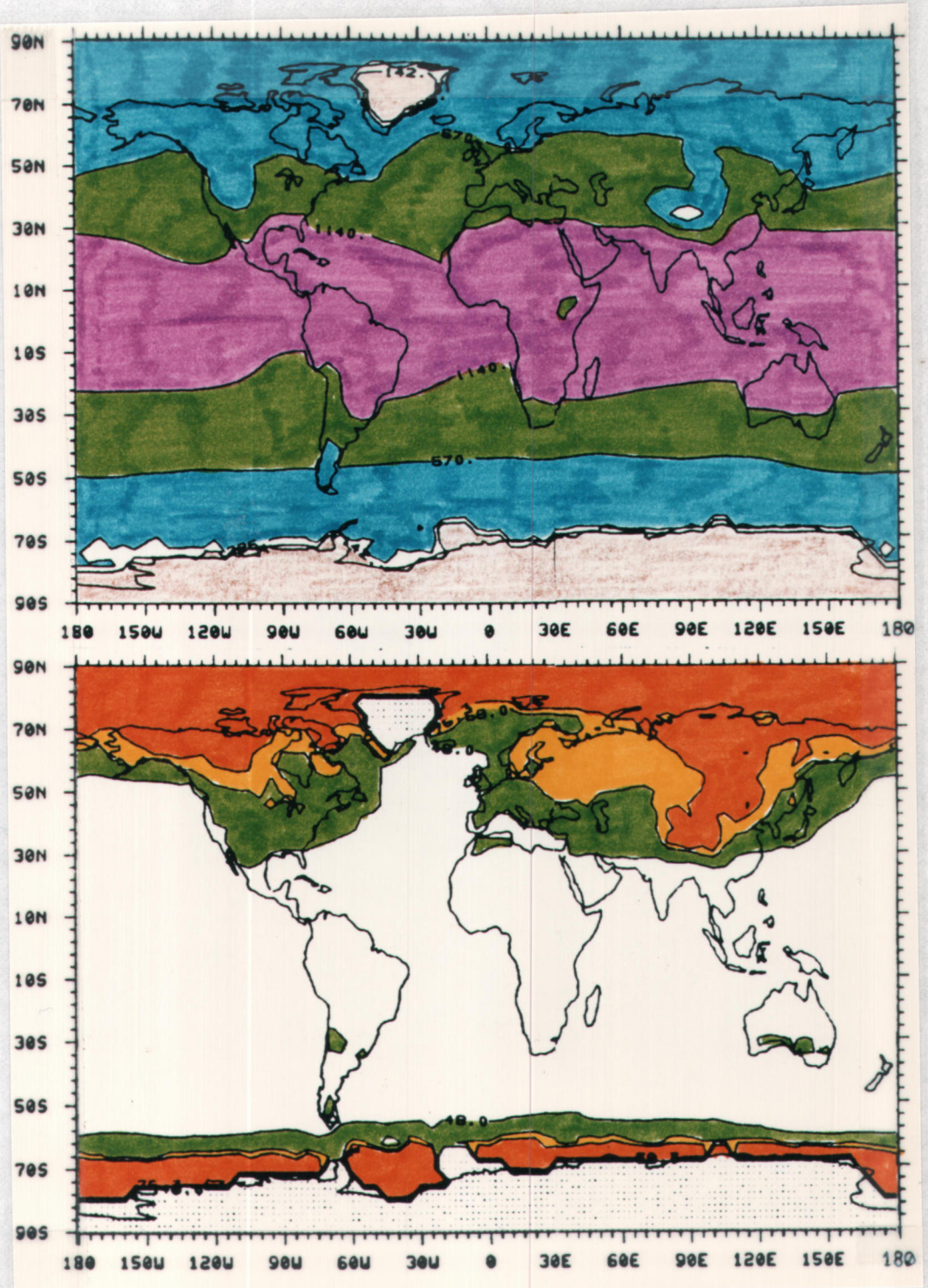

Fig. 22b. Thornthwaite climate maps for QAD: second-level subdivisions (top) of thermal efficiency (A, B, C, D, E) and fourth-level subdivisions (bottom) of summer concentration of thermal efficiency (a, b, c, d). Dotted areas indicate regions where the maximum monthly PE is zero.

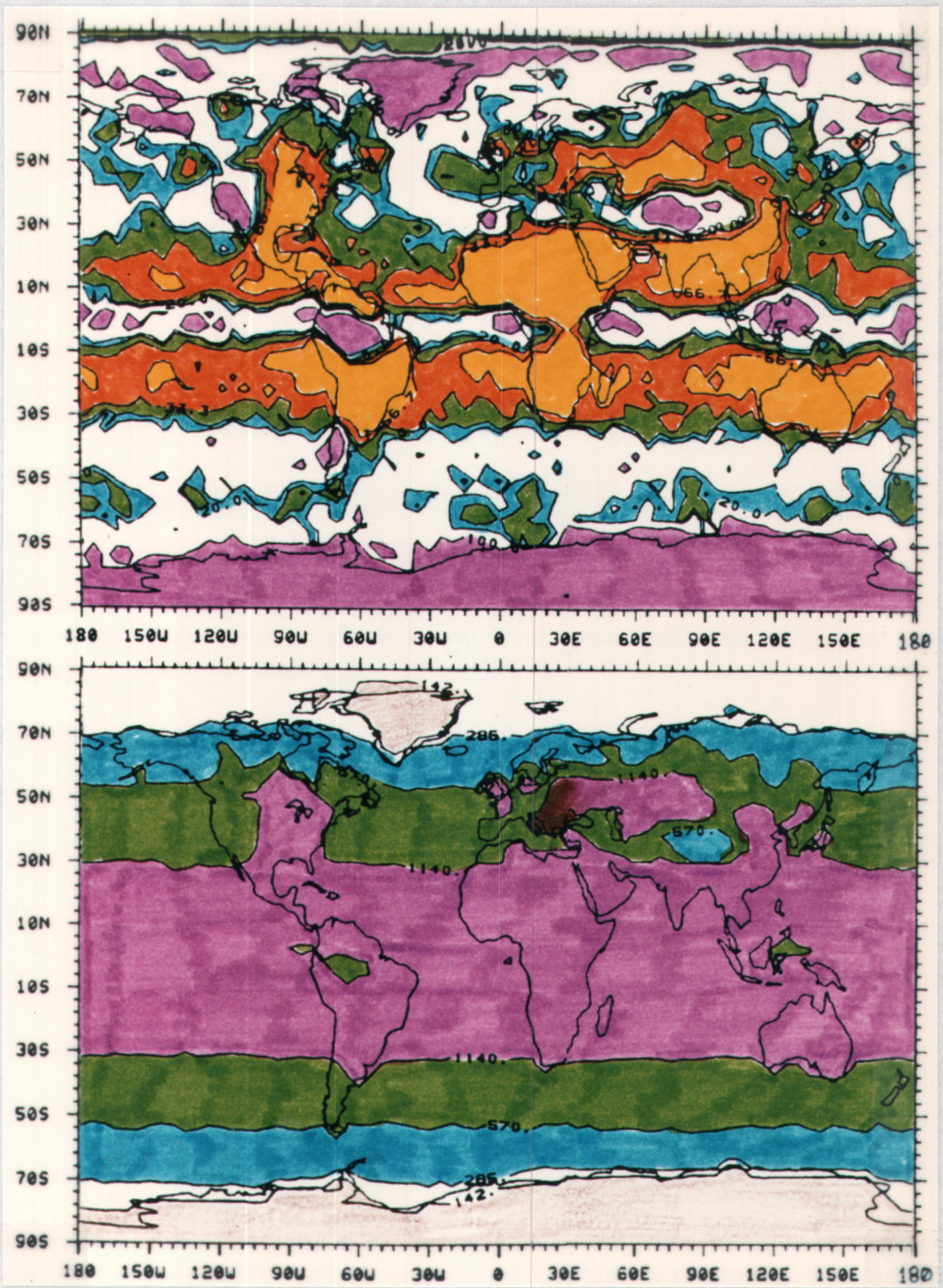

Fig. 23. Thornthwaite climate maps for SWP: first-level subdivisions (top) of moisture regions (A, B, C, D, E, F) and second-level subdivisions (bottom) of thermal efficiency (A, B, C, D, E).

The precipitation field of the swamp model is very noisy, which causes the moisture index field to be noisy because of the sensitivity of the latter to the precipitation. In all regions except around the Gobi Desert, the climate of SWP is more like that of A10 than that of OBS. However, one must remember that the differences in moisture indices between SWP and A10 are not only due to the difference in models, but also to the different methods of calculating the PE used for the moisture index.

The top panel of Fig. 23 shows that the moisture indices of western North America of SWP are similar to those of A10, but the east is considerably drier, with an arid F climate covering Ontario, Manitoba, and all of the eastern half of the United States. This arid climate is due to the very large PE calculated by the model there.

Central America also has an arid F climate which extends into Colombia, Venezuela, and northwestern Brazil in SWP. The equatorial precipitation of SWP is much greater than that of A10, especially in Brazil and Malaysia, so that an unbroken (except in Africa) band of humid B and perhumid A climates exist along the equator. To the south the influence of the large PE is again dominant, leaving arid F climates from Peru and southern Brazil to northern Argentina, and a humid B climate in southern Argentina with a perhumid A section on the western coast, the latter due to the larger amount of precipitation in SWP than in A10 in that area.

Except for the moist equatorial band mentioned above, semi-arid E and arid F climates cover most of the rest of the area between 30° N and 30° S because of the large PE in this band. All of Africa has an

arid F climate (due to the larger PE in SWP than in A10), except for the humid and perhumid climates in Morocco, Algeria, and along the equator on the east and west coasts, where there is more precipitation in SWP than in A10. Australia, eastern China, and Asia south of 30°N all have arid F climates.

Southwestern Europe and southeastern U.S.S.R. have semi-arid E and arid F climates corresponding to the larger PE in SWP than in A10 there. Thus, unlike A10, the Gobi Desert of SWP is dry. As in A10 there is also an island of perhumid A and humid B climates around Tibet in SWP. The rest of Europe and Asia has a dry-subhumid D climate except for some humid B areas along the northern coasts. Antarctica and Greenland have a perhumid A climate, and the rest of the polar regions have perhumid or humid climates because the PE there is small but never zero.

The lower panel of Fig. 23 shows that the distribution of thermal efficiency of SWP is somewhat more zonal than that of A10. Between 30°N and 30°S there is a megathermal climate in SWP, except for a couple of mesothermal patches in Malaysia and southwestern Brazil. There's a band of mesothermal climate between 30° S and 50° S, a band of microthermal climate between 50° S and 70° S, a band of frost covering Antarctica, and a sliver of tundra climate between the microthermal and frost climates.

The distribution of thermal efficiency in SWP is less zonal than that of A10 north of 30°N because of the larger amount of land mass in the Northern Hemisphere than in the Southern Hemisphere. Between about 30°N and 60°N there is a band of mesothermal climate with

regions of microthermal climate in Tibet and megathermal climate in the British Isles, France, northern Germany and Poland, southwestern Europe, southeastern U.S.S.R., eastern China, Japan, and the eastern half of North America. There's a band of microthermal climate between 60° N and 70° N, and a band of tundra climate poleward of 70° N except for the frost climate in Greenland.

4.2.6 Swamp Model Sensitivity to Doubled CO_2 (SCO2 and SWP)

Figs. 19, 21, and 27 of Schlesinger (1984) show the differences and the significance levels of the differences in surface air temperature and precipitation between SWP and SCO2. There are several regions in which the differences in temperature are statistically significant (i.e., there is less than a 1% chance that the difference could occur purely by chance), but almost all of the precipitation differences are statistically insignificant (i.e., there is more than a 10% chance that the difference could occur purely by chance).

The first and second levels of Thornthwaite's scheme for SCO2 are shown in Fig. 24. Mexico is simulated to be 2-3° warmer in SCO2 than in SWP, but there is no difference in climate type since Mexico was simulated to have an arid Fd climate in SWP. Similarly the Sahara Desert, the area east of the Caspian Sea, Saudi Arabia, southern India, China, and Australia are simulated as arid Fd climates in both SWP and SCO2, although these regions are warmer in SCO2 than in SWP.

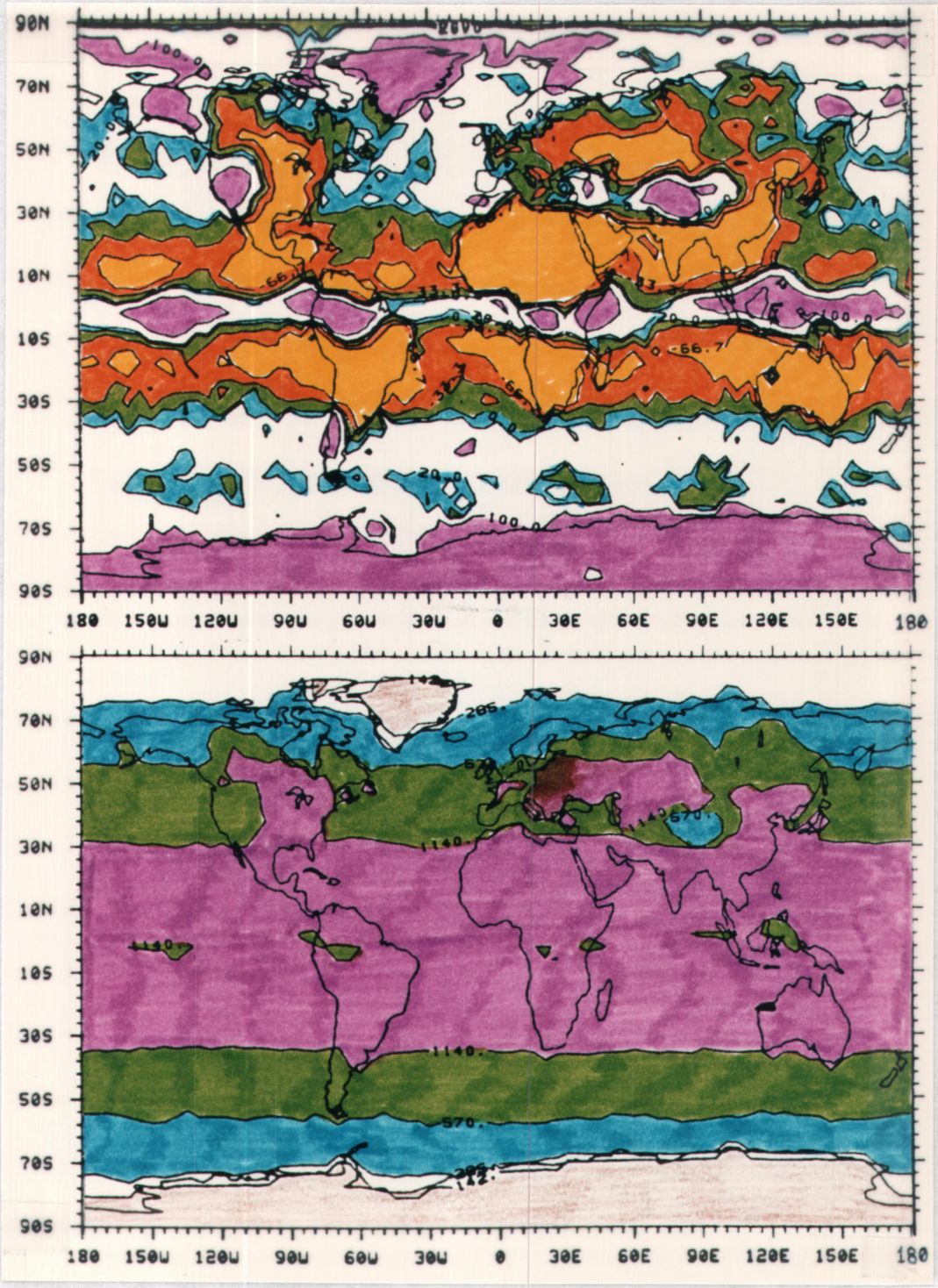

Fig. 24. Thornthwaite climate maps for SC02: first-level subdivisions (top) of moisture regions ([]A, []B, []C, []D, []E, []F) and second-level subdivisions (bottom) of thermal efficiency ([]A, []B, []C, []D, []E).

The simulated warmer-than-SWP temperature in the southern half of South America and the southern tip of Africa results in only a very slight difference in climate types there. However, the 2-4 mm/day increased precipitation in SCO2 compared to SWP in equatorial Africa results in an unbroken band of humid B and perhumid A climates in SCO2.

The distribution of thermal efficiency in SCO2 is basically the same as in SWP. The borders between the subdivisions seem to have moved a few degrees of latitude poleward, indicating a slight global warming. The megathermal regions in central Eurasia and northwestern Africa have expanded slightly. There are a few more patches of mesothermal climate embedded in the megathermal climate along the equator which tend to correspond to the regions of greatest precipitation.

4.3 Summary of Results

This section will summarize the results of the comparisons made in Sections 4.1 and 4.2 to verify the ability of the model to simulate the present climate and to analyze the model's sensitivity to increased CO_2.

4.3.1 Model Verification

The first step in the model verification part of this study was to see how closely the climate of the OSU AGCM matches the present climate. The model did fairly well in simulating the major climate

regions of the world. A summary of how the distribution of the climate types based on model-simulated data differs from those based on observed data is given in Tables 7 and 8. In many cases the model's errors reveal themselves as a shift of the boundaries of the first-level types of each of the climate classification schemes, with the interior regions matching.

Table 7. Differences in Köppen climate maps of A10 compared to those of OBS (Figs. 12 and 11, respectively).

1. Less tundra ET climate in Canada and the U.S.S.R. and much more in Tibet in A10 than in OBS; less perpetual frost EF climate in the Arctic.

2. Border between cold D climate and temperate C climate in A10 is somewhat farther south in Europe, Asia, and western North America than it is in OBS.

3. Extent and intensity of dry climate is greater in A10 than OBS in the southeastern United States, Peru, northern Argentina, southern Africa, the region east of the Caspian Sea, India, eastern China, and Australia.

4. Extent and intensity of dry climates is less in A10 than OBS in the western United States, southern Argentina, and the Gobi Desert.

5. Summers are drier and/or winters are wetter in A10 than OBS in the southern United States, northern Argentina, the southern U.S.S.R., and southern Australia.

6. Winters are drier and/or summers are wetter in A10 than OBS in Brazil, northern and equatorial Africa, Saudi Arabia, and Indonesia.

7. A10 has less monsoon climate than OBS in equatorial South America and equatorial Africa.

Table 8. Differences in Thornthwaite climate maps of A10 compared to those of OBS (Figs. 18 and 19, respectively).

1. Regions of smaller moisture index in A10 than OBS (i.e., less precipitation and/or warmer): southeastern United States, Mexico, South America except northern Brazil and southern Chile, southern Africa, India, eastern China, southeastern Asia, and most of the Australian coast.

2. Regions of larger moisture index in A10 than OBS (i.e., more precipitation and/or cooler): western North America, southern Argentina and Chile, southern tip of Africa, Europe, Tibet, Gobi Desert, Manchuria, and Indonesia.

3. Winters are drier and/or summers are wetter in A10 than OBS in northern Canada, the northern U.S.S.R., equatorial South America, and equatorial Africa.

The next step was to determine the noise level or interannual variability of the climate of the OSU AGCM. This was done by comparing the climate maps of YR1, YR2, YR3, and A10. Tables 9 and 10 contain a summary of the features exhibiting interannual variability based on Köppen's and Thornthwaite's schemes, respectively.

Table 9. Features exhibiting interannual variability using Köppen's scheme (Figs. 12-15).

1. Extent of tundra ET climate in Canada and Tibet.

2. Location of the border between the cold D and temperate C climates of North America and of Europe.

3. Extent and intensity of the dry climates in the southeastern United States, northern Argentina, southern Africa, east of the Caspian Sea, eastern China, India, and southeastern Asia.

4. Seasonality of precipitation everywhere.

Table 10. Features exhibiting interannual variability using Thornthwaite's scheme (Figs. 18-21).

1. Extent and intensity of moist regions in western North America, New England, Quebec, and equatorial Africa.

2. Extent and intensity of dry regions in the southern United States and northern Argentina.

In each of the first three years of the control simulation the extent and intensity of the first-level climate regions is slightly different and the distribution of the precipitation seasonality is generally noisy. Because of the amount of variability shown by the climate maps, it is concluded that a longer averaging time is needed to filter out the interannual variability and noise of the model. It was decided to use the average of as many years of the model simulation as were available for the best representation of the model's climate for this study. The climate maps for the ten-year mean data are definitely less noisy than the ones for the one-year mean data sets.

Table 11 shows how well the OSU AGCM and the GFDL AGCM did relative to each other in simulating the present climate for various areas. Both of the models simulate the major climate types and seasonality of precipitation fairly well. Each has problems near mountain ranges such as the Rockies, the Andes, and the Himalayas. For example, the observed steppe BS climate of the Rockies is not simulated in either model, although MH75 does simulate a steppe BS climate farther eastward.

Table 11. Relative performance of GFDL AGCM (MH75) and OSU AGCM (A10) in simulating the present climate using Köppen's scheme.

Region	MH75 better	A10 better	both good
Canada			X
western third of United States	X		
central third of United States		X	
eastern third of United States	X		
Brazil			X
Argentina	X		
east coast of South America			X
north coast of Gulf of Guinea	X		
tropical Africa	X		
southern Africa		X	
Mediterranean Coast		X	
northern Europe		X	
Europe	X		
Saudi Arabia and Pakistan		X	
India	X		
east of the Caspian Sea	X		
U.S.S.R.	X		
Gobi Desert	X		
Tibet			X
eastern China	X		
southeastern Asia		X	
Indonesia and New Guinea	X		
Australia	X		

The above model intercomparison is not really valid because of the problems of differing resolutions, observed data sets, and lengths of simulation. MH75 compare their gridpoint data with a horizontal resolution of approximately 265 km to the observed data of T68 with a different resolution. This paper compares the A10 gridpoint data with a horizontal resolution of 4° latitude by 5° longitude to the observed data of OBS with the same resolution. When trying to compare two data sets with different resolutions, it is difficult to determine whether the differences are due to the data or to the resolution.

Also, A10 is the mean of ten years of model simulation, while MH75 is only one year of model simulation. We have no way of knowing what the interannual variability of the GFDL AGCM is like. As stated earlier, one-year-mean model simulation data should not be used as being representative of the model climate when the interannual variability of the model is unknown. Too small a sampling size and differing resolutions, as well as errors in the model can contribute to differences between MH75 and T68. Climate classification schemes are based on several (preferable at least 30 or 40) years of data. Therefore it's not really realistic to base a description of climate on only one year (especially the first year of a model simulation) of data.

4.3.2 Model Sensitivity to Increased CO_2

The second part of this paper concerns the sensitivity of the climate of the OSU AGCM to an increase in the atmospheric CO_2 concentration. The interannual variability part of this study demonstrated that a sampling size of one year of model simulation data may not be representative of the model climate. However, since only one year of simulation data was available from the quadrupled CO_2 experiment, the comparison was made between it and the control ten-year mean data while keeping in mind the fact that a longer time period for QAD is required to reveal any statistically significant climate change.

The changes due to a quadrupling of atmospheric CO_2 in the climate types of the model are summarized in Tables 12 and 13. The

magnitudes of these changes are no larger than those due to interannual variability. Thus, one year of model simulation with a quadrupling of CO_2 resulted in no statistically significant climate changes compared to A10, based on Köppen's and Thornthwaite's schemes. The differences summarized in Tables 12 and 13 are very small and are given solely for completeness, and should not be regarded as significant.

Table 12. Differences in Köppen climate maps of QAD compared to those of A10 (Figs. 16 and 12, respectively).

1. QAD has slightly less precipitation than A10 in southern United States, the region east of the Caspian Sea, eastern China, and Australia.
2. ET region in Tibet is slightly smaller in QAD than in A10.
3. Border between cold D climate and temperate C climate in QAD is slightly farther south than in A10 in North America and Europe.
4. Summer (winter) of QAD is generally drier (wetter) than that of A10 in eastern North America, Europe, and Asia.
5. Winter (summer) of QAD is generally drier (wetter) than that of A10 along the northern Canadian and U.S.S.R. coasts, in eastern North America, and in southern Australia.

Table 13. Differences in Thornthwaite climate maps of QAD compared to those of A10 (Figs. 22 and 18, respectively).

1. Regions of slightly smaller moisture index (drier and/or warmer) of QAD compared to A10: west coast of North America, southeastern United States, northern Argentina, southern Africa, east of the Caspian Sea, eastern China, the Gobi Desert, and Europe.
2. Regions of slightly larger moisture index (wetter and/or cooler) of QAD compared to A10: central Canada, equatorial South America, equatorial Africa, and southeastern Asia.

No significant climate change was expected for a model with prescribed sea-surface temperatures, since the ocean temperatures weren't allowed to react to the increased CO_2; a model with a swamp ocean is more likely to produce a climate change. But both Köppen's and Thornthwaite's schemes were designed to use monthly-mean data, which is not available from a model with a swamp ocean because of the annually-averaged insolation. However, part of Thornthwaite's scheme can be used with annually-averaged data if the model-calculated (using the bulk aerodynamic method) PE is used instead of using Thornthwaite's method (for which the monthly-mean temperatures are needed).

The next logical step in this study would be to redo the model verification using Thornthwaite's scheme with the model-calculated PE and AE for both the model with prescribed sea-surface temperatures and the model with a swamp ocean. From this, the effects of an annual cycle and differing methods of calculating PE could be determined. However, one step would still be missing: the model results could not be compared to the observed data since the observed global distribution of PE is not available.

Due to time limitations, only the sensitivity of the swamp model to a doubling of atmospheric CO_2 using model-calculated PE with Thornthwaite's scheme was examined. The climate changes are summarized in Table 14.

Table 14. Differences in Thornthwaite climate maps of SCO2 compared to SWP (Figs. 24 and 23, respectively).

1.	Regions of smaller moisture index (drier and/or warmer) of SCO2 compared to SWP: central Canada, Manchuria, and the central U.S.S.R.
2.	Regions of larger moisture index (wetter and/or cooler) of SCO2 compared to SWP: equatorial Africa.

As stated in Chapter 2, a doubling of the atmospheric CO_2 concentration in the swamp model resulted in a global surface temperature warming of 2° C, which is a large climate change since this warming is about half that from the ice age climate to the present interglacial. But when using the model-calculated PE, Thornthwaite's climate classification scheme does not directly use temperature; only the precipitation and model-calculated PE are used. And the noise in the global distribution of precipitation makes any significant changes in precipitation hard to detect. Also, since Thornthwaite's moisture index is very sensitive to precipitation, significant climate changes are also hard to detect when the precipitation field is very noisy. Therefore the differences listed in Table 14 are not large.

5. CONCLUSIONS

Comparing the climate type definitions and the climate maps based on Köppen's and Thornthwaite's schemes, one can see some similarity; Table 15 tries to generalize this similarity. As shown in Table 15, the first three levels of Thornthwaite's scheme define climatic types that are similar to the first two levels of Köppen's scheme. For example, Köppen's temperate, even rainfall Cf climate corresponded to Thornthwaite's humid, mesothermal, little or no water deficiency BBr climate in the examples discussed in Chapter 2.

Table 15. Comparison of Köppen and Thornthwaite climate types.

Köppen climate type	Corresponding Thornthwaite climate type(s)	
1st Level	1st Level	2nd Level
A	A,B	A
BS	D,E	A
BW	E,F	A
C	A,B,C,D	A,B
D	A,B,C,D	B,C,D
ET		D
EF		E
2nd Level	3rd Level	
f	r,d	
s	s	
w	w	

Looking at the Köppen maps for OBS (Fig. 11), one can see that except for the desert and steppe regions, the other first-level

climate types are somewhat zonal. Although the Thornthwaite maps for OBS (Fig. 17) show about the same detail as Köppen's for the arid and semi-arid regions, more detail is shown by the other Thornthwaite first-level divisions. For example, the simulated drier-than-observed region in central South America and the simulated wetter-than-observed region in southern South America are more obvious in the Thornthwaite maps (Fig. 18a compared to Fig. 17a) than in the Köppen maps (Fig. 12 compared to Fig. 11). This difference in sensitivity could be due to the combination of variables used to delineate the first-level subdivisions, or it could be due to the subdivisions themselves, i.e., maybe it would be better to subdivide Köppen's tropical and temperate climate types further.

Köppen's second-level and Thornthwaite's third-level subdivisions define seasonal precipitation characteristics. Thornthwaite's scheme differs from Köppen's in that it makes a distinction whether a water surplus/deficiency is exceptional for a region. For example, the simulated winter is drier than the simulated summer in northern Australia and vice versa in southern Australia. These two regions are shown by the Köppen scheme in Fig. 12 as a desert dry winter BWw climate and a desert dry summer BWs climate, respectively. However, Thornthwaite's scheme makes no distinction between these two regions, since neither region has a season of exceptional water surplus and a dry season is not unusual in a desert climate. Therefore, all of Australia is shown as an arid Fd climate with little or no water surplus in Fig. 18a.

Both schemes give complementary information about the seasonal precipitation characteristics: Köppen's scheme defines a relative dry season while Thornthwaite's scheme differentiates whether a season of precipitation surplus/deficit is unusual for a region.

As stated earlier, the climate of an area is not determined by any single factor, but rather by the distinctive regional integration of several factors. Except for the two dry climate types (BS and BW), Köppen's first-level subdivisions (A, C, D, ET, and EF) are based upon temperature only, and all the second-level subdivisions are based upon precipitation only. Thornthwaite's scheme uses combinations of temperature and precipitation in all four levels. Use of a scheme which bases its climatic boundaries upon the interaction of climatic elements, such as Thornthwaite's scheme, would complement the examination of the raw data from GCM's.

Neither Köppen's nor Thornthwaite's schemes take into account intramonthly variability. When monthly-mean data are used, the effects of the extremes are smoothed out. The mean rainfall of a month with 30 days of 1 mm/day is the same as for a month with 30 mm of rain for one day and no rain for the other 29 days.

Both Köppen's and Thornthwaite's schemes were designed to be used with long-term monthly-mean data, so that the effect of interannual variability is averaged out. Since the actual climate is affected by anomalies as well as the mean, the climate type based on one year's data may be different from the climate type based on the mean of ten years of data. Unless long-term mean data from GCMs is

always used, it is important to determine the magnitude of the interannual variability of the climate of the model; otherwise noise of the model may be mistaken as a definite climate change.

The comparison of the climate maps of YR1, YR2, YR3, and A10 illustrates the interannual variability of the model. While the distribution of the main climate types of Köppen's scheme remains fairly constant for the four data sets, the distribution of the second-level climate types is very noisy in YR1, YR2, and YR3. However, if you were to place the Thornthwaite climate maps for these four data sets side by side, it would be less apparent which maps were based upon one year's worth of data and which were based upon the mean of ten years of data. This difference between Köppen and Thornthwaite is probably due to the fact that Köppen's second level is based on values of precipitation only, while Thornthwaite's corresponding third level is based upon a combination of precipitation and temperature. The effect of the interannual variability of the precipitation is lessened when combined with temperature.

While a perturbation may result in a change in the temperature and precipitation patterns of a region, it may not imply a change in the climatic type of that region. The climate changes due to a quadrupling of CO_2 in the model with seasonal insolation and prescribed sea surface temperatures and due to a doubling of CO_2 in the swamp model appeared to be insignificant using the climate classification schemes.

The results from the quadrupled CO_2 experiment are not conclusive, since only one year of model simulation was available. The

magnitude of the differences between the climate maps of QAD and A10 are no larger than those due to interannual variability. As discussed earlier, several years of model simulation are needed to eliminate the interannual variability.

However, the doubled-CO_2 simulation was shown to have reached equilibrium after 300 days of simulation (Schlesinger, 1984) and the data used in this study were the means of the last 180 days of a 720 day simulation. There is essentially no difference in climate types between SWP and SCO2, except for equatorial Africa. The locations of the boundaries between the climate types of the various regions differ only slightly between SCO2 and SWP. The moisture regions simulate by the swamp model are rather noisy compared to those simulated by the seasonal model; filtering of the precipitation field could eliminate some of this noise.

The statistical significance of the differences in temperature and precipitation is discussed in Schlesinger (1984). Although there are several regions in which the temperature differences are statistically significant, almost all the precipitation differences are statistically insignificant. Whether a change in climate types is statistically significant is difficult to determine with climate classification schemes, since the types themselves are not pure numbers. However, one could determine the statistical significance of differences in PE, PESC, and the moisture index of Thornthwaite's scheme.

The global warming due to doubled CO_2 in the swamp model was 2°C which is about half that from the ice age climate to the present

interglacial. Yet there was no apparent change in climate types based on Thornthwaite's scheme. One explanation for this discrepancy is that Thornthwaite's scheme is accurate in its finding that there is no vegetation climate change due to doubled CO_2 simulated by the swamp model. Although there may be statistically significant temperature changes in various regions, the process of classifying the climate combines the effects of several variables, thereby obscuring the individual effects.

Another explanation is that Thornthwaite's scheme is not sensitive enough to detect climate changes of the magnitude due to a doubling of atmospheric CO_2. Maybe climate classification schemes need to use more climatic variables since climate is the result of the interaction of many variables, of which temperature and precipitation are just two. Or maybe the schemes just need to use different combinations of variables to represent the climate.

One of the weaker sections of Thornthwaite's scheme is his computation of PE; although it gives reasonable results in the mid-latitudes (Bailey and Johnson, 1972), it is not to be trusted in very hot or cold regions (Thornthwaite, 1948; Bailey and Johnson, 1972). A possible improvement would be to use the PE and AE calculated (using the bulk aerodynamic method) by GCMs. Thornthwaite's PE formula is a function of temperature and latitude only, while the bulk aerodynamic formula is a function of surface air density, surface elevation, surface wind speed, surface air water vapor mixing ratio, and the surface saturation mixing ratio at ground temperature (Ghan et al., 1982). It is possible that the non-dry Gobi Desert in A10

and many other model simulation "errors" as well as the lack of sensitivity of Thornthwaite's climate classification to climate change induced by doubled CO_2 in the swamp model are the result of using the moisture budget PE instead of the model-calculated PE.

The calculation of PE based on the bulk aerodynamic method would also be accessible to annual-averaged models. However, the third level (relative dry season) subdivisions using annual-averaged data would be questionable, since the annual water surplus (deficit) needed to compute the humidity (aridity) index would have to rely solely on the annual-mean precipitation (P), PE, and AE (Mather,1974):

$$S = P - AE$$

$$D = PE - AE$$

due to the lack of monthly-mean data required to determine a moisture budget. When using the model-calculated PE the numerical boundaries of the moisture regions might be changed slightly to allow a more even distribution. For example, instead of considering a region where $Im < -66.7$ as arid, the boundary might be changed to $Im < -75$.

One problem with using the model-calculated PE and AE is the lack of global distributions of observed PE and AE. Therefore, only comparisons between GCM runs can be made without considering variance due to different methods of calculating PE and AE (i.e., if climate maps using the model-calculated PE and AE were compared to climate maps using the Thornthwaite-calculated PE and AE based on the

observed temperature and precipitation, then the differences could be due to either the model simulation or the different methods of calculating PE and AE used by the model and by Thornthwaite.)

The variety of data provided by GCM simulations offers an excellent opportunity to derive a new classification scheme (perhaps based on vegetation, perhaps based on something else) using multivariate statistical techniques. This would also allow for a more rigorous way of determining the statistical significance of climate changes. For example, perhaps a "distance measure" could be chosen to describe how a climate type resulting from a perturbation compares to the climate type of the control.

BIBLIOGRAPHY

Bailey, H. P. and C. W. Johnson, 1972: "Potential evapotranspiration in relation to annual waves of temperature," Publ. Clim., 25(2), 4-12.

Bregman, L. D., 1978: "The performance of the Rand atmospheric general circulation model in terms of Koppen's classification of climates," Rand Internal Note 23928-AF, Santa Monica, CA, 20 pp.

Carter, D. B., 1966: "Characteristics of climate classification," Publ. Clim., 19(4), 305-308.

Crutcher, H. L. and J. M. Meserve, 1970: Selected Level Heights, Temperatures, and Dew Points for the Northern Hemisphere, NAVAIR 50-1C-52, Naval Weather Service Command, Washington, D.C.

Flohn, H., 1950: "Neue Anschauungen ueber die allgemeine Zirkulation der Atmosphaere und ihre klimatische Beduetung," Erdkunde, 4, 141-162.

Gates, W. L., E. S. Batten, A. B. Kahle, and A. B. Nelson, 1971: "A Documentation of the Mintz-Arakawa Two-Level Atmospheric General Circulation Model," R-877-ARPA, The Rand Corporation, Santa Monica, 408 pp.

Gates, W. L. and M. E. Schlesinger, 1977: "Numerical simulation of the January and July global climate with a two-level atmospheric model," JAS, 34(1), 36-76.

Gates, W. L., K. H. Cook, and M. E. Schlesinger, 1981: "Preliminary analysis of experiments on the climatic effects of increased CO_2 with an atmospheric general circulation model and a climatological ocean," J. Geophys. Res., 86, 6385-6393.

Ghan, S. J., J. W. Lingaas, M. E. Schlesinger, R. L. Mobley, and W. L. Gates, 1982: "A documentation of the OSU two-level atmospheric general circulation model," Report No. 35, Climatic Research Institute, Oregon State University, Corvallis, 395 pp.

Hansen, J., A. Lacis, D. Rind, and G. Russell, 1984: Climate Processes and Climate Sensitivity, (Maurice Ewing Series, 5, editors J. E. Hansen and T. Takahashi), American Geophysical Union, Washington, D.C., 368 pp.

Haurwitz, B. and J. M. Austin, 1944: Climatology, McGraw-Hill, New York.

Hendl, M., 1963: Einfuehrung in die Physikalische Klimatologie, 2, VEP Deutscher Verlag der Wissenschafter, Berlin, 40 pp.

Jaeger, L., 1976: "Monatskarten des Niederschlags fuer die ganze Erde," Ber. Deutsch. Wetterdienstes, Nr. 139, Offenbach, 38 pp.

Köppen, W., 1931: Grundriss der Klimakunde, Walter de Gruyter, Berlin.

Köppen, W., 1936: Das geographische system der Klimate, in Handbuch der Klimatologie 1, part C, ed. W. Koppen and G. Geiger, Boentraeger, Berlin.

Manabe, S. and J. L. Holloway, 1975: "The seasonal variation of the hydrological cycle as simulated by a global model of the atmosphere," J. Geophy. Res., 80(12), 1617-1649.

Manabe, S., K. Bryan, and M. J. Spelman, 1979: "A global ocean-atmosphere climate model with seasonal variation for future studies of climate sensitivity," Dyn. Atmos. Oceans, 3, 393-426.

Mather, J. R., 1966: "Elements of the classification," Publ. Clim., 19(4), 341-352.

Mather, J. R., 1974: Climatology: Fundamentals and Applications, McGraw-Hill Book Company, San Francisco, CA, 412 pp.

Saltzman, B., 1978: "A survey of statistical-dynamical models of the terrestrial climate," Advances in Geophysics, 20, 183-304.

Schlesinger, M. E., 1984: "Mathematical Modeling and Simulation of Climate and Climate Change," invited lecture at the Institut D'Astronomie et de Geophysique Georges Lemaitre, Universite Catholique de Louvain, Louvain-la-Neuve, Belgique, May, 1984.

Schlesinger, M. E. and W. L. Gates, 1980: "The January and July performance of the OSU two-level atmospheric general circulation model," JAS, 37, 1914-1943.

Schneider, S. H. and R. E. Dickinson, 1974: "Climate Modeling," Rev. of Geophys. and Space Phys., 12(3), 447-493.

Taljaard, J. J., H. van Loon, H. L. Crutcher, and R. L. Jenne, 1969: Climate of the Upper Air: Southern Hemisphere, Vol. 1, Temperatures, Dew Points and Heights at Selected Pressure Levels, NAVAIR 50-1C-55, Naval Weather Service Command, Washington, D.C.

Thornthwaite, C. W., 1948: "An approach toward a rational classification of climate," Geogr. Rev., 38(1), 54-94.

Thornthwaite, C. W., 1954: "The determination of potential evapotran spiration," Publ. Clim., 7, (1), 218-225.

Thornthwaite, C. W. and J. R. Mather, 1955: "Instructions for evaluating the water balance," Publ. Clim., 8(1), 87-104.

Trewartha, G. T., 1968: Introduction to Climate, McGraw-Hill Book Company, San Francisco, CA, 408 pp.

Trewartha, G. T. and L. H. Horn, 1980: An Introduction to Climate, McGraw-Hill Book Company, New York, 416 pp.

Willmott, C. J., 1977: "WATBUG: A FORTRAN IV algorithm for calculating the climatic water budget," Publ. Clim., 30(2), 55 pp.

APPENDICES

Appendix A. Flowchart of Water Balance Routine

The first of the following two pages shows a flowchart of the main portion of the water balance routine used in the code in Appendix C; the second page contains the flowchart of a module shown in the main flowchart. Abbreviations used in the flowcharts are:

FC = field capacity
ST = soil moisture storage
SST = snowpack storage
MELT = snowmelt

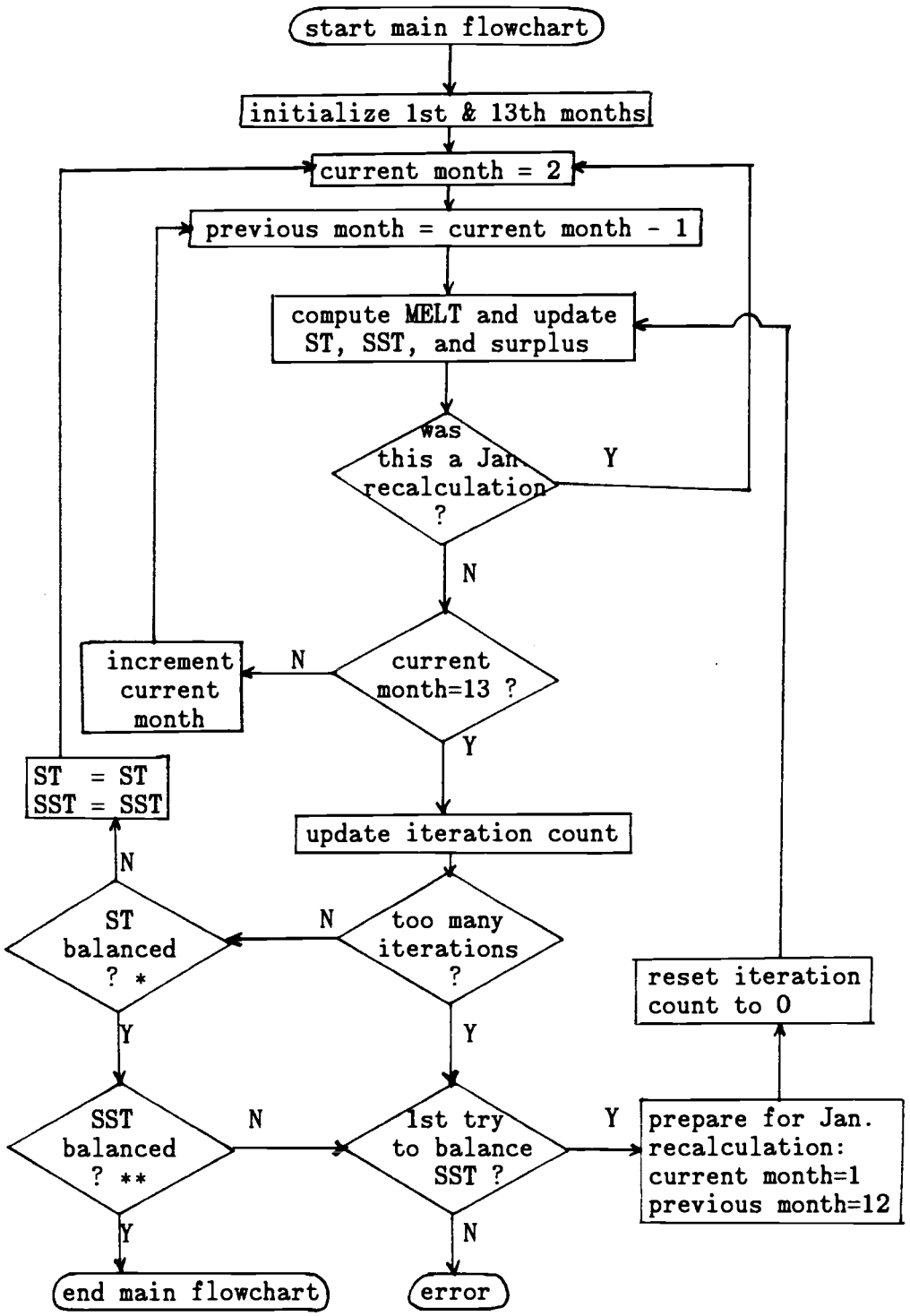

* ST is defined to be "balanced" if $ST_{Jan} = ST_{Dec}$.

** SST is defined to be "balanced" if the difference between SST_{Jan} and SST_{Dec} is either negligible or has not increased from last year.

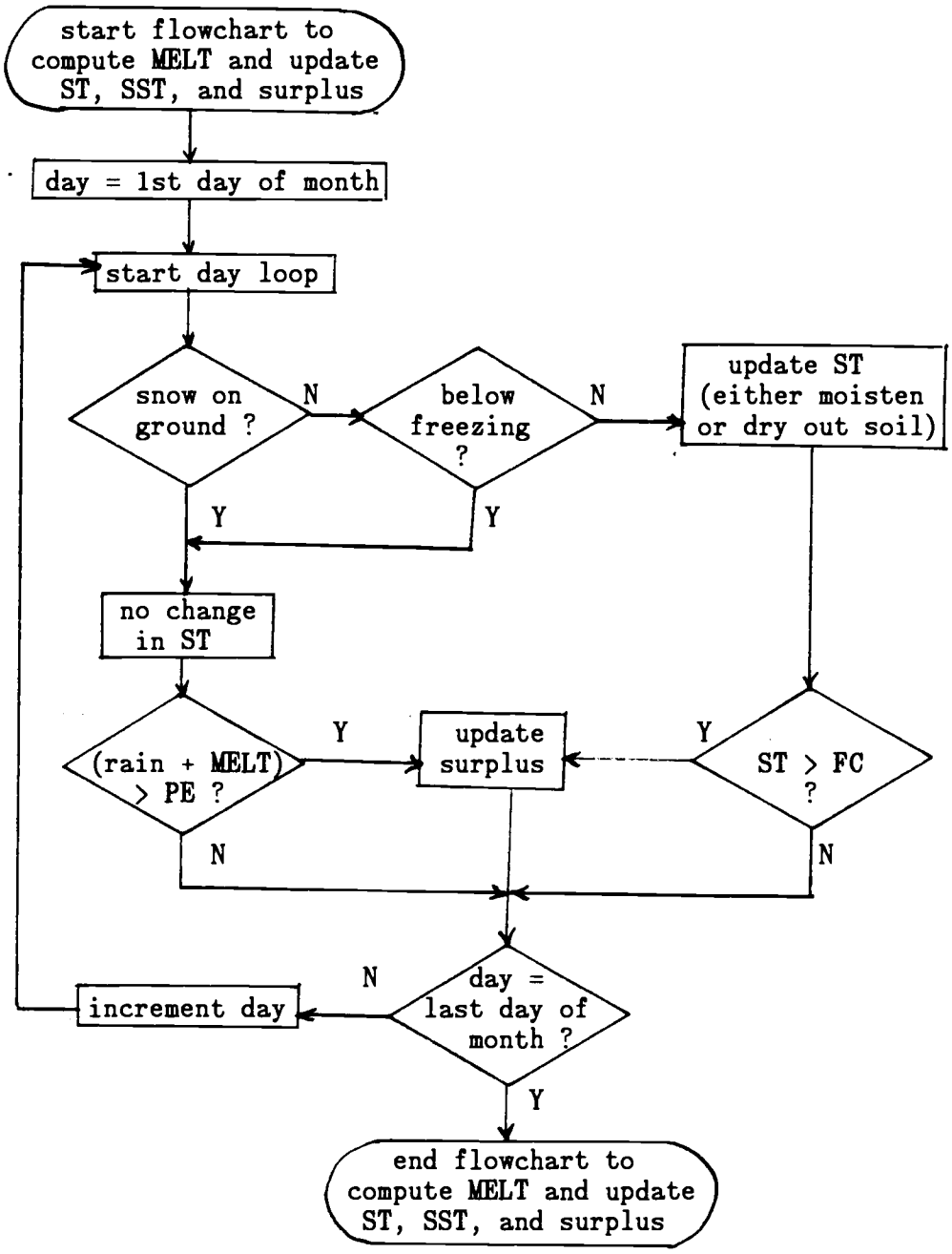
start flowchart to compute MELT and update ST, SST, and surplus
day = 1st day of month
start day loop
snow on ground ?
N
below freezing ?
N
update ST (either moisten or dry out soil)
Y
Y
no change in ST
(rain + MELT) > PE ?
Y
update surplus
Y
ST > FC ?
N
N
day = last day of month ?
N
increment day
Y
end flowchart to compute MELT and update ST, SST, and surplus

Appendix B. Listing of Köppen Classification Code

```
      PROGRAM KOPPEN
C
C -----------------------------------------------------------------
C
C     INPUT FOR THIS CODE FOR EACH COORDINATE:
C
C        R(12) = MONTHLY RAINFALL IN MM/DAY
C        T(12) = MONTHLY AVERAGED TEMPERATURE IN DEG C
C
C     ALL CALCULATIONS ARE DONE IN INCHES AND DEG F.
C
C     USING KOPPEN'S METHOD OF CLASSIFICATION, EACH COORDINATE IS
C     ASSIGNED A CLASSIFICATION CODE = DESCRP(L,I,1),
C     WHICH CONSISTS OF NOT MORE THAN 4 DESCRIPTORS:
C
C        DESCRP(L,1,1)  DESCRP(L,2,1)  DESCRP(L,3,1)  DESCRP(L,4,1)
C
C         A             F,W,M                         I
C         B             W,S             W,S,F         H,K,P
C         C             W,S,F           A,B,C         I
C         D             W,S,F           A,B,C,D       I
C         E             T,F
C
C -----------------------------------------------------------------
C
      COMMON /Z1/ T(12),R(12),AT,AR,TMIN,TMAX,RMIN,RMAX,
     XWW,WS,DW,DS,DIEM(12),IT4,L
      DIMENSION IX(46)
      BYTE DESCRP(3312,4,1)
      CHARACTER*3 XPRMT
      CHARACTER*20 FILE
C
      DATA DIEM/31.,28.,31.,30.,31.,30.,31.,31.,30.,31.,30.,31./
      DATA FILE/'LB:[102,3]XT    .DAT '/
C
      OPEN(UNIT=5,NAME='TI:',TYPE='NEW',CARRIAGECONTROL='LIST')
      WRITE(5,2040)
      READ(5,2050) XPRMT
      FILE(13:15)=XPRMT(1:3)
      OPEN(UNIT=1,NAME=FILE,TYPE='OLD',FORM='UNFORMATTED',
     XREADONLY)
      FILE(12:12)='P'
      OPEN(UNIT=3,NAME=FILE,TYPE='OLD',FORM='UNFORMATTED',
     XREADONLY)
C
      DO 9900 L=1,3312
C
C --- SET UP INITIAL VALUES ---------------------------------
```

```
C
      READ(1) T
      READ(3) R
      CALL AVG
      DO 10 I=1,4
   10 DESCRP(L,I,1)=' '
C
C --- B CLIMATES ------------------------------------------
C
      IF(WS.GE.(10.*DW)) GO TO 100
      IF(WW.GE.(3.*DS)) GO TO 200
C
C --- EVEN RAINFALL
C
      IF(AR.GT.(.22*AT-4.25)) GO TO 300
      DESCRP(L,2,1)='W'
      DESCRP(L,3,1)='F'
      GO TO 700
  300 IF(AR.GT.(.44*AT-8.5)) GO TO 1000
      DESCRP(L,2,1)='S'
      DESCRP(L,3,1)='F'
      GO TO 700
C
C --- RAINFALL MAX IN SUMMER
C
  100 IF(AR.GT.(.22*AT-1.5)) GO TO 150
      DESCRP(L,2,1)='W'
      DESCRP(L,3,1)='W'
      GO TO 700
  150 IF(AR.GT.(.44*AT-3.)) GO TO 1000
      DESCRP(L,2,1)='S'
      DESCRP(L,3,1)='W'
      GO TO 700
C
C --- RAINFALL MAX IN WINTER
C
  200 IF(AR.GT.(.22*AT-7.)) GO TO 250
      DESCRP(L,2,1)='W'
      DESCRP(L,3,1)='S'
      GO TO 700
  250 IF(AR.GT.(.44*AT-14.)) GO TO 1000
      DESCRP(L,2,1)='S'
      DESCRP(L,3,1)='S'
C
C --- ADDITIONAL DESCRIPTORS (4TH LEVEL)
C
  700 DESCRP(L,1,1)='B'
      IF(TMAX.GE.64.4) GO TO 750
      DESCRP(L,4,1)='P'
      GO TO 9000
  750 IF(AT.LT.64.4) DESCRP(L,4,1)='K'
```

```
      IF(AT.GE.64.4) DESCRP(L,4,1)='H'
      GO TO 9000
 1000 IF(TMIN.GT.64.4) GO TO 1500
      IF(TMAX.GT.50.) GO TO 1200
C
C --- E CLIMATE ------------------------------------------------
C
      DESCRP(L,1,1)='E'
      DESCRP(L,2,1)='F'
      IF(TMAX.GT.32.) DESCRP(L,2,1)='T'
      GO TO 9000
C
C --- A CLIMATE ------------------------------------------------
C
 1500 DESCRP(L,1,1)='A'
      IF(RMIN.LT.2.4) GO TO 1550
      DESCRP(L,2,1)='F'
      GO TO 1980
 1550 DESCRP(L,2,1)='M'
      IF(RMIN.LT.(3.94-AR/25.)) DESCRP(L,2,1)='W'
      GO TO 1980
C
C --- C CLIMATE ------------------------------------------------
C
 1200 IF(TMIN.LT.26.6) GO TO 1400
      DESCRP(L,1,1)='C'
      GO TO 1600
C
C --- D CLIMATE ------------------------------------------------
C
 1400 DESCRP(L,1,1)='D'
C
C --- ADDITIONAL DESCRIPTORS (2ND LEVEL)
C
 1600 IF(DS.GT.DW) GO TO 1610
C
C ... CHECK FOR S BEFORE CHECKING FOR W
C
      IF(WW.LT.(3.*DS)) GO TO 1610
      IF(DS.GE.1.2) GO TO 1610
      DESCRP(L,2,1)='S'
      GO TO 1800
C
 1610 IF(WS.LT.(10.*DW)) GO TO 1650
      DESCRP(L,2,1)='W'
      GO TO 1800
 1650 IF(WW.LT.(3.*DS)) GO TO 1700
      IF(DS.GE.1.2) GO TO 1700
      DESCRP(L,2,1)='S'
      GO TO 1800
 1700 DESCRP(L,2,1)='F'
```

```
C
C --- MORE DESCRIPTORS (3RD LEVEL)
C
 1800 IF(DESCRP(L,1,1).NE.'D') GO TO 1900
      IF(TMIN.GE.-36.4) GO TO 1900
      DESCRP(L,3,1)='D'
      GO TO 1980
 1900 IF(TMAX.LE.71.6) GO TO 1950
      DESCRP(L,3,1)='A'
      GO TO 1980
 1950 DESCRP(L,3,1)='C'
      IF(IT4.EQ.1) DESCRP(L,3,1)='B'
C
C --- EVEN MORE DESCRIPTORS (4TH LEVEL)
C
 1980 IF((TMAX-TMIN).LT.9.) DESCRP(L,4,1)='I'
C
 9000 CONTINUE
C
 9900 CONTINUE
C
C ------ WRITE INTO PRINT FILE ----------------------------
C
      CLOSE(1)
      FILE='SY:[101,46]K    .PRT '
      FILE(13:15)=XPRMT(1:3)
      OPEN(UNIT=1,NAME=FILE,TYPE='NEW')
      DO 50 I=1,46
   50 IX(I)=I
      DO 55 K=1,2
      I1=24
      IF(K.EQ.1) I1=1
      WRITE(1,2010) (IX(I),I=I1,I1+22)
      DO 60 J=1,72
   60 WRITE(1,2020) J,((DESCRP(72*I-72+J,JX,1),JX=1,4),I=I1,I1+22)
   55 CONTINUE
C
C ------ WRITE INTO KMAP PLOT FILE ------------------------
C
      CLOSE(1)
      FILE(17:19)='DAT'
      OPEN(UNIT=1,NAME=FILE,TYPE='NEW',FORM='UNFORMATTED')
      DO 65 J=1,72
   65 WRITE(1) J,((DESCRP(72*I-72+J,JX,1),JX=1,4),I=1,46)
C
C --- FORMAT STATEMENTS --------------------------------------
C
 2010 FORMAT(1H1,5X,23(I2,3X),/)
 2020 FORMAT(1X,I2,2X,23(4A1,1X))
 2040 FORMAT(' INPUT EXPERIMENT CODE NAME (A3)')
 2050 FORMAT(A3)
```

```
C
      STOP
      END
C
      SUBROUTINE AVG
C
C -------------------------------------------------------------
C
C     INPUT FOR THIS SUB:
C
C        T(12) = MONTHLY AVG TEMPERATURE IN DEG C
C        R(12) = MONTHLY RAINFALL IN MM/DAY
C
C     OUTPUT FROM THIS SUB:
C
C        TMIN = MINIMUM MONTHLY AVG TEMP IN DEG F
C        TMAX = MAXIMUM MONTHLY AVG TEMP IN DEG F
C
C        IT4 = INDICATOR THAT AT LEAST 5 MO. HAVE T>50 C (IT4=1)
C
C        RMIN = MINIMUM MONTHLY RAINFALL IN INCHES
C        RMAX = MAXIMUM MONTHLY RAINFALL IN INCHES
C
C        WW = RAINFALL OF WETTEST WINTER MONTH IN INCHES
C        WS = RAINFALL OF WETTEST SUMMER MONTH IN INCHES
C        DW = RAINFALL OF DRIEST WINTER MONTH IN INCHES
C        DS = RAINFALL OF DRIEST SUMMER MONTH IN INCHES
C
C -------------------------------------------------------------
C
      COMMON /Z1/ T(12),R(12),AT,AR,TMIN,TMAX,RMIN,RMAX,
     XWW,WS,DW,DS,DIEM(12),IT4,L
C
C --- CONVERT DEG C TO DEG F AND MM/DAY TO INCHES ---------------
C
      DO 40 I=1,12
      T(I)=9.*T(I)/5.+32.
   40 R(I)=R(I)/25.4*DIEM(I)
C
C --- TEMPERATURE CALCULATIONS ----------------------------------
C
      TMIN=T(1)
      TMAX=T(1)
      AT=0.
      DO 10 I=1,12
      TMIN=AMIN1(T(I),TMIN)
      TMAX=AMAX1(T(I),TMAX)
   10 AT=AT+T(I)*DIEM(I)/365.
C
C --- IT4 INDICATOR THAT AT LEAST 5 MONTHS HAVE T>50 DEG C
C
```

```
      J=0
      DO 15 I=1,12
      IF(T(I).GT.50.) J=J+1
   15 CONTINUE
      IT4=0
      IF(J.GT.4) IT4=1
C
C --- PRECIPITATION CALCULATIONS --------------------------------
C
      RMIN=R(1)
      RMAX=R(1)
      AR=0.
      DO 20 I=1,12
      RMIN=AMIN1(R(I),RMIN)
      RMAX=AMAX1(R(I),RMAX)
   20 AR=AR+R(I)
C
      IF(L.GT.1656) GO TO 50
C
C --- COORDINATE IN SOUTHERN HEMISPHERE -----------------------
C
   25 WW=R(4)
      DW=R(4)
      DO 30 I=4,9
      WW=AMAX1(R(I),WW)
   30 DW=AMIN1(R(I),DW)
C
      WS=R(1)
      DS=R(1)
      DO 90 I=1,3
      WS=AMAX1(R(I),WS)
      WS=AMAX1(R(I+9),WS)
      DS=AMIN1(R(I),DS)
   90 DS=AMIN1(R(I+9),DS)
      GO TO 80
C
C --- COORDINATE IN NORTHERN HEMISPHERE -----------------------
C
   50 WW=R(1)
      DW=R(1)
      DO 60 I=1,3
      WW=AMAX1(R(I),WW)
      WW=AMAX1(R(I+9),WW)
      DW=AMIN1(R(I),DW)
   60 DW=AMIN1(R(I+9),DW)
C
      WS=R(4)
      DS=R(4)
      DO 70 I=4,9
      WS=AMAX1(R(I),WS)
   70 DS=AMIN1(R(I),DS)
```

```
C
   80 CONTINUE
C
      RETURN
      END
```

Appendix C. Listing of Seasonal Thornthwaite Classification Code

```
      PROGRAM THORN
C
C -------------------------------------------------------------
C
C     THIS CODE CLASSIFIES CLIMATES ACCORDING TO
C     THORNTHWAITE'S 1955 SCHEME, USING GLOBAL DATA.
C
C -------------------------------------------------------------
C
C     UNITS ARE DEGREES CELSIUS AND MILLIMETERS.
C
C -------------------------------------------------------------
C
C     T(12)       = MONTHLY MEAN TEMP FOR A GRID POINT
C     P(12)       = MONTHLY PRECIP FOR A GRID POINT
C     RN(12)      = MONTHLY RAINFALL
C     SF(12)      = MONTHLY SNOWFALL
C     ST(12)      = MONTHLY SOIL MOISTURE (RAINFALL) STORAGE
C     SST(12)     = MONTHLY SOIL MOISTURE (SNOWFALL) STORAGE
C     P12         = ANNUAL PRECIP FOR A GRID POINT
C     AE(12)      = MONTHLY ACTUAL EVAPOTRANSPIRATION FOR A
C                   GRID POINT
C     AE12        = ANNUAL ACTUAL EVAPOTRANSPIRATION FOR A
C                   GRID POINT
C     HINDEX      = HEAT INDEX
C     UNADJ       = UNADJUSTED MONTHLY PE
C     PE(12)      = MONTHLY POTENTIAL EVAPOTRANSPIRATION
C                   FOR A GRID POINT
C     PE12        = ANNUAL PE FOR A GRID POINT
C     SUM3        = SUM OF PE FOR SUMMER MONTHS
C     PESC        = SUMMER CONCENTRATION OF PE
C     RMPE(12)    = R - PE
C     SUR(12)     = MONTHLY MOISTURE SURPLUS
C     SUR12       = ANNUAL MOISTURE SURPLUS
C     DEF(12)     = MONTHLY MOISTURE DEFICIT
C     DEF12       = ANNUAL MOISTURE DEFICIT
C     XIH         = ANNUAL HUMIDITY INDEX
C     XIA         = ANNUAL ARIDITY INDEX
C     XIM         = ANNUAL MOISTURE INDEX
C
C -------------------------------------------------------------
C
C     >TKB
C     TKB>THORN=THORN
C     TKB>/
C     Enter options:
C     TKB>UNITS=6
```

```
C     TKB>ACTFIL=6
C     TKB>LIBR=FCSRES:RO
C     TKB>//
C
C ------------------------------------------------------------
C
      DIMENSION TEMP(12),PRECIP(12),HSUN(12,46),ISWM(6,2)
      COMMON /Z1/ RMPE(13),ST(13),FC,SUR(13),DST(13),
     XDAYSPM(13),DEF(13),L,L1,DEC,PI,P(13),T(13),PE(13),
     XSF(13),RN(13),SST(13),SMT(13),DS,AE(13),JVERIF(10,2),JV
      CHARACTER*1 LAND(72)
      CHARACTER*8 XPRMT
      CHARACTER*20 FILE
      BYTE DESCRP(3312,4,1)
C
      DATA FILE/'LB:[102,3]XT    .DAT '/
      DATA FC/150./
      DATA PI,L72,L46/3.14159,72,46/
      DATA DAYSPM/31.,28.,31.,30.,31.,30.,31.,31.,
     X30.,31.,30.,31.,31./
      DATA ISWM/4,5,6,7,8,9,10,11,12,1,2,3/
C
C ------ OPEN FILES ---------------------------------------
C
      OPEN(UNIT=1,NAME='XOUCH.DAT',TYPE='NEW',
     XFORM='UNFORMATTED')
      OPEN(UNIT=5,NAME='TI:',TYPE='OLD',
     XCARRIAGECONTROL='LIST')
      WRITE(5,2040)
      READ(5,2050) XPRMT
      WRITE(1) XPRMT
      FILE(13:15)=XPRMT(1:3)
      OPEN(UNIT=2,NAME=FILE,TYPE='OLD',FORM='UNFORMATTED',
     XREADONLY)
      FILE(12:12)='P'
      OPEN(UNIT=3,NAME=FILE,TYPE='OLD',FORM='UNFORMATTED',
     XREADONLY)
      OPEN(UNIT=6,NAME='SY:TMAP.DAT',TYPE='OLD',READONLY)
C
C ..... VERIFICATION FILE INFO .........................
C
      OPEN(UNIT=4,NAME='VERIFY.PRT',TYPE='NEW')
      WRITE(5,2070)
      READ(5,2060) JV
      DO 650 J=1,JV
      WRITE(5,2080) J
      READ(5,2090) (JVERIF(J,I),I=1,2)
  650 CONTINUE
C
C ------ HRS SUN PER DAY (DAILY SUMS) EQUATORWARD OF 50 ----
C
```

```
      DO 520 L1=11,36
C
      PHI=(FLOAT(L1)-23.5)*4.*PI/180.
      IF(PHI.GT.50.*PI/180.) PHI=50.*PI/180.
      IF(PHI.LT.-50.*PI/180.) PHI=-50.*PI/180.
      DAYSVE=284.
      DO 40 M=1,12
      HSUN(M,L1)=0.
      KDM=DAYSPM(M)+.1
      DO 45 KD=1,KDM
      DAYSVE=DAYSVE+1.
      IF(DAYSVE.GT.365.) DAYSVE=DAYSVE-365.
      DEC=23.46*SIN(DAYSVE/365.*2.*PI)*PI/180.
      IF(DEC.EQ.0.) THEN
C
C ..... EQUINOX
C
        HSUN(M,L1)=HSUN(M,L1)+12.
      ELSE
        HSUN(M,L1)=HSUN(M,L1)+
     X  2.*ACOS(COS((90.+5./6.)*PI/180.)/COS(PHI)/COS(DEC)
     X  -TAN(PHI)*TAN(DEC))*12./PI
      END IF
   45 CONTINUE
      HSUN(M,L1)=HSUN(M,L1)/DAYSPM(M)
   40 CONTINUE
  520 CONTINUE
C
C ------ USE HSUN AT 50 FOR POLEWARD OF 50 -----------------
C
      DO 540 M=1,12
      DO 530 L1=1,10
      HSUN(M,L1)=HSUN(M,11)
      HSUN(M,L1+36)=HSUN(M,36)
  530 CONTINUE
  540 CONTINUE
C
C ------ START LATITUDE (L1) LOOP ------------------------
C
      DO 510 L1=1,L46
      PHI=(FLOAT(L1)-23.5)*4.*PI/180.
C
C ..... READ IN SURFACE TYPES ............................
C
      REWIND(6)
      DO 50 I=1,47-L1
   50 READ(6,2100)
      READ(6,2110) LAND
C
C ........ TERMINAL PROGRESS MESSAGES .....................
C
```

```
      IF(L1.EQ.1) WRITE(5,1010)
      IF(L1.EQ.2) WRITE(5,1040)
      IF(L1.EQ.20) WRITE(5,1020) 46-L1
      IF(L1.EQ.40) WRITE(5,1030) 46-L1
C
C ..... INDICES FOR SUMMER MONTHS .....................
C
      IF(L1.LE.23) THEN
        IS=2
        IW=1
      ELSE
        IS=1
        IW=2
      END IF
      ISMAX=ISWM(3,IS)
      ISMAX1=ISWM(4,IS)
      ISMAX2=ISWM(5,IS)
      ISMIN=ISWM(3,IW)
      ISMIN1=ISWM(4,IW)
      ISMIN2=ISWM(5,IW)
C
C ------ START LONGITUDE (L) LOOP ----------------------
C
      DO 500 L=1,72
C
C ..... WRITE HEADER FOR STATION CHECK ................
C
      DO 640 J=1,JV
      IF(L1.EQ.JVERIF(J,1).AND.L.EQ.JVERIF(J,2)) THEN
        WRITE(4,2025) (I,I=1,12)
      END IF
  640 CONTINUE
C
      L3312=(L1-1)*72+L
      READ(2) TEMP
      READ(3) PRECIP
C
C ..... SHORT RUN FLAG & STATION PROGRESS INFO .........
C
      IF(L.GT.L72) GO TO 500
      WRITE(5,3020) L1,L
 3020 FORMAT(2I3)
C
C ..... CONVERT MM/DAY TO MM/MONTH .....................
C
      CFLAG=0.
      DO 70 M=1,12
      T(M)=TEMP(M)
      P(M)=PRECIP(M)*DAYSPM(M)
C
C ..... SET COLD STATION FLAG .........................
```

```
C
      IF(T(M).LT.-1.0) CFLAG=CFLAG+1.
   70 CONTINUE
C
C ------ ZEROES ----------------------------------------
C
      HINDEX=0.
      SUM3=0.
      SUR12=0.
      DEF12=0.
      AE12=0.
      PE12=0.
      P12=0.
C
C ------ PE --------------------------------------------
C
      DO 10 M=1,12
      IF(T(M).GT.0.) HINDEX=HINDEX+(T(M)/5.)**1.514
   10 CONTINUE
      A=6.75E-07*HINDEX**3-7.71E-05*HINDEX**2+
     X0.01792*HINDEX+.49239
      DO 20 M=1,12
      IF(T(M).LE.0.) THEN
        UNADJ=0.
      ELSE IF(T(M).LT.26.5) THEN
        UNADJ=16.*(10.*T(M)/HINDEX)**A
      ELSE
        UNADJ=-415.8547+32.2441*T(M)-.4325*T(M)**2
      END IF
      PE(M)=UNADJ*HSUN(M,L1)*DAYSPM(M)/30./12.
      IF(M.EQ.ISMAX.OR.M.EQ.ISMAX1.OR.M.EQ.ISMAX2)
     XSUM3=SUM3+PE(M)
C
C ------ DEFINE RAINFALL AND SNOWFALL --------------------
C
      IF(T(M).LE.-1.0) THEN
        RN(M)=0.
        SF(M)=P(M)
      ELSE
        RN(M)=P(M)
        SF(M)=0.
      END IF
C
C ..... RMPE .....................................
C
      RMPE(M)=RN(M)-PE(M)
   20 CONTINUE
C
C ------ WATER BALANCE CALCULATIONS ----------------------
C
      IF(CFLAG.EQ.12.0.OR.LAND(L).EQ.'7') THEN
```

```
C
C ..... POLAR OR OCEAN GRID POINT .....................
C
        DO 30 M=1,12
        SUR(M)=0.
        DEF(M)=0.
        AE(M)=PE(M)
   30   CONTINUE
C
C ..... ALL OTHER GRID POINTS .........................
C
      ELSE
        CALL BALNCE
        DO 80 M=1,12
        AE(M)=RN(M)+SMT(M)-DST(M)-SUR(M)
        IF((PE(M)-AE(M)).LT.0.) THEN
          DEF(M)=0.
        ELSE
          DEF(M)=PE(M)-AE(M)
        END IF
   80   CONTINUE
      END IF
C
C ------ ANNUAL AE, PE, P ---------------------------------
C
      DO 90 M=1,12
      AE12=AE12+AE(M)
      PE12=PE12+PE(M)
      P12=P12+P(M)
      SUR12=SUR12+SUR(M)
      DEF12=DEF12+DEF(M)
   90 CONTINUE
C
C ------ ANNUAL HUMIDITY, ARIDITY, & MOISTURE INDICES ------
C
      IF(PE12.EQ.0.) THEN
        XIH=0.
        XIA=0.
        XIM=0.
      ELSE
        XIH=100.*SUR12/PE12
        XIA=100.*DEF12/PE12
        XIM=100.*(P12/PE12-1.)
      END IF
C
C ..... SUMMER=# OF MOIST SUMMER HALF-YR MONTHS ..........
C ..... WINTER=# OF MOIST WINTER HALF-YR MONTHS ..........
C
      SUMMER=0.
      WINTER=0.
      DO 200 M=1,6
```

```
      IF(RMPE(ISWM(M,IS)).GT.0.) SUMMER=SUMMER+1.
      IF(RMPE(ISWM(M,IW)).GT.0.) WINTER=WINTER+1.
  200 CONTINUE
C
C ------ SUMMER CONCENTRATION OF PE -----------------------
C
      IF(PE12.EQ.0.) THEN
        PESC=0.
      ELSE
      PESC=SUM3/PE12*100.
      END IF
C
C ------ 1ST LEVEL: MOISTURE REGIONS ----------------------
C
C     A=PERHUMID              D=DRY SUBHUMID
C     B=HUMID                 E=SEMI-ARID
C     C=MOIST SUBHUMID        F=ARID
C
C ..........................................................
C
      IF(XIM.GE.100.) THEN
        DESCRP(L3312,1,1)='A'
      ELSE IF(XIM.GE.20.) THEN
        DESCRP(L3312,1,1)='B'
      ELSE IF(XIM.GE.0.) THEN
        DESCRP(L3312,1,1)='C'
      ELSE IF(XIM.GE.-33.3) THEN
        DESCRP(L3312,1,1)='D'
      ELSE IF(XIM.GE.-66.7) THEN
        DESCRP(L3312,1,1)='E'
      ELSE IF(XIM.GE.-100.) THEN
        DESCRP(L3312,1,1)='F'
      ELSE
        DESCRP(L3312,1,1)='X'
      END IF
C
C ------ 2ND LEVEL: THERMAL EFFICIENCY --------------------
C
C     A=MEGATHERMAL           D=TUNDRA
C     B=MESOTHERMAL           E=FROST
C     C=MICROTHERMAL
C
C ..........................................................
C
      IF(PE12.GE.1140.) THEN
        DESCRP(L3312,2,1)='A'
      ELSE IF(PE12.GE.570.) THEN
        DESCRP(L3312,2,1)='B'
      ELSE IF(PE12.GE.285.) THEN
        DESCRP(L3312,2,1)='C'
      ELSE IF(PE12.GE.142.) THEN
```

```
        DESCRP(L3312,2,1)='D'
      ELSE
        DESCRP(L3312,2,1)='E'
      END IF
C
C ------ 3RD LEVEL: RELATIVE DRY SEASON --------------------
C
C     R=EVENLY MOIST
C     D=EVENLY DRY
C     S=SUMMER DRIEST
C     W=WINTER DRIEST
C
C ..........................................................
C
      IF(XIM.GE.0.) THEN
C
C ..... MOIST CLIMATES ..................................
C
        IF(XIA.LT.10.0.OR.LAND(L).EQ.'7') THEN
          DESCRP(L3312,3,1)='R'
        ELSE IF(SUMMER.LT.WINTER) THEN
          DESCRP(L3312,3,1)='S'
        ELSE IF(WINTER.LT.SUMMER) THEN
          DESCRP(L3312,3,1)='W'
        ELSE
          DESCRP(L3312,3,1)='R'
        END IF
C
C ..... DRY CLIMATES ....................................
C
      ELSE
        IF(XIH.LT.16.7.OR.LAND(L).EQ.'7') THEN
          DESCRP(L3312,3,1)='D'
        ELSE IF(SUMMER.GT.WINTER) THEN
          DESCRP(L3312,3,1)='W'
        ELSE IF(WINTER.GT.SUMMER) THEN
          DESCRP(L3312,3,1)='S'
        ELSE
          DESCRP(L3312,3,1)='D'
        END IF
      END IF
C
C ------ 4TH LEVEL: SUMMER CONC. OF THERMAL EFFICIENCY -----
C
C     A=SMALLEST CONCENTRATION
C     B=SMALLER CONCENTRATION
C     C=LARGER CONCENTRATION
C     D=LARGEST CONCENTRATION
C
C ..........................................................
C
```

```
      IF(PESC.LE.48.) THEN
        DESCRP(L3312,4,1)='A'
      ELSE IF(PESC.LE.68.) THEN
        DESCRP(L3312,4,1)='B'
      ELSE IF(PESC.LE.76.3) THEN
        DESCRP(L3312,4,1)='C'
      ELSE
        DESCRP(L3312,4,1)='D'
      END IF
C
C ------ WRITE OUT TO POST-PROCESSOR FILE --------------
C
      WRITE(1) XIM,XIA,XIH,PE12,AE12/365.,PESC,HINDEX,
     X(PE(M)/DAYSPM(M),M=1,12)
C
C ------ WRITE OUT SAMPLE STATION DATA -------------------
C
      DO 630 J=1,JV
      IF(L1.EQ.JVERIF(J,1).AND.L.EQ.JVERIF(J,2)) THEN
        WRITE(4,2020)
        WRITE(4,2030) LAND(L),PHI*180./PI
        WRITE(4,2000) 'HSUN',(HSUN(M,L1),M=1,12)
        WRITE(4,2000) 'T   ',T
        WRITE(4,2000) 'P   ',P
        WRITE(4,2000) 'RN  ',RN
        WRITE(4,2000) 'SF  ',SF
        WRITE(4,2000) 'PE  ',PE
        WRITE(4,2000) 'AE  ',AE
        WRITE(4,2000) 'R-PE',RMPE
        WRITE(4,2000) 'SUR ',SUR
        WRITE(4,2000) 'DEF ',DEF
        WRITE(4,2000) 'ST  ',ST
        WRITE(4,2000) 'SST ',SST
        WRITE(4,2000) 'DST ',DST
        WRITE(4,2000) 'SMT ',SMT
        WRITE(4,2000) 'AE  ',AE12
        WRITE(4,2000) 'PE  ',PE12
        WRITE(4,2000) 'PESC',PESC
        WRITE(4,2000) 'P   ',P12
        WRITE(4,2000) 'SUR ',SUR12
        WRITE(4,2000) 'DEF ',DEF12
        WRITE(4,2000) 'IH  ',XIH
        WRITE(4,2000) 'IA  ',XIA
        WRITE(4,2000) 'IM  ',XIM
        WRITE(4,2010) (DESCRP(L,K,1),K=1,4)
      END IF
  630 CONTINUE
  500 CONTINUE
  510 CONTINUE
C
C ------ WRITE CLIMATE CODE INTO TEXT FILE ----------------
```

```
C
      CLOSE(1)
      FILE='DR1:T    .PRT          '
      FILE(6:8)=XPRMT(1:3)
      OPEN(UNIT=1,NAME=FILE,TYPE='NEW')
      DO 610 N=1,2
      K=(N-1)*23+1
      WRITE(1,4000)(I,I=K,K+22)
      DO 600 L=1,72
  600 WRITE(1,4010) L,((DESCRP(72*I-72+L,J,1),J=1,4),
     XI=K,K+22)
  610 CONTINUE
C
C ------ WRITE CLIMATE CODE INTO TMAP PLOT FILE -----------
C
      CLOSE(1)
      FILE(10:12)='DAT'
      OPEN(UNIT=1,NAME=FILE,TYPE='NEW',
     XFORM='UNFORMATTED')
      DO 620 L=1,72
  620 WRITE(1) L,((DESCRP(72*I-72+L,J,1),J=1,4),I=1,46)
C
C ------ FORMAT STATEMENTS --------------------------------
C
 1010 FORMAT(' GO TAKE A BREAK!',/)
 1020 FORMAT(' HANG IN THERE!',/,
     X' ONLY ',I2,' MORE LATITUDES TO GO',/)
 1030 FORMAT(' YES, IT IS ALMOST FINALLY COMPLETELY DONE!',/,
     X' ONLY ',I2,' MEASLY LATITUDES TO GO')
 1040 FORMAT(' 1 DOWN AND ONLY 45 TO GO!')
 2000 FORMAT(1X,A4,13F9.2)
 2010 FORMAT(1X,4A1)
 2020 FORMAT(/)
 2025 FORMAT(1H1,2X,12(7X,I2),/)
 2030 FORMAT(1X,A1,F7.2)
 2040 FORMAT(' INPUT EXPERIMENT CODE NAME (A8)')
 2050 FORMAT(A8)
 2060 FORMAT(I2)
 2070 FORMAT(' INPUT # OF STATIONS (JV<=10) TO VERIFY (I2)')
 2080 FORMAT('   GRID POINT #',I2,'?   (2I2)')
 2090 FORMAT(2I2)
 2100 FORMAT(1X)
 2110 FORMAT(1X,18A1,3(46(/),1X,18A1))
 4000 FORMAT(1H1,5X,23(I2,3X),/)
 4010 FORMAT(1X,I2,2X,23(4A1,1X))
C
      STOP
      END
C
      SUBROUTINE BALNCE
C
```

```
C -------------------------------------------------------
C
C     THIS SUB BALANCES THE WATER BUDGET ACCORDING TO
C     CORT WILLMOTT'S AUGUST 1981 VERSION OF WATBUG.
C
C -------------------------------------------------------
C
      COMMON /Z1/ RMPE(13),ST(13),FC,SUR(13),DST(13),
     XDAYSPM(13),DEF(13),L,L1,DEC,PI,P(13),T(13),PE(13),
     XSF(13),RN(13),SST(13),SMT(13),DS,AE(13),JVERIF(10,2),JV
C
C ------ DEFINE INITIAL CONDITIONS ----------------------
C
      SST(1)=SF(1)
      ST(1)=FC
      DST(1)=0.
      P(13)=P(1)
      T(13)=T(1)
      ST(13)=0.
      SST(13)=0.
      SF(13)=SF(1)
      RMPE(13)=RMPE(1)
C
C ------ DEFINE OTHER INITIAL CONDITIONS AND FLAGS ------
C
      K=0
      ITC=0
      Z=0.
      Z2=0.
      XX4=0.
      ZZ4=0.
C
C ------ INITIAL CONDITIONS FOR DOING MONTHLY STORAGE ---
C
  230 INIT=2
      IFLAG=0
      NP1=13
C
C ------ IF BALANCED ST & UNBALANCED SNOWPACK, RESET K=0
C
  260 IF(IFLAG.EQ.1) K=0
C
C ------ START MONTH LOOP -------------------------------
C
      DO 200 M=INIT,NP1
C
C ..... IF BALANCED ST & UNBAL. SNOWPACK, DO ST FOR M=12
C
      IF(IFLAG.EQ.1) THEN
        M1=12
      ELSE
```

```
        M1=M-1
      END IF
C
C ..... DEFINE TEMPORARY STORAGE .....................
C
      X1=ST(M1)
      X2=SST(M1)
C
C ..... SET SMOWMELT & SURPLUS TO ZERO ...............
C
      SMT(M)=0.
      SUR(M)=0.
C
C ------ START DAY LOOP --------------------------------
C
      DO 210 J=1,DAYSPM(M)
C
C ..... COMPUTE SNOWMELT .............................
C
      SX=ST(M1)
      SST(M)=SST(M1)+SF(M)/DAYSPM(M)
      TX=T(M)
      PX=P(M)/DAYSPM(M)
      SSTX=SST(M)
      SNMLT=SMELT(TX,PX,SSTX)
      SST(M)=SST(M)-SNMLT
      SMT(M)=SMT(M)+SNMLT
C
C ..... R - PE + SNOWMELT ............................
C
      DS=SNMLT+RMPE(M)/DAYSPM(M)
C
C ..... CALCULATE STORAGE ............................
C
      CALL CALST(SX,M,M1)
  210 CONTINUE
C
C ------ END DAY LOOP ----------------------------------
C
      ST(M1)=X1
      SST(M1)=X2
      DST(M)=ST(M)-ST(M1)
      IF(IFLAG.NE.0) THEN
C
C ..... UNBAL. SNOWPACK: RESET Z,Z2 & REDO MONTHLY ST
C
        Z=ST(M)
        Z2=SST(M)
        GO TO 230
      END IF
  200 CONTINUE
```

```
C ------ END MONTH LOOP --------------------------------
C
 2000 FORMAT(1X,A4,13F9.2)
 2020 FORMAT(1X)
 2030 FORMAT(5X,3I3,8F9.2)
C
C ------ BALANCE ITERATIONS ----------------------------
C
      K=K+1
      IF(K.GT.50) GO TO 250
C
C ..... DEFINE STORAGE BALANCE VARIABLES ..............
C
      XX=ABS(ST(13)-ST(1))
      ZZ=ABS(Z-ST(1))
      XX2=ABS(SST(13)-SST(1))
      ZZ2=ABS(Z2-SST(1))
C
C ..... DEFINE SNOWPACK INCREASE VARIABLES .............
C
      XX3=ABS(XX2-XX4)
      ZZ3=ABS(ZZ2-ZZ4)
      XX4=XX2
      ZZ4=ZZ2
C
C ..... WRITE OUT ITERATION DATA CHECK ................
C
      DO 630 J=1,JV
      IF(L1.EQ.JVERIF(J,1).AND.L.EQ.JVERIF(J,2)) THEN
        WRITE(4,2000) 'ST  ',ST
        WRITE(4,2000) 'DST ',DST
        WRITE(4,2000) 'SST ',SST
        WRITE(4,2000) 'SMT ',SMT
        WRITE(4,2000) 'SUR ',SUR
        WRITE(4,2030) K,ITC,IFLAG,XX,ZZ,XX2,XX3,ZZ2,ZZ3,XX4,ZZ4
        WRITE(4,2020)
      END IF
  630 CONTINUE
C
C
C ..... CHECK FOR BALANCED ST AND SNOWPACK .............
C
      IF(XX.LT.1.0.AND.ZZ.LT.1.0.AND.
     X  (XX2.LT.1.0.OR.XX3.LT.1.0).AND.
     X  (ZZ2.LT.1.0.OR.ZZ3.LT.1.0)) RETURN
C
C ..... IS ST AT LEAST BALANCED? ......................
C
      IF(XX.LT.1.0.AND.XX2.LT.1.0) THEN
        CONTINUE
      ELSE
```

```
C
C ........ NOTHING BALANCED; REDO MONTH LOOP .............
C
        SST(1)=SST(13)
        ST(1)=ST(13)
        GO TO 230
      END IF
C
C ....... INITIALIZATION FOR SNOWPACK BALANCE ITERATIONS .
C
  250 IF(K.GT.50.AND.ITC.EQ.2) THEN
        WRITE(4,1000) L1,L,K,ITC,IFLAG
 1000   FORMAT(' TOO MANY ITERATIONS IN BALANCING',
     X  /,5I3)
        RETURN
      ELSE
        ITC=ITC+1
        IFLAG=1
        INIT=1
        NP1=1
        GO TO 260
      END IF
      END
C
      SUBROUTINE CALST(SX,M,M1)
C
C ---------------------------------------------------------
C
C     THIS SUB COMPUTES THE STORAGE AND SURPLUS FOR ONE
C     MONTH.
C
C ---------------------------------------------------------
C
      COMMON /Z1/ RMPE(13),ST(13),FC,SUR(13),DST(13),
     XDAYSPM(13),DEF(13),L,L1,DEC,PI,P(13),T(13),PE(13),
     XSF(13),RN(13),SST(13),SMT(13),DS,AE(13),JVERIF(10,2),JV
C
      IF(T(M).LT.-1.0.OR.SST(M).GT.1.0) THEN
C
C ------ BELOW ZERO TEMP OR SNOW ON GND -----------------
C
        IF(DS.GT.0.) THEN
C
C ........ SURPLUS .....................................
C
          SUR(M)=SUR(M)+DS
        END IF
        ST(M)=ST(M1)
      ELSE
C
C ------ ABOVE ZERO TEMP OR NO SNOW ON GND --------------
```

```
C
        RATIO=1.-EXP(-6.8*SX/FC)
        IF(DS.GE.0.) RATIO=1.
        ST(M)=ST(M1)+DS*RATIO
C
C ........ SURPLUS .....................................
C
        IF(ST(M).GT.FC) THEN
          SUR(M)=SUR(M)+ST(M)-FC
          ST(M)=FC
        ELSE
          IF(ST(M).LE.0.1) ST(M)=.1
        END IF
      END IF
      SST(M1)=SST(M)
      ST(M1)=ST(M)
      RETURN
      END
C
      FUNCTION SMELT(TX,PX,SSTX)
C
C ------ COMPUTE DAILY SNOWMELT (MM/DAY) ----------------
C
      SMELT=2.63+2.55*TX+0.0912*TX*PX
      IF(SMELT.LE.0.) SMELT=0.
      IF(SMELT.GE.SSTX) SMELT=SSTX
      RETURN
      END
C
```

Appendix D. Listing of Annual-mean Thornthwaite Classification Code

```
      PROGRAM THORN2
C
C -------------------------------------------------------
C
C     THIS CODE CLASSIFIES CLIMATES ACCORDING TO
C     THORNTHWAITE'S 1955 SCHEME, USING ANNUAL MEAN
C     GLOBAL DATA.
C
C -------------------------------------------------------
C
C     UNITS ARE DEGREES CELSIUS AND MILLIMETERS.
C
C -------------------------------------------------------
C
C     T          = ANNUAL MEAN TEMP FOR A GRID POINT
C     P          = ANNUAL MEAN PRECIP FOR A GRID POINT
C     PE12       = ANNUAL PE FOR A GRID POINT
C     XIM        = ANNUAL MOISTURE INDEX
C
C -------------------------------------------------------
C
C     >TKB
C     TKB>THORN2=THORN2
C     TKB>/
C     Enter options:
C     TKB>UNITS=5
C     TKB>ACTFIL=5
C     TKB>LIBR=FCSRES:RO
C     TKB>//
C
C -------------------------------------------------------
C
      DIMENSION JVERIF(10,2)
      CHARACTER*8 XPRMT
      CHARACTER*20 FILE
      BYTE DESCRP(3312,4,1)
C
      DATA FILE/'LB:[102,3]XP    .DAT '/
      DATA PI,L72,L46/3.14159,72,46/
      DATA DAYSPM/30./
C
C ------ OPEN FILES ------------------------------------
C
      OPEN(UNIT=1,NAME='XOUCH.DAT',TYPE='NEW',
     XFORM='UNFORMATTED')
      OPEN(UNIT=5,NAME='TI:',TYPE='OLD',
     XCARRIAGECONTROL='LIST')
```

```
      WRITE(5,2040)
      READ(5,2050) XPRMT
      WRITE(1) XPRMT
      FILE(13:15)=XPRMT(1:3)
      OPEN(UNIT=3,NAME=FILE,TYPE='OLD',FORM='UNFORMATTED',
     XREADONLY)
      FILE(12:13)='PE'
      FILE(14:16)=XPRMT(1:3)
      FILE(17:20)='.DAT'
      OPEN(UNIT=2,NAME=FILE,TYPE='OLD',FORM='UNFORMATTED',
     XREADONLY)
C
C ..... VERIFICATION FILE INFO .........................
C
      OPEN(UNIT=4,NAME='VERIFY.PRT',TYPE='NEW')
      WRITE(5,2070)
      READ(5,2060) JV
      DO 650 J=1,JV
      WRITE(5,2080) J
      READ(5,2090) (JVERIF(J,I),I=1,2)
  650 CONTINUE
C
C ------ START LATITUDE (L1) LOOP --------------------
C
      DO 510 L1=1,46
      PHI=(FLOAT(L1)-23.5)*4.*PI/180.
C
C ........ TERMINAL PROGRESS MESSAGES ..................
C
      IF(L1.EQ.1) WRITE(5,1010)
      IF(L1.EQ.2) WRITE(5,1040)
      IF(L1.EQ.20) WRITE(5,1020) 46-L1
      IF(L1.EQ.40) WRITE(5,1030) 46-L1
C
C ------ START LONGITUDE (L) LOOP ------------------------
C
      DO 500 L=1,72
C
C ..... WRITE HEADER FOR STATION CHECK ................
C
      DO 640 J=1,JV
      IF(L1.EQ.JVERIF(J,1).AND.L.EQ.JVERIF(J,2)) THEN
        WRITE(4,2025) (I,I=1,12)
      END IF
  640 CONTINUE
C
      L3312=(L1-1)*72+L
      READ(2) PE12
      READ(3) P12
C
C ..... CONVERT MM/DAY TO MM/MONTH .....................
```

```
C
      P12=P12*DAYSPM*12.
      PE12=PE12*DAYSPM*12.
C
C ------ COMPUTE MOISTURE INDEX --------------------------
C
      IF(PE12.EQ.0.) THEN
        XIM=0.
      ELSE
        XIM=100.*(P12/PE12-1.)
      END IF
C
C ------ 1ST LEVEL: MOISTURE REGIONS ----------------------
C
C     A=PERHUMID              D=DRY SUBHUMID
C     B=HUMID                 E=SEMI-ARID
C     C=MOIST SUBHUMID        F=ARID
C
C ..........................................................
C
      IF(XIM.GE.100.) THEN
        DESCRP(L3312,1,1)='A'
      ELSE IF(XIM.GE.20.) THEN
        DESCRP(L3312,1,1)='B'
      ELSE IF(XIM.GE.0.) THEN
        DESCRP(L3312,1,1)='C'
      ELSE IF(XIM.GE.-33.3) THEN
        DESCRP(L3312,1,1)='D'
      ELSE IF(XIM.GE.-66.7) THEN
        DESCRP(L3312,1,1)='E'
      ELSE IF(XIM.GE.-100.) THEN
        DESCRP(L3312,1,1)='F'
      ELSE
        DESCRP(L3312,1,1)='X'
      END IF
C
C ------ 2ND LEVEL: THERMAL EFFICIENCY --------------------
C
C     A=MEGATHERMAL           D=TUNDRA
C     B=MESOTHERMAL           E=FROST
C     C=MICROTHERMAL
C
C ..........................................................
C
      IF(PE12.GE.1140.) THEN
        DESCRP(L3312,2,1)='A'
      ELSE IF(PE12.GE.570.) THEN
        DESCRP(L3312,2,1)='B'
      ELSE IF(PE12.GE.285.) THEN
        DESCRP(L3312,2,1)='C'
      ELSE IF(PE12.GE.142.) THEN
```

```
        DESCRP(L3312,2,1)='D'
      ELSE
        DESCRP(L3312,2,1)='E'
      END IF
C
C ------ 3RD AND 4TH LEVELS ----------------------------
C
      DESCRP(L3312,3,1)=' '
      DESCRP(L3312,4,1)=' '
C
C ------ WRITE OUT TO POST-PROCESSOR FILE --------------
C
      WRITE(1) XIM,PE12
C
C ------ WRITE OUT SAMPLE STATION DATA -------------------
C
      DO 630 J=1,JV
      IF(L1.EQ.JVERIF(J,1).AND.L.EQ.JVERIF(J,2)) THEN
        WRITE(4,2020)
        WRITE(4,2030) PHI*180./PI
        WRITE(4,2000) 'PE  ',PE12
        WRITE(4,2000) 'P   ',P12
        WRITE(4,2000) 'IM  ',XIM
        WRITE(4,2010) (DESCRP(L,K,1),K=1,4)
      END IF
  630 CONTINUE
  500 CONTINUE
  510 CONTINUE
C
C ------ WRITE CLIMATE CODE INTO TEXT FILE ----------------
C
      CLOSE(1)
      FILE='DR1:T    .PRT        '
      FILE(6:8)=XPRMT(1:3)
      OPEN(UNIT=1,NAME=FILE,TYPE='NEW')
      DO 610 N=1,2
      K=(N-1)*23+1
      WRITE(1,4000)(I,I=K,K+22)
      DO 600 L=1,72
  600 WRITE(1,4010) L,((DESCRP(72*I-72+L,J,1),J=1,4),
     XI=K,K+22)
  610 CONTINUE
C
C ------ WRITE CLIMATE CODE INTO TMAP PLOT FILE -----------
C
      CLOSE(1)
      FILE(10:12)='DAT'
      OPEN(UNIT=1,NAME=FILE,TYPE='NEW',
     XFORM='UNFORMATTED')
      DO 620 L=1,72
  620 WRITE(1) L,((DESCRP(72*I-72+L,J,1),J=1,4),I=1,46)
```

```
C
C ------ FORMAT STATEMENTS --------------------------------
C
 1010 FORMAT(' GO TAKE A BREAK!',/)
 1020 FORMAT(' HANG IN THERE!',/,
     X' ONLY ',I2,' MORE LATITUDES TO GO',/)
 1030 FORMAT(' YES, IT IS ALMOST FINALLY COMPLETELY DONE!',/,
     X' ONLY ',I2,' MEASLY LATITUDES TO GO')
 1040 FORMAT(' 1 DOWN AND ONLY 45 TO GO!')
 2000 FORMAT(1X,A4,13F9.2)
 2010 FORMAT(1X,4A1)
 2020 FORMAT(/)
 2025 FORMAT(1H1,2X,12(7X,I2),/)
 2030 FORMAT(1X,F7.2)
 2040 FORMAT(' INPUT EXPERIMENT CODE NAME (A8)')
 2050 FORMAT(A8)
 2060 FORMAT(I2)
 2070 FORMAT(' INPUT # OF STATIONS (JV<=10) TO VERIFY (I2)')
 2080 FORMAT('   GRID POINT #',I2,'?   (2I2)')
 2090 FORMAT(2I2)
 2100 FORMAT(1X)
 2110 FORMAT(1X,18A1,3(46(/),1X,18A1))
 4000 FORMAT(1H1,5X,23(I2,3X),/)
 4010 FORMAT(1X,I2,2X,23(4A1,1X))
C
      STOP
      END
C
```